Blue Transition Pilot DK-1: 3D geological model of the Bylderup-Bov area

Peter B. E. Sandersen, Christian Brandes, Jesper Pedersen,
Ulrich Polom, Lærke T. Andersen, Reinhard Kirsch,
Angelos Almpanis & Agnieszka T. Bentzen

Blue Transition | Interreg North Sea

Co-funded by the European Union

CLIMATE RESILIENCE, BIODIVERSITY AND POLLUTION

GEOLOGICAL SURVEY OF DENMARK AND GREENLAND
DANISH MINISTRY OF CLIMATE, ENERGY AND UTILITIES

GEUS

Blue Transition Pilot DK-1: 3D geological model of the Bylderup-Bov area

Peter B. E. Sandersen, Christian Brandes, Jesper Pedersen,
Ulrich Polom, Lærke T. Andersen, Reinhard Kirsch,
Angelos Almpanis & Agnieszka T. Bentzen

Blue Transition | Interreg North Sea

Co-funded by the European Union

CLIMATE RESILIENCE, BIODIVERSITY AND POLLUTION

GEOLOGICAL SURVEY OF DENMARK AND GREENLAND
DANISH MINISTRY OF CLIMATE, ENERGY AND UTILITIES

GEUS

Title:
Blue Transition Pilot DK-1:
3D geological model of the Bylderup-Bov area

Authors:
Sandersen, P.B.E., GEUS
Brandes, C., Leibniz University, Hannover, Germany
Pedersen, J., HydroGeophysics Group, Institute for Geoscience, Aarhus University Polom, U., LIAG
Andersen, L.T., GEUS
Kirsch, R., Kirsch GeoImpuls
Almpanis, A., HydroGeophysics Group, Institute for Geoscience, Aarhus University Bentzen, A.T., Southern Region of Denmark

Digital version (suitable for printing).

January 9th, 2026

Øster Voldgade 10
DK-1350 København K
Telephone: 38 14 20 00
E-mail: geus@geus.dk

ISBN 978-87-7871-629-3

Table of contents

1. Foreword

This report is prepared as a part of the project “BlueTransition – How to make my region climate resilient”. Blue Transition is a transnational EU-project supported by the Interreg North Sea Region programme. The consortium has 24 partners and 19 stakeholders from research, government, technical authorities, and public service providers, who have activities in 16 pilot areas in 6 European countries. The main goal of Blue Transition is a systemic change by an integrated water and soil management in times of climate change. Focus areas balance around activities in urban, agricultural, or natural areas, considering a transition in land-use and fosters political structures and governance.

This report describes geological conditions for area pilot DK-1 “Climate-hydrological models for two groundwater catchments for flood and contamination protection in the urban area”.

The Blue Transition Pilot DK-1 covers two areas within Aabenraa Municipality, Aabenraa city and the town of Bylderup-Bov (Figure 1.1), which are areas threatened by excess groundwater and surface water related to a changing climate. The excess water comes from increased precipitation, flooding from streams, and rising groundwater levels, but the low-lying parts of Aabenraa are also exposed to storm water overflow from the nearby fjord. Apart from the risk of flooding of houses and infrastructure, there is also a risk of potential mobilization of contamination related to former urban activities. In order to be able to point to possible mitigation activities, modelling of the geology and hydrology including subsequent scenario calculations is therefore necessary.

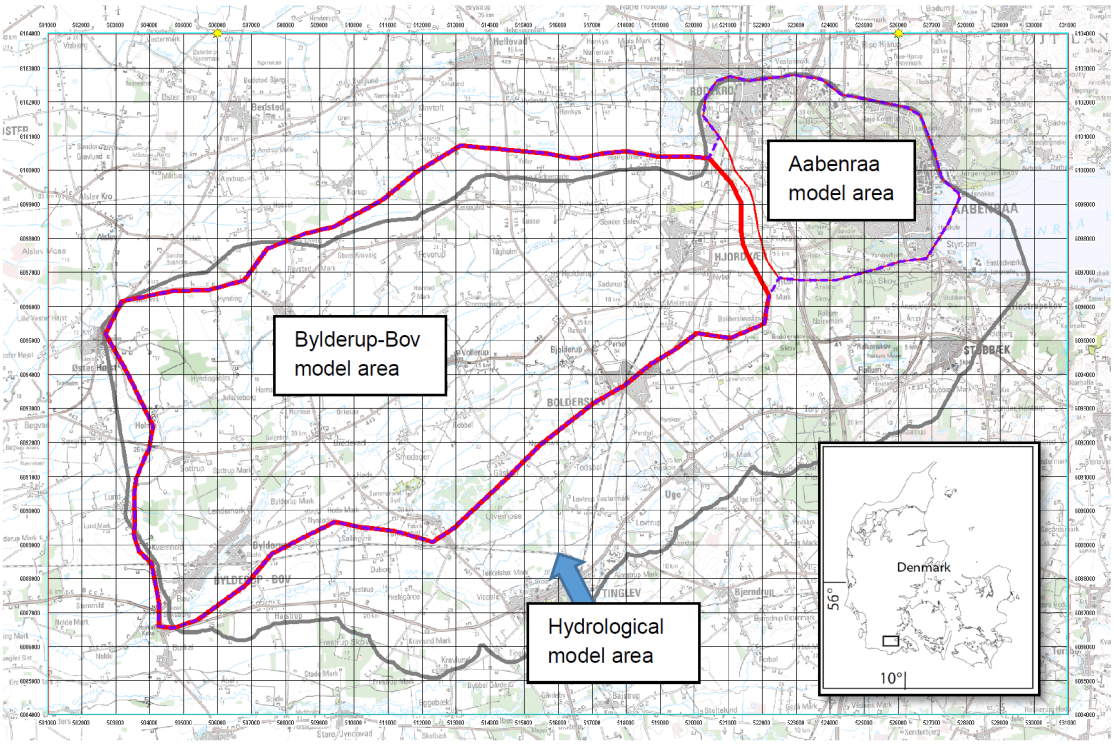

Figure 1.1. Location of the Bylderup-Bov and Aabenraa geological model areas, and the hydrological model area. The area inside the outer rectangle is the extent of the final model (20 x 30 km).

Geological models have been made for both areas, where the Aabenraa area has been modelled by the consulting engineers Niras, and the Bylderup-Bov area has been modelled by GEUS. This report covers the work on the geological model in Bylderup-Bov only, whereas the geological model of Aabenraa is reported separately by Niras. However, because the two model areas lie back-to-back, the hydrological modelling will cover both geological models, and therefore the geological modelling has been focused on securing that the two models could be merged into one. This has happened in a collaboration between Niras and GEUS. In areas not covered by the two geological models, model layer interpretations are collected from the existing hydrostratigraphic FOHM model (a national hydrostratigraphic model constructed by the Danish Environmental Protection Agency; Miljøstyrelsen, 2020). GEUS has performed the merging of the geological models and therefore this report will include a description of the procedure. For details about the Aabenraa model, we refer to the report by Niras (Niras, 2025). The hydrological model will be performed by GEUS and will be reported separately.

It should be noted that the Bylderup-Bov geological model focuses on the uppermost 50 m of the subsurface, and therefore the reporting will largely do the same. Both the geological modelling and the reporting will follow the national guidelines for geological modelling intended for hydrological modelling (Sandersen et al., 2018), but the reporting will be condensed to include only what is considered needed for the documentation specifically related to the Blue Transition DK-1 pilot.

2. Rationale

At present and in years to come, a changing climate is expected to create groundwater and surface water challenges in many parts of Denmark. In general, climate models for Denmark foresee a significant increase in winter precipitation, resulting in more groundwater recharge and higher water tables, especially during winter and spring in many areas (Seidenfaden et al., 2022). Specifically in areas around Aabenraa and Bylderup-Bov groundwater and surface water challenges have been occurring in recent years, calling for action both on the short and the long term.

Climate change, however, is not the only factor which affect the level and flow of surface water and groundwater. For instance, anthropogenic alterations of terrain and drainage, variations in groundwater abstraction and in the surface water administration should be included in the equation (e.g. Rasmussen et al., 2023). Furthermore, the geological framework will affect the groundwater flow depending on the layer architecture and the hydraulic properties of the sediments. Especially in areas with geological complexity created by faults, deformed layers or deep erosions, obstructions and corridors for groundwater flow and groundwater leakage between aquifers are likely to occur (e.g. Kidmose et al., 2025; Arnaud et al., 2025; Sandersen & Jørgensen, 2003; Bense et al., 2003). The impact of climate-induced changes in groundwater and surface water may therefore be sensitive to variations in the subsurface geological framework.

Situated on a Lateglacial sandy and gravelly outwash plain, the area around Bylderup-Bov would be expected to be well-drained, but as experienced locally this is obviously not the case. So why does this area of the outwash plain encounter such high groundwater levels? From previous knowledge of the geology in the area we know that a deep graben structure - The Tønder Graben - located underneath a large part of the stream catchment is riddled by faults, deformations, and deep erosions (Friborg et al., 2002; Jørgensen et al., 2014; Sandersen & Jørgensen, 2016). In addition to this, the unusual and highly irregular topography in the area points to near-surface complexity and very young tectonic events (Sandersen & Jørgensen, 2015).

In order to test the geological impact on groundwater and surface water flow and to calculate both present-day and future groundwater level scenarios, geological modelling in 3D and subsequent hydrological modelling has been performed. In this Blue Transition DK-1 pilot, it has been chosen to add more detail to especially the upper parts of the subsurface by using newly acquired geophysical data and water level measurements in new wells. The geological model is focused on aquifers and aquitards and is therefore constructed with layers that corresponds with the existing hydrostratigraphic FOHM model in the area. The model is focused on the uppermost 50 meters, but because of the presence of the deep graben structure, modelling of some of the deeper layers has been necessary.

3. General geology of the study area

3.1 Geomorphology

The Aabenraa and Bylderup-Bov areas are situated behind and in front of the Late Weichselian Main Stationary Line (MSL), respectively (see Figure 3.1). The MSL represent the westernmost location of the Late Weichselian ice sheet.

The Aabenraa area is located in an irregular terrain dominated by ice-marginal moraine hills sloping down towards the Aabenraa Fjord to the east. The hills are dominantly clayey. West of Aabenraa, the moraine hills outline the Main Stationary Line (MSL).

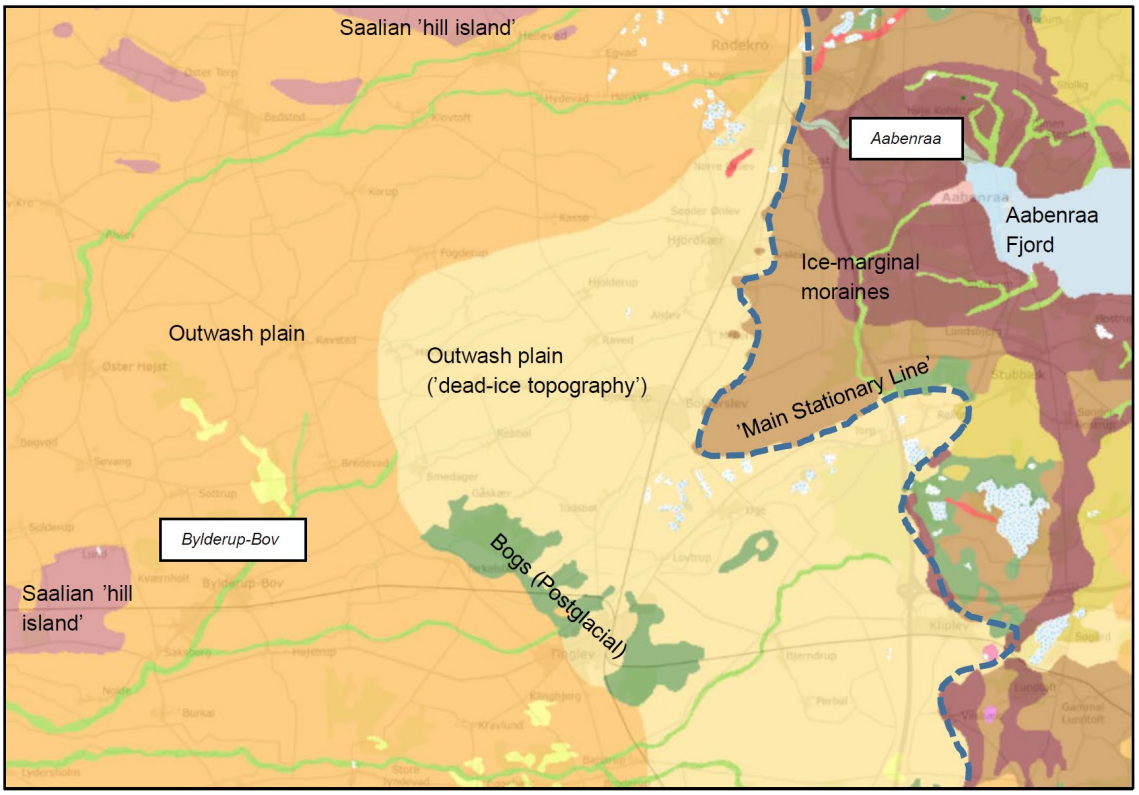

Figure 3.1. Geomorphology (Jakobsen, 2022). The figure shows main geomorphological elements. The map area is approximately the same as Figure 1.1.

From the west side of the clayey hills and further westwards the geomorphology is dominated by the Lateglacial Tinglev outwash plain which was formed by sedimentation of meltwater sand and gravel when the margin of the Late Weichselian ice sheet was at the MSL (Houmark-Nielsen, 2007). The outwash plain has a westerly oriented slope from around 50 m a.s.l. at the former ice margin to the east, to a few metres below sea level at the North Sea coast farther to the west. The outwash sediments generally consist of sand and gravel and attain thicknesses of up to around 20 m (Friborg 1996). On Figure 3.1, a large part of the outwash plain is described by Jacobsen (2022) as having a dead-ice topography (see also

Hansen, 1978). However, the irregularities of the topography in large parts of this area has been proven to be the result of Postglacial tectonic movements caused by deglaciation-induced reactivation of the faults of the Tønder Graben (Sandersen & Jørgensen, 2015; see later description). Depressions in the outwash plain surface is illustrated on Figure 3.1 by the presence of a large NW-SE oriented area with bogs a few kilometres east of Bylderup-Bov.

On the outwash plain there are isolated glacial hills of Saalian age lying as 'islands' surrounded by the outwash plain sediments (Figure 3.1).

3.2 Structural framework

The study area is situated south of the WNW−ESE orientated Ringkøbing-Fyn High (RFH) at the northern margin of the North German Basin – see Figure 3.2 (NGB; Vejbæk 1997). South of RFH is the WNW−ESE oriented Rømø Fracture Zone (RFZ), marking the transition between the RFH and the NGB (Lyngsie 2007). According to Lyngsie (2007), the RFZ is a sinistral en-echelon fault zone offsetting the Top pre-Zechstein. Strike-slip movements and block rotation in the RFH during the Palaeozoic made an impact both north and south of the RFH. According to Rasmussen (2009), the RFH was inverted in the early Miocene as part of the Alpine Orogeny and reactivation of former structural elements took place. A Late Cenozoic inversion of the basement structures south of the RFH deformed most of the Cenozoic succession in a compression event (Clausen & Huuse 1999).

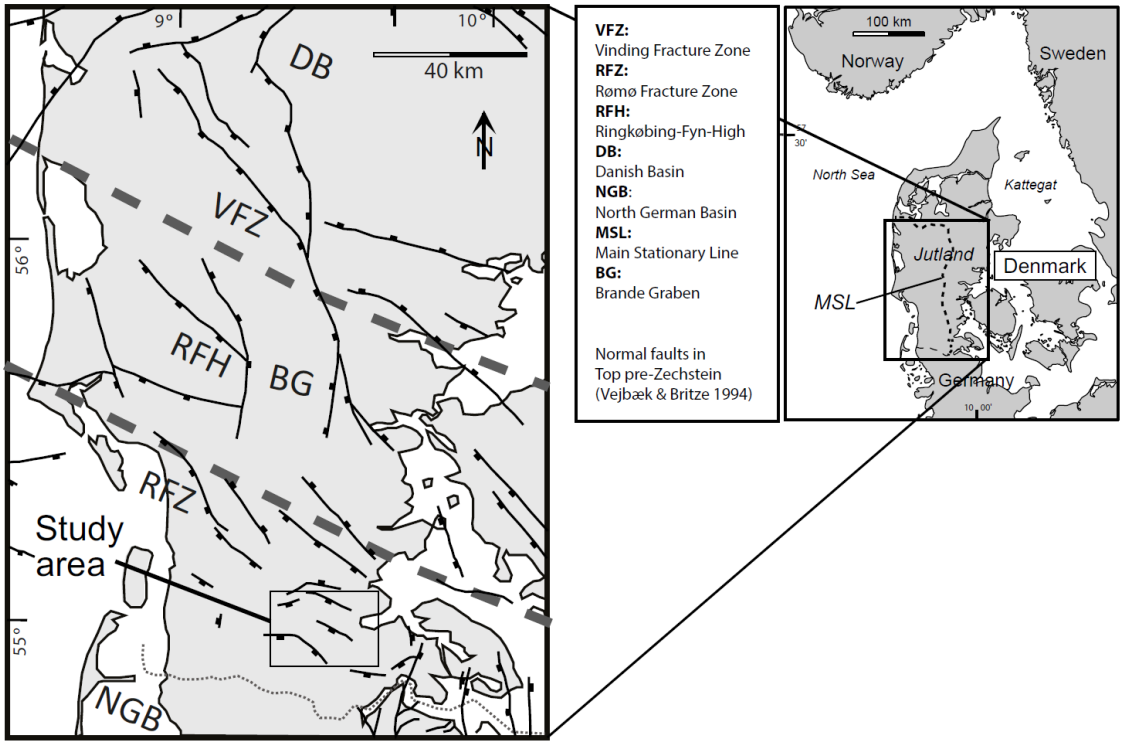

Figure 3.2. Study area and the general structural framework. Modified from Sandersen & Jørgensen (2015).

The Tønder Graben farther to the south developed along the RFZ, and mobilized Zechstein salt in the NGB added to the evolution of the graben impacting on the Mesozoic and Cenozoic sedimentation (e.g. Clausen & Pedersen 1999). Differential subsidence and faulting of the

cover sediments south of the RFH during the Cenozoic was caused by reactivation of Zechstein salt triggered by sediment load (Clausen et al., 2012). The salt acted as a detaching surface, meaning that faults offsetting the Top pre-Zechstein may be detached from the succession above, and faults offsetting the Top Chalk surface generally may be detached from the basement (Clausen & Huuse 1999; Clausen et al. 2012).

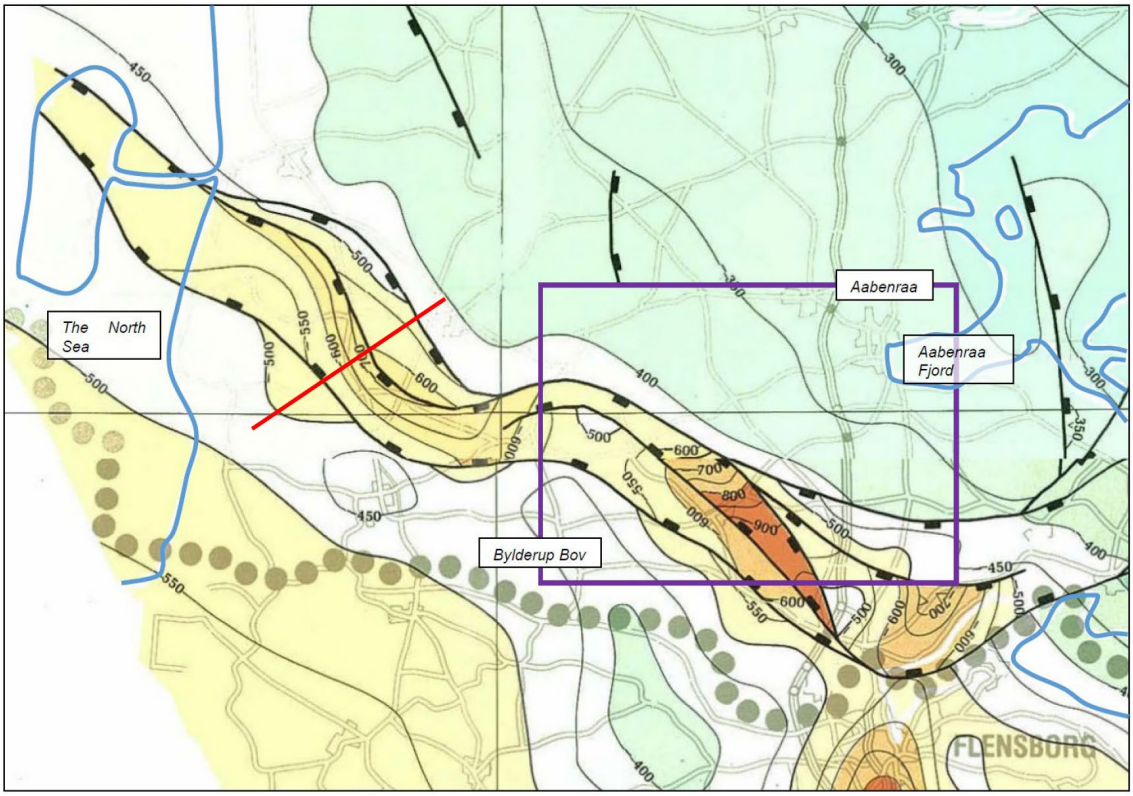

Figure 3.3. The Tønder Graben visualized in the Top Chalk Group (m a.s.l.); Ter-Borch, 1991. Black lines mark faults and a violet rectangle marks the approximate location of the study area. The coastline is enhanced with a blue line. A red line marks the approximate location of the seismic profile ST87T-005 shown in Figure 3.4

The Tønder Graben can be seen expressed in the Top Chalk surface as a W−E and NW−SE trending depression across southern Denmark (Figure 3.3; Ter-Borch 1991). Large offsets in the Top Chalk Group along the faults of the graben structure have created depressions of several hundred metres depth. Fault-related subsidence took place during the Neogene (Clausen et al. 2012), and some faults bounding the Tønder Graben offset the sedimentary succession including at least the Miocene deposits above the Chalk Group - see Figure 3.4 and Figure 3.6 (Friborg et al., 2002; Sandersen & Jørgensen, 2015). The main faults of the Tønder graben are also visualized in Figure 3.5.

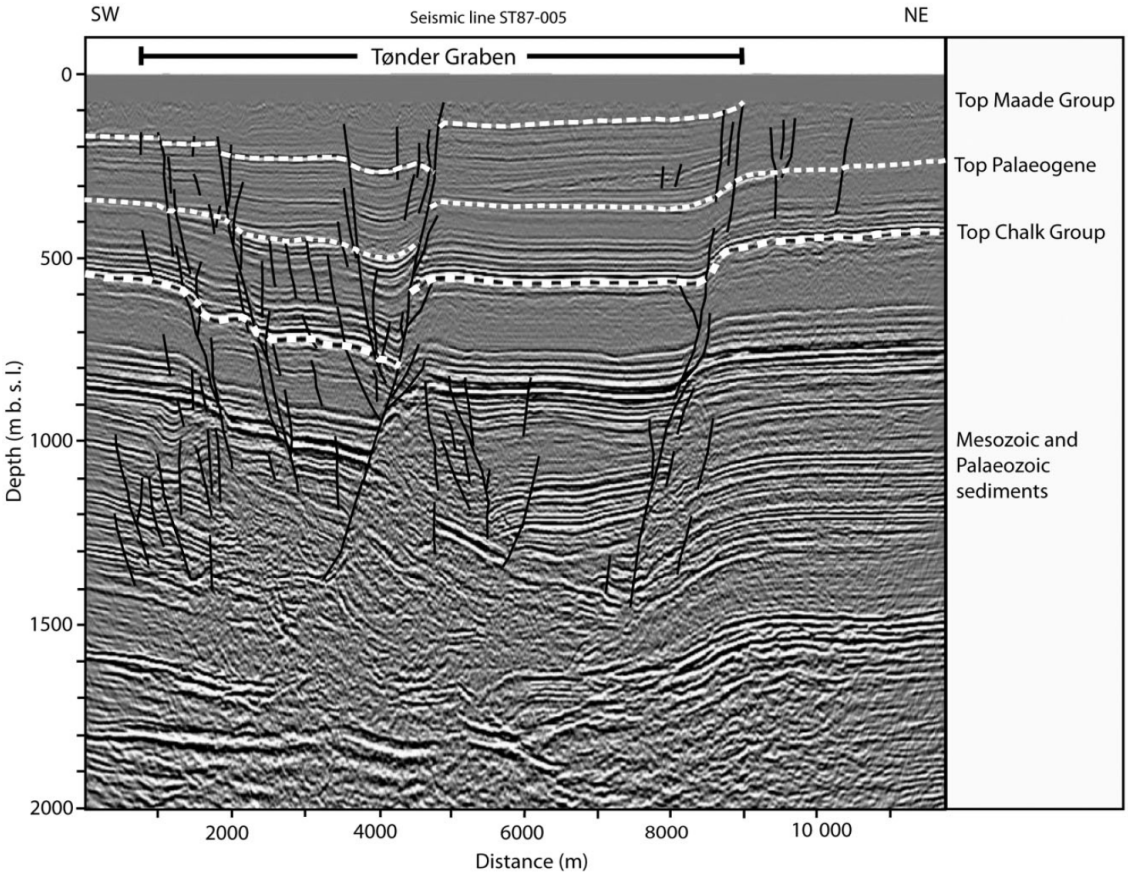

Figure 3.4. Seismic profile ST87T-005 oriented SW-NE. For location see Figure 3.3. From Sandersen & Jørgensen (2015).

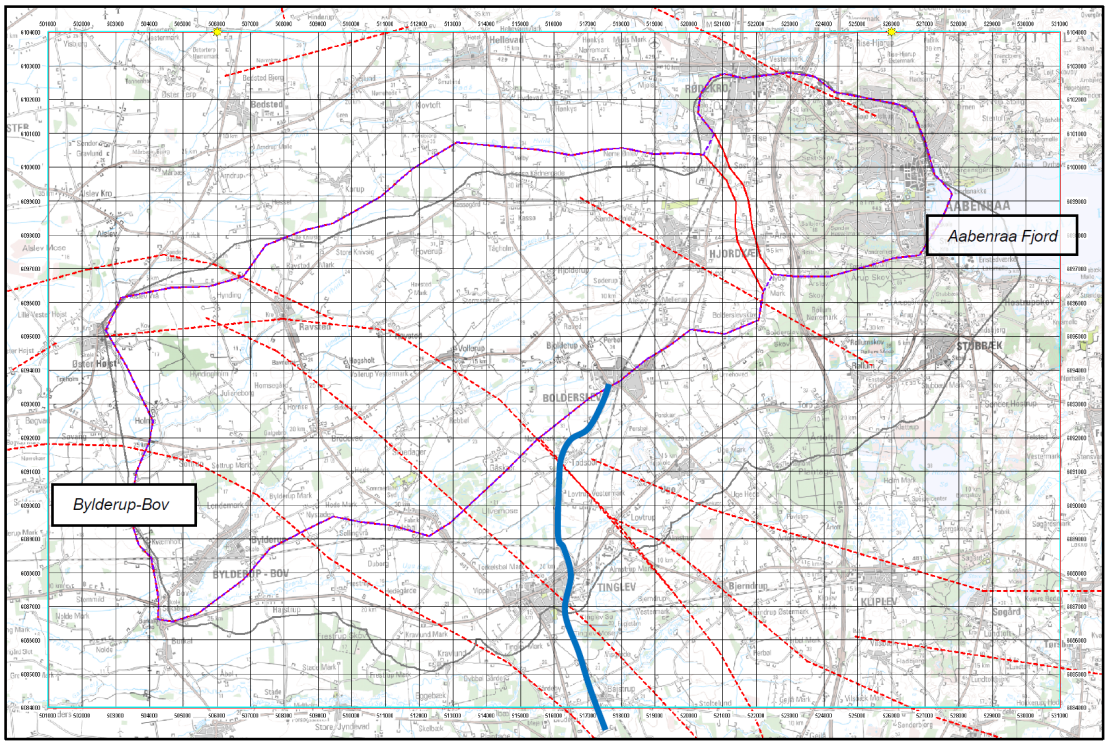

Figure 3.5. The main faults of the Tønder Graben sketched as red hatched lines with the outline of the geological model areas (purple line). The S-N blue line through the city of Tinglev shows the location of the right half of the conceptual profile in Figure 3.6.

3.3 The sedimentary succession

The sedimentary succession above the Top Chalk Group (Figure 3.3) described shortly in the following, comprises the youngest pre-Quaternary sediments from Paleogene and Neogene, and the Quaternary sediments from Pleistocene and Holocene. An earlier conceptual understanding of the layer succession is shown in (Figure 3.6). To the right on the profile, the main faults of the Tønder Graben are seen offsetting the pre-Quaternary succession in the order of 100-150 m causing the Miocene sediments within the main graben to be positioned deeper than outside the graben. From the profile it can be seen that the youngest Miocene layers attain greater thicknesses within the graben (Friborg et al., 2002).

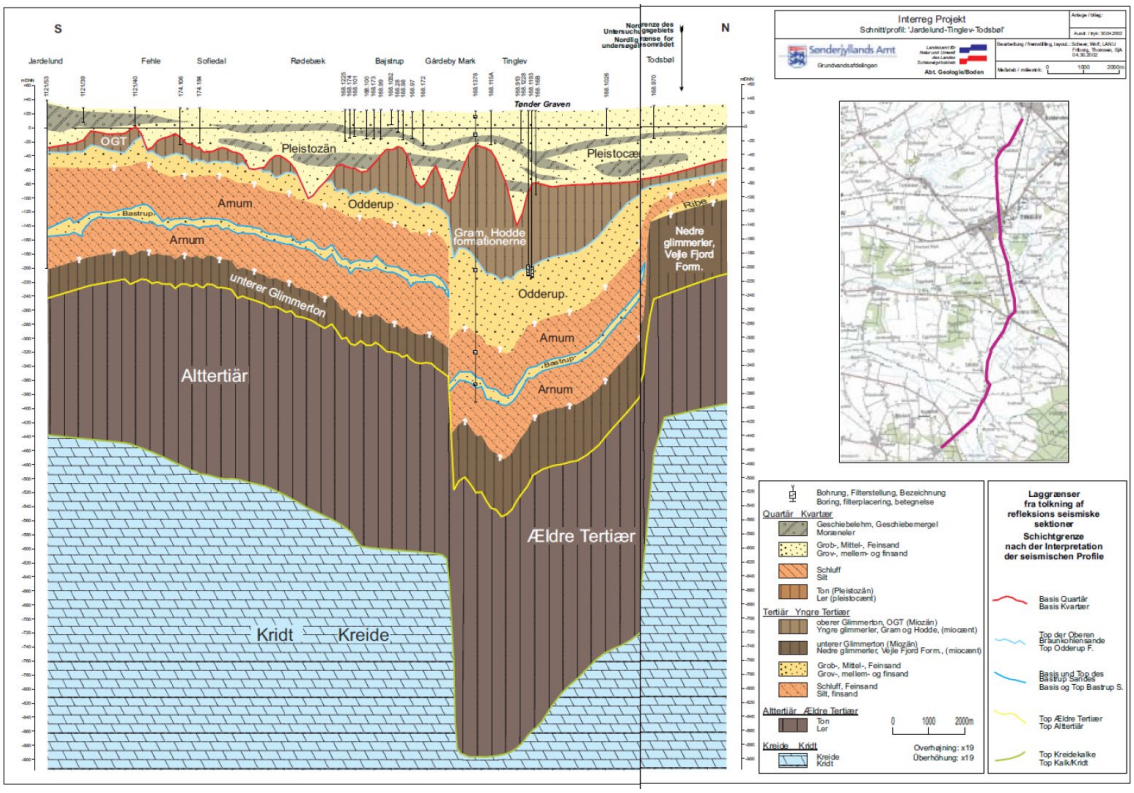

Figure 3.6. Conceptual geological profile interpreted along a S-N seismic profile across the Tønder Graben at Tinglev. From Friborg et al. (2002). See location on Figure 3.5. 'Kridt/Kreide' = Limestone and chalk

3.3.1 Pre-Quaternary sediments

Paleogene sediments

The Paleogene sediments ('Ældre Tertiær' on Figure 3.6) are dominated by Paleocene, Eocene and Oligocene clays. In the deep well Aabenraa-1 (DGU no. 160.101), the clays attain a total thickness of close to 160 m.

Neogene sediments

The Miocene formations have been subject to intense investigation during the last 25 years mainly because of the aquifer potential of the sandy formations (e.g. Rasmussen et al., 2010). The mapped formations within the study area can be seen in the Tinglev boreholes to the left on Figure 3.7:

The Ribe Group includes the Vejle Fjord, Billund, Klintinghoved, Bastrup, Arnum og Odderup Formations from the Lower Miocene. Three cycles with varying dominance of clay and sand are found. The sediments were deposited in delta systems that were prograding from north to south. The Ribe Group has a total thickness of up to 200 m or more.

- The Vejle Fjord Formation (VFF) consists of mainly dark brown, clayey silt and occasionally with thin lamination of grey sand and silt. The sediments of the VFF were deposited in a brackish to full marine environment and are expected to be around 30 m thick.
- The Klintinghoved Formation (KF) consists of dark brown, silty clay with intercalated layers of sand. The sand is homogeneous or finely laminated. KF was deposited in a storm and tidally influenced marine environment. KF attains thicknesses of up to 100 m.
- The Bastrup Formation (BF) is dominated by grey sand with occasional gravel and occurrences of clay. The sand is mainly quartz with mica minerals. The depositional environment was deltaic and fluvial with point bars and channels. BF is up to 25 m thick.
- The Arnum Formation (AF) consists of dark brown, silty clay with numerous thin layers of shell-containing silty sand layers. The thin sand layers can have a high content of heavy minerals and glauconite. The AF is deposited in a deep, full marine environment. AF interfingers with the sandy Bastrup and Odderup Formations, but can attain a thickness of up to 50-60 m.
- The Odderup Formation (OF) consists of fine to coarse sand with thin clay layers. OF is subdivided into two members, the Stauning and Fasterholt Members, where the Fasterholt Member contains coal layers. However, this member is not expected to be found in the study area. The formation is quartz rich with mica and occasionally heavy minerals. The OF was deposited in a coast/coastal plain environment. The thickness varies but is expected to be up to or more than 50 m.

The Maade Group is from the Middle and Upper Miocene and includes the Hodde, Ørnhøj, Gram and Marbæk Formations. The total thickness is expected to be varying in the study area with thicknesses of occasionally over 100 m.

- The Hodde Formation (HF) is a brown, organic rich silty clay with thin sand lenses. The upper parts consist of laminated, silty clays with glauconite, while the basal part of the formation consists of a gravel layer. HF is deposited in a full marine environment with the basal gravel layer representing the initial transgression. The thickness of the HF is expected to be around 25 m.
- The Ørnhøj Formation (ØF) consists of green and brown clay with a high clauconite content deposited in a marine environment. The expected thickness is up to 5 m.
- The Gram Formation (GF) consists of predominantly dark brown clay with an increasing silt content towards the top. In the upper part, thin sand layers occur. Concretions of siderite are numerous, and the pyrite content is high. The GF is deposited in a full marine environment. The GF is expected to be up to around 100 m thick.
- The Marbæk Formation (MF) is dominated by white to reddish, fine- to medium-grained, mica-rich sand with a few thin silt and coarse-grained sand or gravel layers.

The sand beds show parallel lamination. The pyrite content is very high. The formation was deposited in a storm-dominated marine environment. The expected thickness is up to around 10 m.

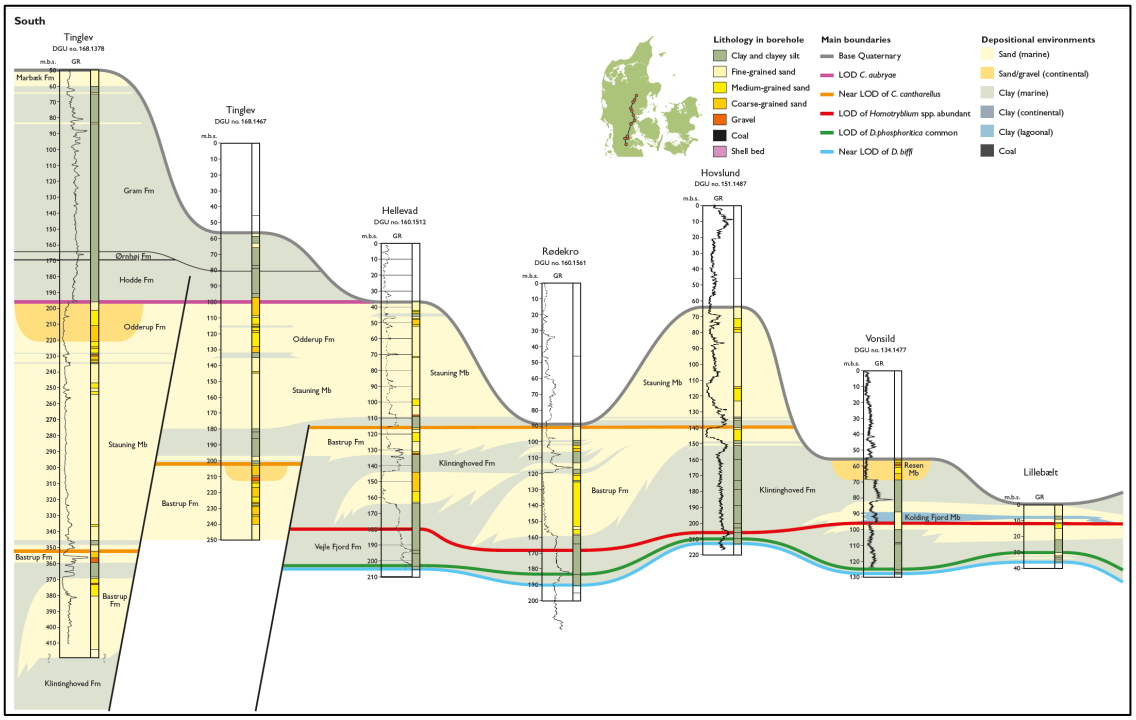

Figure 3.7. Log correlation panel from Piasecki & Rasmussen (2010). The panel shows the seven southernmost boreholes from Tinglev (left) to Lillebælt (right), see the insert map. Note that the elevation of the boreholes is arranged relative to top Odderup Formation and top Bastrup Formation. The faults of the Tønder Graben are illustrated by to sub-vertical lines intersecting the succession.

The top of the Miocene sediments represents the surface of the pre-Quaternary succession, and as illustrated on Figure 3.6, intense erosion and deformation has formed the surface.

3.3.2 Quaternary sediments

In the southern part of the Jutland peninsula traces of four glaciations and three interglacials have been found, but within and close to the study area, sediments from only two glaciations (Weichselian, Saalian) and one interglacial (Eemian) have been identified with certainty. The glacial sediments consist mostly of tills and meltwater sand/gravel while the sediments from the interglacials consist of marine and freshwater sandy and clayey sediments. In addition to this, organic rich freshwater sediments from the Holocene have also been found.

During the Saalian glaciation three large ice advances are known (Figure 3.8). 'The Norwegian Ice Advance' from the north was the oldest, and a sandy and quartz-rich till was deposited (Houmark-Nielsen, 2011). The Drenthe advance from north-east deposited coarse meltwater sediments and tills with a Swedish provenance, but according to Sjørring & Frederiksen (1980), local ice advances from north-westerly directions can be found. Finally, the Warthe advance came from east/south-east resulted in deposition of clayey, quarts-poor, and calcareous tills with a Baltic provenance.

The Eemian interglacial is represented in boreholes in Tinglev (e.g. borehole DGU no. 168.16), where molluscs confirmed a marine Eemian age (Ødum 1933; see Sandersen & Jørgensen, 2015). Additional findings of marine sediments at deeper levels could indicate the presence of older interglacial sediments around Tinglev. The interglacial sediments are only found occasionally pointing to former presence of fjords allowing narrow marine incursions into the glacial terrain (Sandersen & Jørgensen, 2015).

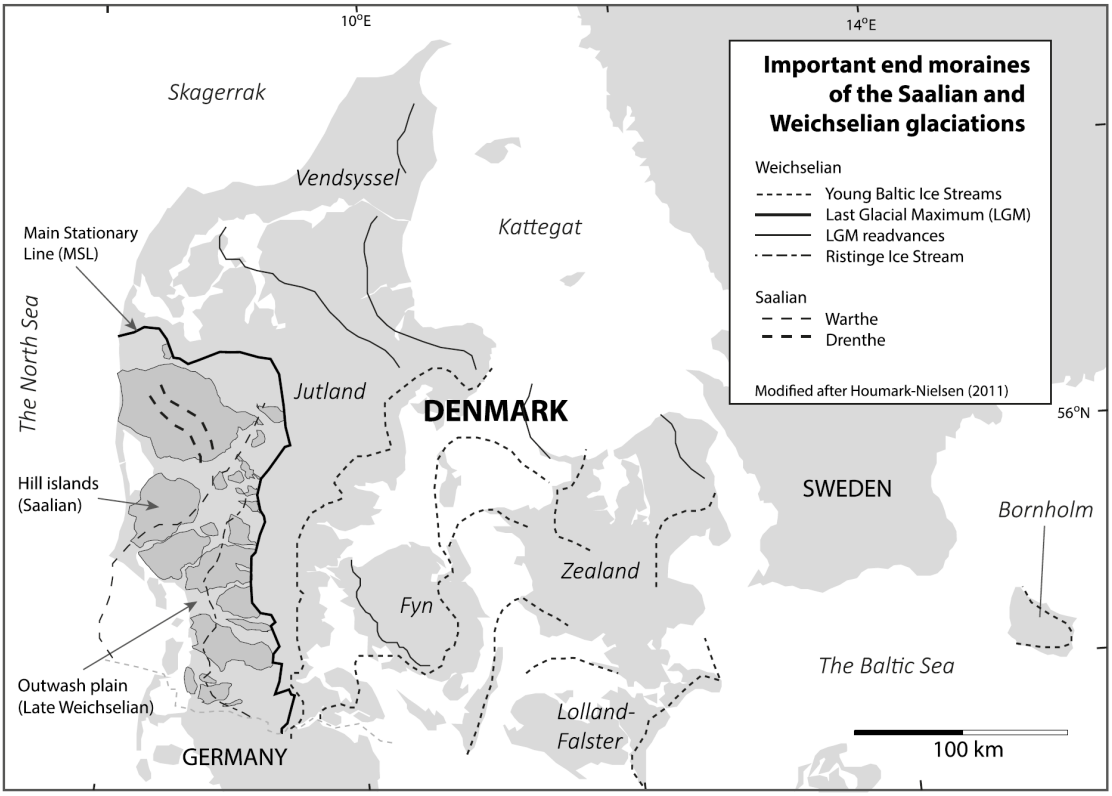

Figure 3.8. Distribution of Saalian and Weichselian ice advances and moraines. From Sandersen & Jørgensen (2022); modified after Houmark-Nielsen (2011).

As shown on Figure 3.8, the LGM advance in the Late Weichselian reached the MSL, and only one earlier ice advance, the Ristinge Ice Stream, is believed to have reached farther west than the MSL largely based on geomorphological observations of the Saalian hills and of irregularities on the Weichselian outwash plain (Houmark-Nielsen, 2007; 2011). However, as mentioned previously, later interpretations of the outwash plain topography have found that the irregular terrain on parts of the Tinglev outwash plain is caused by deglaciation-induced reactivation of faults in the Tønder Graben (Sandersen & Jørgensen, 2015). These findings therefore question the westerly extent of the Ristinge Advance in the Bylderup-Bov/Tinglev area. No sedimentological observations of a more westerly ice margin than the MSL have been found in this part of Jutland (e.g. Kolstrup & Havemann, 1984).

3.3.3 Buried valleys

Buried tunnel valleys were created underneath the Pleistocene ice sheets by high-pressure meltwater erosion (Jørgensen & Sandersen, 2006), whereas other valley-like forms can be created as depressions or as other types of erosions into the substrate. Valley erosions are

particularly important in relation to groundwater flow and vulnerability because they may be eroded deep into the subsurface, thereby creating possible pathways for groundwater transport between shallow and deep aquifers (Sandersen & Jørgensen, 2003, 2016).

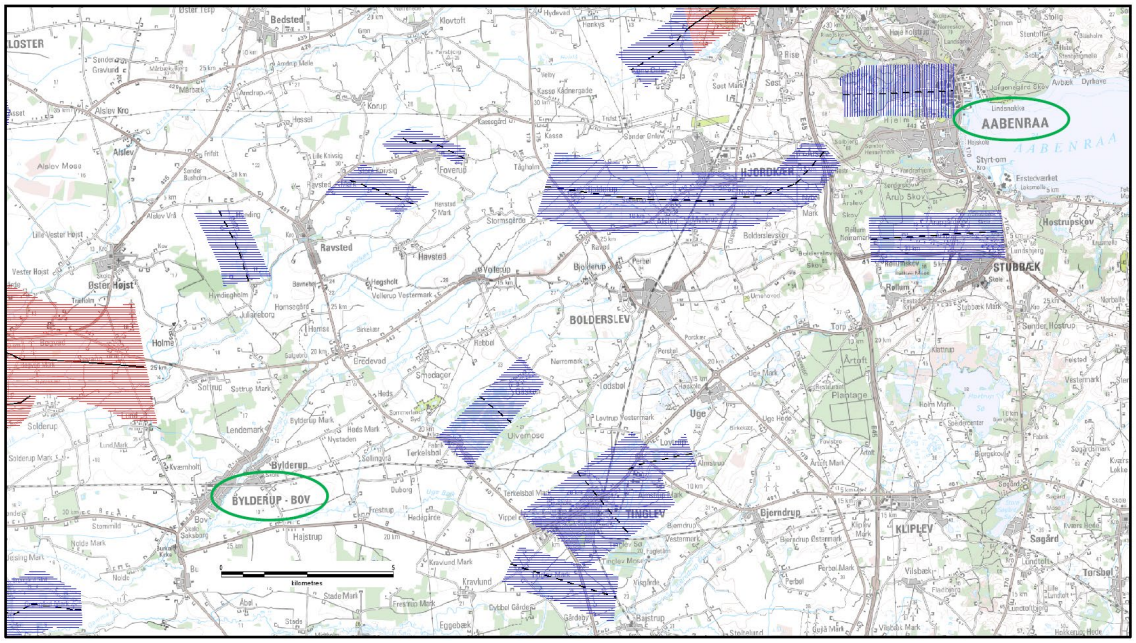

Figure 3.9. Mapped buried valleys as of 2021. Red polygons are well-documented buried valleys, whereas blue valleys are weakly documented. The map is based on data from www.buriedvalleys.dk. The town of Bylderup-Bov and the city of Aabenraa are marked with green. Compare with Figure 1.1.

In and around the study area a few buried valley structures have been mapped (Figure 3.9; Sandersen & Jørgensen, 2016). The interpretation uncertainty is varying because in some cases the presence of the valleys is not supported by independent datasets, and in other cases the presence of valleys is ambiguous because of a high degree of geological complexity and because of the challenges for the geophysics to resolve the geological variations.

3.3.4 Glaciotectonics

Apart from the sandy outwash plains and the hills bordering the Aabenraa area, the Weichselian glaciation has not directly contributed to the sedimentary succession within the Bylderup-Bov model area. Glaciotectonic deformations and glacial deposits within the area must therefore be related to earlier glaciations, most likely from the Saalian and the preceding Elsterian glaciation. Glaciotectonics is already known from several areas in the region, for instance in the Tønder area (Jørgensen et al., 2012; 2014), north of the Bylderup-Bov model area (Sandersen et al., 2021), and in the Eastern North Sea (Andersen et al., 2005; Andersen & Pedersen, 2025).

Figure 3.10 shows two profiles through the glaciotectonic complex at Tønder west of the Bylderup-Bov model area. From the lowermost panel, it can be seen that the glaciotectonic deformations reach as deep as 200 m b.s.l., or even more. It also appears as if the low-resistive Miocene clay in the upper part of the Miocene succession to the right (dark blue colour) has been deformed and broken up into isolated and irregular low-resistivity blocks

(see between 15,000 and 25,000 m). Farther west, Andersen & Pedersen (2025) found that the basal décollement surface of the Fanø Bugt Glaciotectonic Complex developed in the fine-grained sediments of the Arnum Fm (Early Miocene) whereas the upper décollement surface developed in the fine-grained sediments of the Hodde Fm (Middle Miocene).

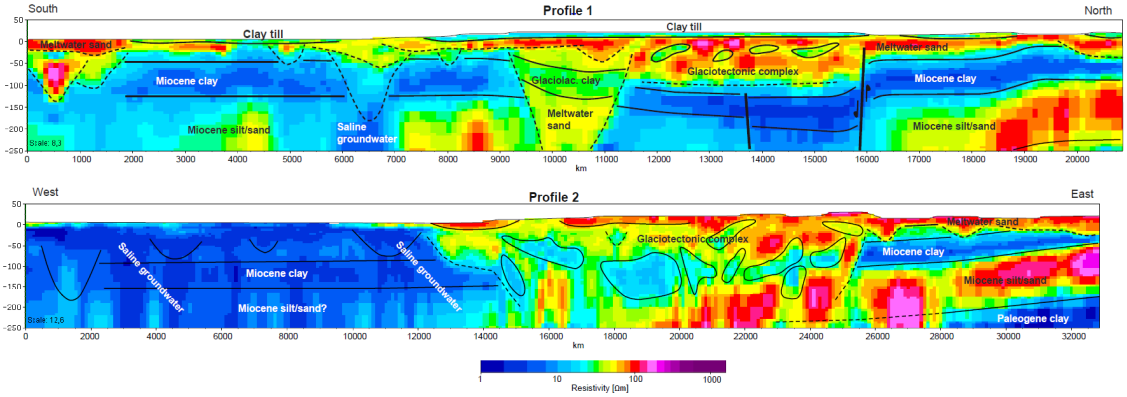

Figure 3.10. The glaciotectonic complex in the Tønder area. Two profiles through a SkyTEM 3-D resistivity grid. From Jørgensen et al. (2012).

Figure 3.11 shows a profile through the uppermost 70 m of the sedimentary succession north of Bylderup-Bov. Deformed Quaternary clays are seen along the profile, pointing to a glaciotectonic push from northerly directions. The sediments appear to be disturbed down to 50 m b.s.l. and probably deeper (Sandersen et. al., 2021).

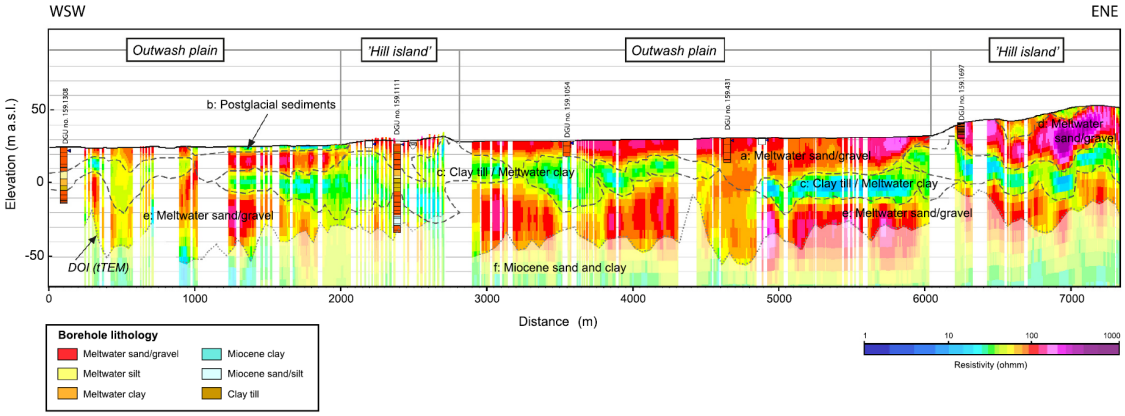

Figure 3.11. A WSW-WNW cross-section through tTEM data and boreholes at Bolbro north of the Bylderup-Bov model area. From Sandersen et al. (2021).

3.4 Geological and hydrogeological considerations

Before starting the work on the 3D geological model, it is important to discuss geological and hydrogeological issues that may have an importance for the transport of groundwater in the study area.

As seen in the preceding sections, the sedimentary succession is expected to be structurally influenced by a series of tectonic movements within the Tønder Graben. The tectonic history

of the graben is long, and we know that the faults have been reactivated as late as the Early Holocene, which is seen as deformations of the present-day topography. Depressions in the topography above the Tønder Graben are highlighted by the presence of bogs (Figure 3.1), but more obvious is the dark blue area highlighted with black arrows in Figure 3.12. This is a large NW-SE oriented, rectangular area with very shallow groundwater which is located right above the central part of the Tønder Graben. The sandy and gravelly outwash plain would be expected to be well drained, but the graben structure obviously has an impact on the present-day drainage.

Glaciotectonism is, as previously mentioned, well-known in the region. Large deformations of the sedimentary successions are found in several areas around the study area. Here the deformations reach depths of more than 200 m resulting in the creation of highly complex Quaternary geological architectures in large areas. In and around the Bylderup-Bov study area, boreholes show that the base of the Quaternary is found at varying depth – occasionally down to more than 200 m below sea-level. In addition to this, it has been found that buried valley structures have been carved into the subsurface by glacial meltwater underneath the ice sheets during the Pleistocene glaciations. Because these structures can erode through aquifers and confining layers, connections may have been created between aquifers, thereby enabling groundwater transport from shallow to deep layers or vice versa.

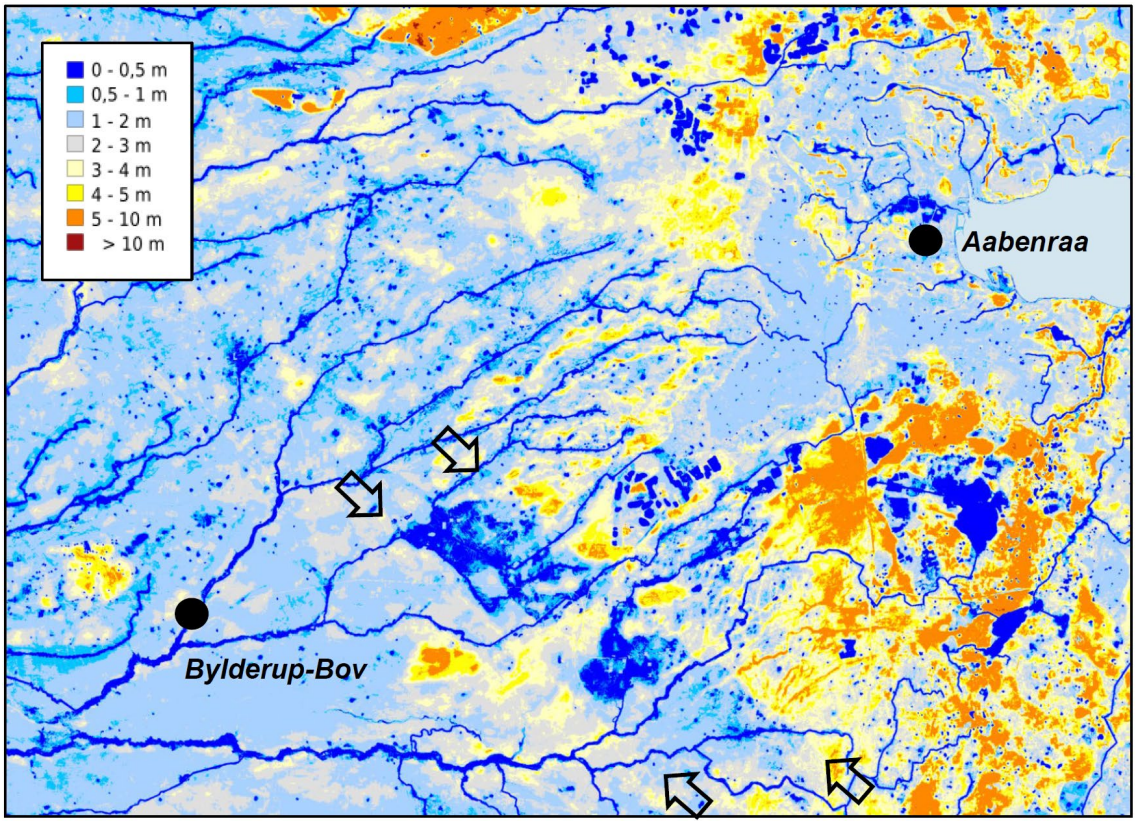

Figure 3.12. Near-surface groundwater scenario; 10 m grid – depth to groundwater; summer (The Danish Agency for Climate Data; hipdata.dk; see Henriksen et al., 2020). The figure shows approximately the same area as on Figure 3.2. Black arrows outline a rectangular area with very shallow groundwater.

The two different types of large-scale deformations found in the area - glaciotectonics and deep tectonics - combined with deep erosions, result in not only a high subsurface complexity, but also a high degree of geological uncertainty. Added to the uncertainties are also known ambiguities in the age of the sediments in several borehole descriptions. The above mentioned represent important issues to map and investigate, but at the same time they also represent challenges for the geological modelling. A high geological complexity produced by large-scale faults, erosions, and deformations disrupts the common conception of the subsurface consisting of laterally extended layers in a layer-cake setting.

The overarching aim of the Blue Transition DK-1 pilot is to try to sketch possible solutions to climate-related groundwater challenges by means of both geological and hydrological mapping and modelling, and hopefully provide answers to main research questions such as:

- To which extent do the variations of the present-day topography affect the drainage of surface water and shallow groundwater?
- To which extent does the complex geological setting affect the drainage of the shallow groundwater in Bylderup-Bov?
- To which extent does the complex geological setting impact the exchange of groundwater between deep and shallow aquifers?

3.4.1 Challenging the existing geological model interpretations

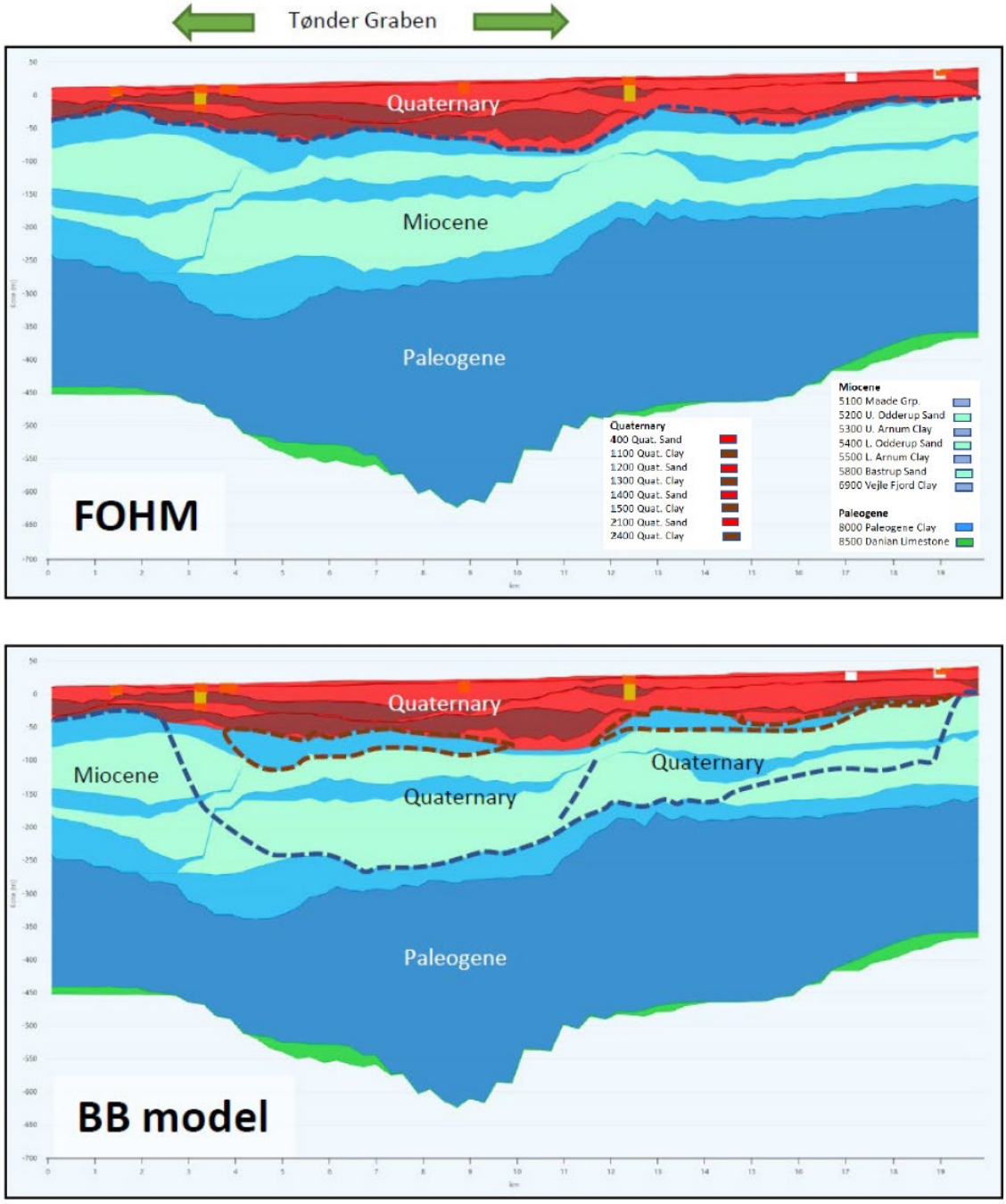

Figure 3.13. Conceptual geology of the FOHM vs. the Bylderup-Bov model (BB)

The National Hydrostratigraphic model called 'FOHM' is layer-cake model based on a merging of local geological and hydrostratigraphical models (Miljøstyrelsen, 2020).

In Figure 3.13, the upper profile shows the FOHM layers and the corresponding layer boundary names along a SW-NE transect through the Bylderup-Bov model area. The profile shows, that the Tønder Graben is visible in the deep parts of the FOHM model, where the top of the Danian limestone (green layer) and the Paleogene (dark blue layer) lie considerably deeper in the central parts of the profile. In the Miocene, and Quaternary sediments above, however, the Tønder Graben is only vaguely represented in the form of slightly thicker layers.

Because of the signs in several boreholes that the Quaternary sediments are considerably thicker than the up to 70 m as shown on the upper profile, an alternative conceptual geology was made as a working hypothesis. This alternative conceptual geology is sketched on the lower profile, where the blue hatched lines show a fundamentally different geology with Quaternary sediments within and northeast of the Tønder Graben down to depths of more than 200 m below the surface. This alternative conceptual geology was tested during the geological modelling; see the following text.

4. Data

4.1 Topography and geomorphology

For the geological modelling, a standard Digital Elevation Model (DEM) available via the modelling software GeoScene3D (i-gis.dk; Geocloud) has been used (25 m grid). No detailed analyses of the topography have been made in connection with the modelling. Instead we refer to Sandersen & Jørgensen (2015), where elaborate analyses of a high-resolution DEM have been made.

The geomorphology shown in Figure 3.1 is from Jacobsen et al. (2022).

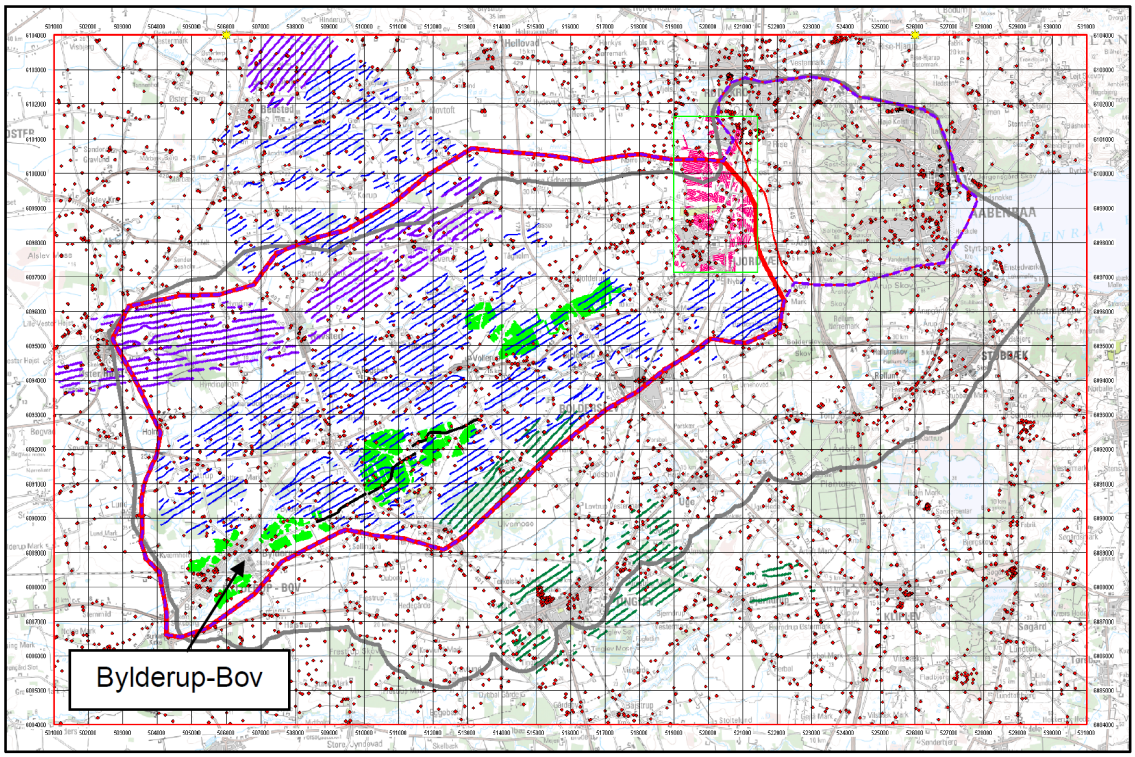

Figure 4.1. Main data used in the geological modelling. Red dots: Boreholes from the Jupiter database. SkyTEM surveys: Dark green lines: Tinglev (2012), purple lines: Ravsted-Bedsted (2012), and blue lines: MST (2024). tTEM surveys: Hjordkær: pale red dots (2024), and Bylderup-Bov: light green dots. Blue Transition seismic: Black line. The shown grid is a one-kilometre grid.

4.2 Borehole data

Borehole data from GEUS' Jupiter Database (Hansen & Pjetursson, 2011) has been accessed in GeoScene3D via Geocloud) and as direct database search via the GEUS webpage (https://data.geus.dk/JupiterWWW/index.jsp). The boreholes are shown in Figure 4.1 as red dots. Figure 4.2 shows boreholes deeper than 75 m, totalling 8 boreholes within the BB model

area. Of these boreholes, two have geophysical down-hole logs and one of these two also have biostratigraphical analyses of sediments samples (boreholes DGU no. 159.1444 and 160.1378). Some of the deep boreholes outside the BB model area shown in Figure 4.2, however, have logs and biostratigraphy that have contributed to the geological interpretations within the BB model area.

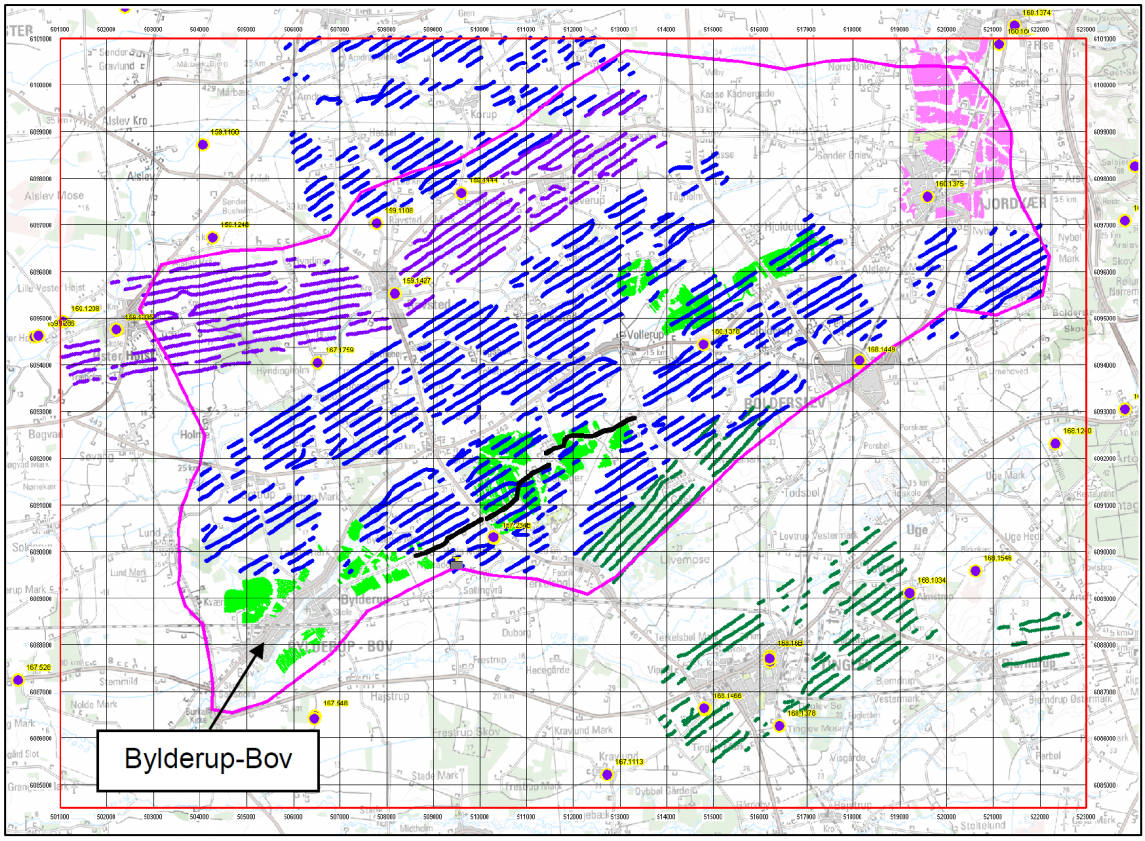

Figure 4.2. Boreholes deeper than 75 m (purple dots) and geophysical data points (see Figure 4.1). Data from the GEUS Jupiter database. The shown grid is a one-kilometre grid.

4.3 Geophysical data

4.3.1 SkyTEM and tTEM

Data from the following TEM surveys has been used (see Figure 4.1):

SkyTEM:

- Tinglev (Rambøll, 2012a): The survey was carried out in 2011 and data processing performed by Rambøll in 2012. The SkyTEM models were downloaded from the GEUS National geophysical database (GERDA).
- Ravsted-Bedsted (Rambøll, 2012b): The survey was carried out in 2011 and data processing performed by Rambøll in 2012. The SkyTEM models were downloaded from the GEUS National geophysical database (GERDA).

- MST (SkyTEM 2023): The survey was carried out in 2023 and the processing was performed by Niras (Niras 2024). The SkyTEM models were delivered directly from the Danish Environmental Agency (MST; Miljøstyrelsen) to GEUS.

tTEM surveys

- Hjordkær: Survey data from 2024 downloaded from the GEUS National geophysical database (GERDA).
- Bylderup-Bov (Aarhus University, 2025): tTEM survey performed by Aarhus University 2023-2024.

4.3.2 Seismic data

Oil exploration seismic and 'groundwater seismic'

Only two seismic profiles shown in Figure 3.4 and Figure 3.6 have been used as background data for the geological interpretations. These two seismic lines and all other lines lie outside the area covered by the Bylderup-Bov model and have therefore not been used in the 3D modelling.

The Blue Transition seismic survey

The seismic lines performed as a part of the Blue Transition DK-1 is shown on Figure 4.1, Figure 4.2 and Figure 4.3 as black lines. Figure 4.3 is an enlargement of the southwestern part of Figure 4.2.

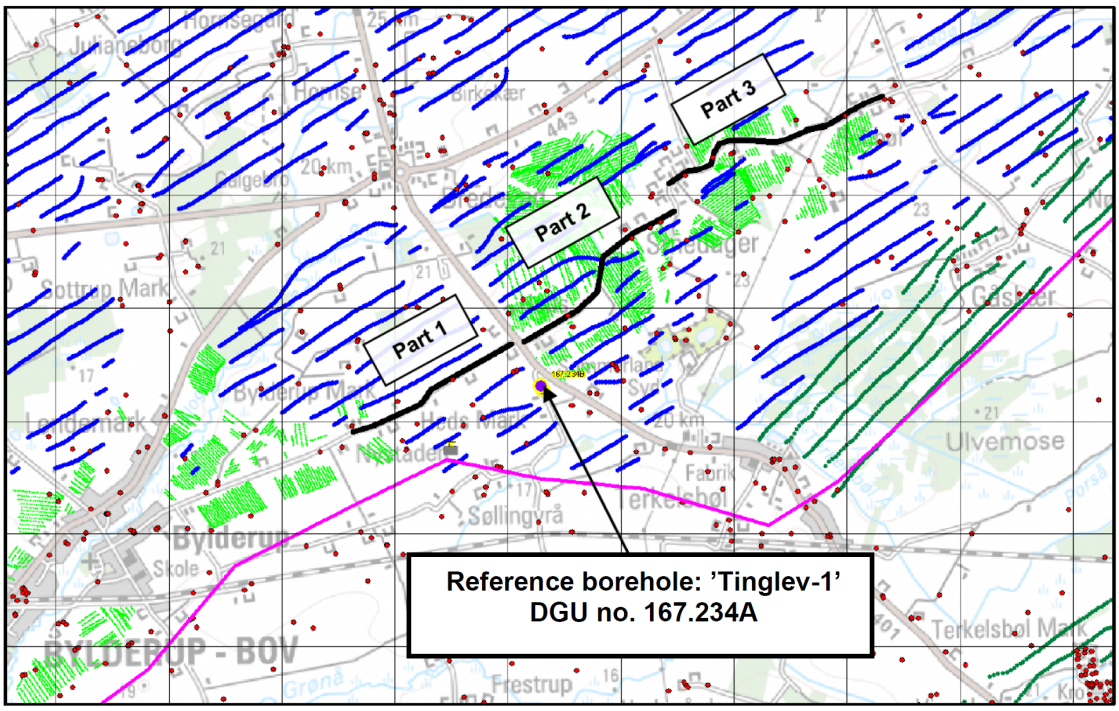

Figure 4.3. The three parts of the Blue Transition seismic survey marked with black lines. The reference borehole 'Tinglev-1' is used for the interpretations. Boreholes from the Jupiter database are shown as small red dots. This figure is an enlargement of the southwestern area shown in Figure 4.1. The shown grid is a one-kilometre grid.

The reflection seismic survey was carried out by LIAG during 9 days in June 2023, applying the high-resolution shear wave technique utilizing a land streamer receiver unit combined

with an Elvis7 microvibrator seismic source (Polom et al., 2013). Due to the specific requirements of the method, the profiling was restricted to operation on paved roads. In the Bylderup-Bov profiling area two independent acquisition setups were used simultaneously to cover the amount of profiling aspired.

Conditions during the survey were good except some noise generated by wind and farming activities. Reflection seismic data processing was carried out by LIAG in 2023, resulting in three profiling segments (Fig 4.1) of 1.5 km, 1.9 km, and 2 km, respectively, with small interruptions between the segments due to local physical conditions. Based on the detailed Root Mean Square (RMS) stacking velocities analysed during data processing, the sections are converted from time to depth domain for final imaging and interpretation. Elevation reference datum (zero m line at the imaged sections) was finally set to 30 m DNN with respect to the highest elevation level along the three profiling segments. Resulting section trace interval (Common Midpoint interval, CMP) of the profiling segments is 0.5 m, the maximum depth penetration reached ca. 150-200 m below surface by a vertical structure resolution of 0.5-2 m.

Data interpretation was carried out by LUH and LIAG referenced by the deep borehole Tinglev-1 (DGU no. 167.234A) and some shallow boreholes (< 50 m depth) along the profiling (Figure 4.3).

4.4 Structural data

The current knowledge of the deep faults in the Danish area mainly comes from the seismic data collected in relation to oil/gas exploration in the last decades of the 1900's. Of special interest for the Bylderup-Bov model are the faults of the Tønder Graben which penetrate the Top Pre-Zechstein (Vejbæk & Britze, 1994) and the Top Chalk Group (Ter-Borch, 1991; see Figure 3.3). A vectorization of these faults shown in Figure 3.5 is from Sandersen & Jørgensen (2015).

4.5 FOHM model interpretation data

The FOHM layers contribute to the Bylderup-Bov/Aabenraa modelling as boundary conditions outside the modelled areas. The FOHM interpretation points have been merged with relevant interpretation points of the Bylderup-Bov/Aabenraa model layers and eventually interpolated to form horizontally coherent layer boundaries for a larger area (see later sections).

The FOHM layer interpretation points have been downloaded from the GEUS website: https://data.geus.dk/geusmap/?mapname=fohm#baslay=baseMapDa&optlay=&extent=-81074.07407407399,5902208.333333333,1123074.0740740742,6547791.666666667.

5. 3D geological modelling

5.1 Focus

As described in the preceding, the complex geological setting due to presence of faults, glaciotectonics, and deep erosions, combined with ambiguous borehole data pose challenges for the 3D geological modelling. The challenges arise mainly from the anticipated difficulties in modelling the geological complexities to a sufficient degree of detail for the subsequent hydrological modelling. To fulfil the aim of the project, the physical framework for the groundwater transport should be modelled as detailed as possible with the given data, modelling tools, and economy.

Because of the high groundwater levels in the study area, the focus described in the DK-1 pilot is on geology and groundwater in the uppermost 50 m. However, as it is expected that the geological complexity in the Bylderup-Bov area may result in a larger transport of groundwater between deep and shallow aquifers than hitherto assumed, a modelling of deeper layers has proven necessary. The modelling activity has therefore been expanded to a greater 3D volume than previously planned.

5.2 General model choices

The geological modelling of both the Bylderup-Bov (BB) and the Aabenraa model (AA) is performed using the GeoScene3D software from i-gis (i-gis.dk). Although a traditional layer-cake modelling is not optimal for modelling a complex geological setting, this has been chosen over voxel modelling and combined layer/voxel modelling, because the number of layers could be kept fairly low. In addition to this, voxel modelling and combined modelling alternatives were not considered viable within the given budget.

It has been chosen to use the hydrostratigraphic layers defined in the FOHM model, in order to ease merging with the Bylderup-Bov/Aabenraa models. The layers of the FOHM model act as a boundary model outside the Bylderup-Bov and Aabenraa models (see Figure 1.1). The advantage of this is, that existing interpretations outside the new model areas can be used to create one single model covering a large area.

The layers of the new geological models should therefore contain layers similar to the layers of the FOHM model. Niras and GEUS have coordinated the modelling and chosen adequate model layer names to align with FOHM for all modelled layer boundaries. However, as the new models introduce new geological interpretations based on new data, elevation changes of the layer boundaries along the border between the models can be expected (see later description).

The Bylderup-Bov model-interpretations are based on geology and therefore we consider it as a geological model per se. But because simplification of the layer succession has been

necessary and because of the merging with the hydrostratigraphic layers of the FOHM model, the resulting model can be considered as a hydrostratigraphical model showing aquifers and aquitards.

5.3 Model setup

5.3.1 Profiles

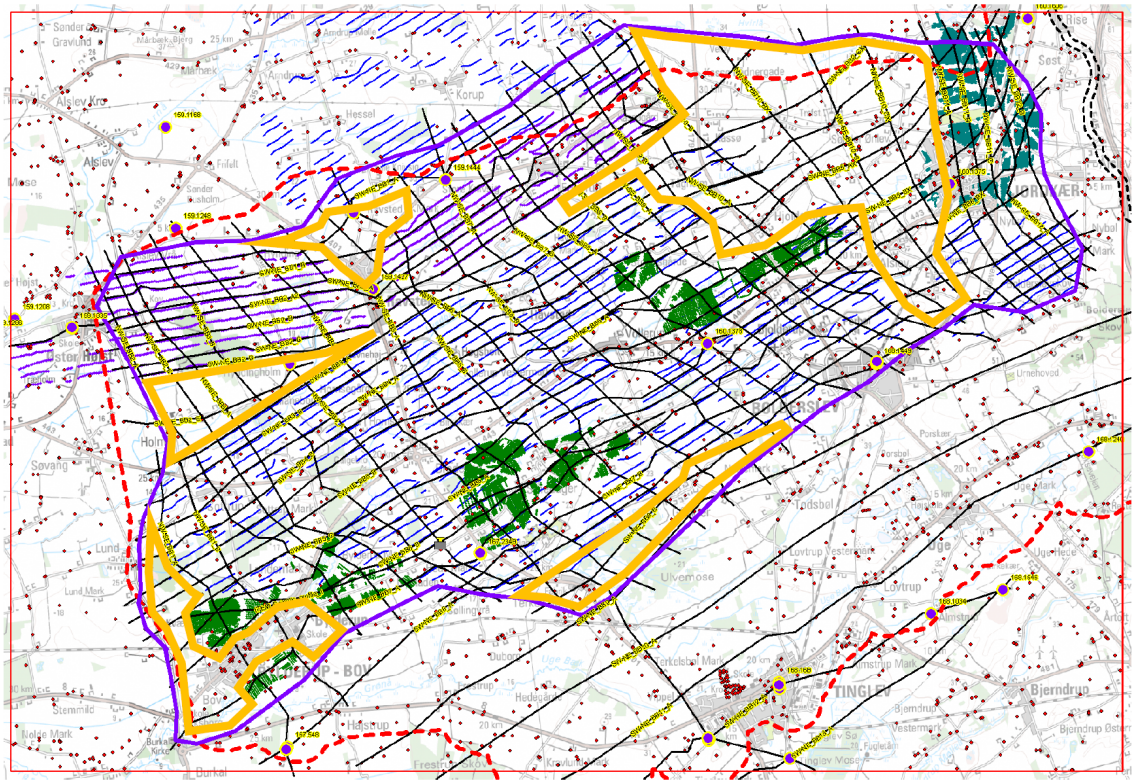

Figure 5.1. Profile grid of the Bylderup-Bov (BB) model (black lines SW-NE and NW-SE). Boreholes are seen as red dots, SkyTEM as thin blue and purple lines, and green areas are tTEM data. Thick purple polygon represents the outline of the BB model, and Orange polygons are areas without geophysical data. See text for further explanation.

The Bylderup-Bov geological model (BB model) is built around 60 profiles of varying length, generally oriented SW-NE and NW-SE (Figure 5.1). The SW-NE profiles follows the SkyTEM data lines, whereas the NW-SE profiles are roughly perpendicular to the SkyTEM lines. On Figure 5.1 the BB model area is outlined by a thick purple polygon. The profiles southeast of this area are only meant as support for the modelling and are not included in the BB model.

The profiles are named with prefixes SW-NE or NW-SE dependent on orientation, and profile numbers on NW-SE profiles are low to the NW and high to the SE, and on the SW-NE profiles they are low to the SW and high to the NE – for instance the profile 'NW-SE_BB1_A' is the south-westernmost profile, while profile 'SW-NE_BB1_A' is the north-westernmost profile.

On Figure 5.1, orange polygons delineate areas without TEM data. In these areas, the BB model interpretations are based on a few shallow boreholes and relies heavily on interpretations in neighbouring areas with more data.

The geological interpretations are generally made along these model profiles. The profiles have a data buffer of 100 m for the boreholes, 50 m for the SkyTEM, and 15 m for the tTEM, meaning that data from a zone of two times the buffer on each side of the profile are included. The distance between the profiles are typically between 200 and 1000 m in the data dense areas and between 400 and 1400 m in the data poor areas (orange polygons). Due to time constraints, geological interpretations outside the profiles have not been made.

5.3.2 Layer sequence

Figure 5.2 shows a conceptual geological profile sketch SW-NE through the BB model area based on preliminary interpretations. The conceptual geology takes faults, deformations, and the deeper position of the Quaternary sediments inside and east of the Tønder Graben into account (see Figure 3.13). Apart from the Maade Group layers, the deeper Miocene layers are is not well resolved in the SkyTEM data, and individual sand and clay layers cannot be defined. The same can be said about the deep parts of the Quaternary sediments, where the boundary to the Miocene below is uncertain, because the high-resistive 'Quaternary' sediments may be Miocene. Lithological details can be obtained from borehole data, but only a few boreholes are available. This means that the interpretation of the bottom of the Quaternary sediments is based on very few data points, and that a precise distinction between Quaternary sandy sediments and Miocene sandy sediments cannot be made.

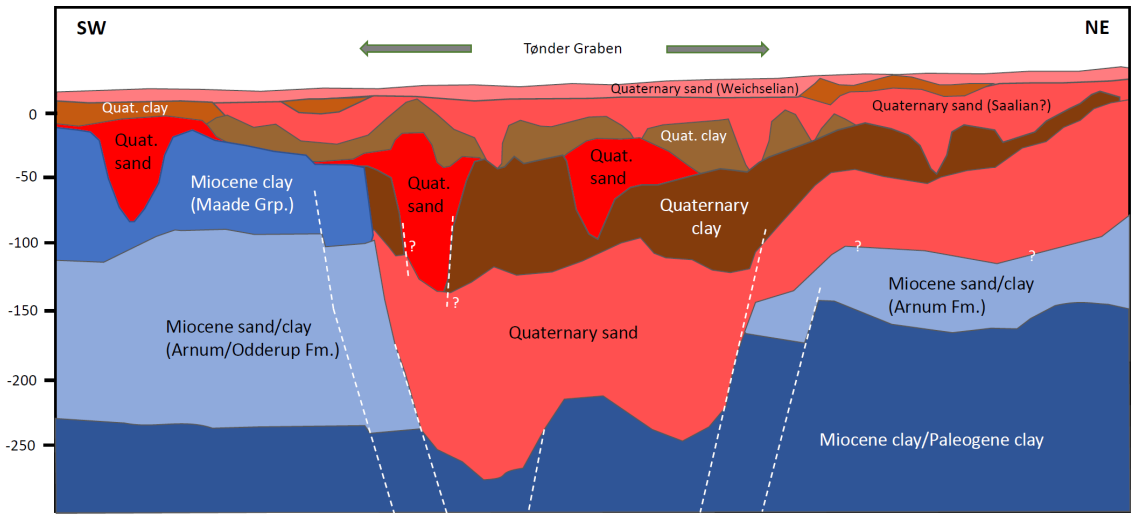

Figure 5.2. Conceptual SW-NE geological sketch across the BB area. White hatched lines denote tentative deep faults. See text for further explanation.

Above the deep, sandy Quaternary sediments in the Tønder Graben we find a fairly thick, but very irregular clay layer, with occurrences of Quaternary sand. Some of these are interpreted as buried tunnel valley erosions. Above, the Quaternary layers alternate between sand and clay where the degree of deformation seems to be less pronounced compared to deeper levels. At the top we find layers of Lateglacial, sandy outwash plain sediments with

patches of Postglacial peat and gyttja in low-lying areas. Because of the patchy tTEM mapping, the bottom of the Postglacial sediments has not been modelled. Instead, a Postglacial layer will be handled in the hydrological model based on current soil maps.

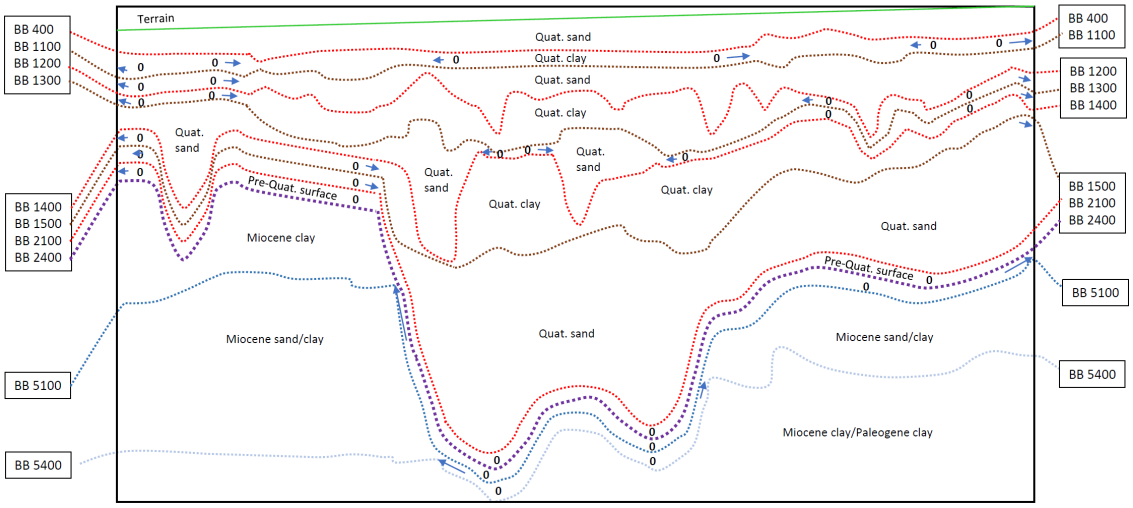

Figure 5.3. Sketch of the BB layer boundaries named with 'BB' followed by the corresponding FOHM layer number (see Table 1). Zeroes inserted above layer boundaries denotes zero thickness (between blue arrows along the profile).

Table 1. Model layer boundaries of the FOHM and the new merged AA/BB-FOHM model.

	Boundary name in FOHM	Boundary name in AA/BB-FOHM	Geology	Layer modelled in: FOHM	AA	BB	Search radius (m) Interpolation
Quaternary	0050_Antropocaen_bund	AA_BB_FOHM_0050_Antropocaen_bund	Bottom of Anthropocene layer		X		200
	0100_Postglacial_tørv_bund	AA_BB_FOHM_0100_Postglacial_toerv_bund	Bottom of Postglacial peat		X		200
	0120_Postglacial_sand_bund	AA_BB_FOHM_0120_Postglacial_Sand_bund	Bottom of Postglacial sand		X		500
	0200_Kvartaer_sand_bund	AA_BB_FOHM_0200_KS_bund	Bottom of glacigenic sand	X			500
	0300_Kvartær_Ler_bund	AA_BB_FOHM_0300_KL_bund	Bottom of glacigenic clay	X			500
	0400_Kvartær_sand_bund	AA_BB_FOHM_0400_KS_bund	Bottom of glacigenic sand	X	X	X	2500
	1100_Kvartær_ler_bund	AA_BB_FOHM_1100_KL_bund	Bottom of glacigenic clay	X	X	X	2500
	1200_Kvartær_sand_bund	AA_BB_FOHM_1200_KS_bund	Bottom of glacigenic sand	X	X	X	2500
	1300_Kvartær_ler_bund	AA_BB_FOHM_1300_KL_bund	Bottom of glacigenic clay	X	X	X	2500
	1400_Kvartær_sand_bund	AA_BB_FOHM_1400_KS_bund	Bottom of glacigenic sand	X	X	X	2500
	1500_Kvartær_ler_bund	AA_BB_FOHM_1500_KL_bund	Bottom of glacigenic clay	X	X	X	2500
	2100_Kvartær_sand_bund	AA_BB_FOHM_2100_KS_bund	Bottom of glacigenic sand	X	X	X	2500
	2200_Kvartær_ler_bund	AA_BB_FOHM_2200_KL_bund	Bottom of glacigenic clay		X		2500
	2400_Kvartær_ler_bund	AA_BB_FOHM_2400_KL_bund	Bottom of glacigenic clay	X		X	2500
Miocene	5100_Maadegruppen_Gram_og_Hodde_Bund	AA_BB_FOHM_5100_MaadeGramHodde_bund	Bottom of Maade Group clays	X		X	5000
	5200_Oevre_Odderup_ODS3_Bund	AA_BB_FOHM_5200_ODS3_bund	Bottom of Upper_Odderup Fm	X			5000
	5300_Oevre_Arnum_ARL3_Bund	AA_BB_FOHM_5300_ARL3_bund	Bottom of Upper Arnum Fm	X			5000
	5400_Nedre_Odderup_ODS2_Bund	AA_BB_FOHM_5400_ODS2_bund	Bottom of Lower Odderup Fm	X			5000
	5500_Nedre_Arnum_ARL2_Bund	AA_BB_FOHM_5500_ARL2_bund	Bottom of Lower Arnum Fm	X			5000
	5700_Klintinghoved_KRL6_Bund	AA_BB_FOHM_5700_KRL6_bund	Bottom of Klintinghoved Fm	X			5000
	5800_Bastrup_BADS5_Bund	AA_BB_FOHM_5800_BADS5_bund	Bottom of Bastrup Fm	X			5000
	6900_Vejle_Fjord_VFL6_Bund	AA_BB_FOHM_6900_VFL6_bund	Bottom of Vejle Fjord Fm	X			5000
Palaeogene	8000_Palaeogen_ler_Bund	AA_BB_FOHM_8000_Palaeogen_Ler_bund	Bottom of Palaeogene clays	X			5000

In Figure 5.3, the BB model layer boundaries with their respective FOHM related numbers are shown in a simplified manner. Apart from the bottom of the '5100' layer (the bottom of the Maade Group Clays), the Miocene succession has not been modelled in the BB model and interpretation points from the FOHM model have been used (see Table 1).

5.3.3 Point interpretation

In GeoScene3D, the geological interpretations have been made using three types of interpretation points: 1) Interpretation points with snap to data, 2) Interpretation points without snap to data, and 3) Supporting points for guiding the gridding (Table 2). For each interpretation point the point type is registered.

Table 2. Interpretation point types used

Point type no.	Point type	Category	Description
1	Interpretation points with snap to data	Interpretation points	Interpretation points for the spatial position of a boundary surface. A snapped interpretation point is attached to a data point in the model space. This will normally be a layer boundary in a borehole but can also be boundaries in a TEM sounding or on a seismic profile.
2	Free interpretation points (no snap to data)	Interpretation points	Interpretation points for the spatial position of a boundary surface, but as opposed to a snapped interpretation point, the free interpretation points are not directly linked to a data point in the model space. Free interpretation points can be used based on data close by or general geological knowledge.
3	Guiding interpretation points	Supporting points	A guiding interpretation point is a free point only used as support for the gridding process. The guiding points are not geological interpretation points per se, and they can be used to form the gridded surface in a pre-defined way or for interpretations in data sparse areas.

However, due to a technical error, the point types have not been properly stored in the points database, meaning that the column 'PointType' should not be used. This said, point types used are predominantly point type 2 in areas with a high data density, and point type 3 typically in areas with low data density.

In connection with performing the interpretations along the geological profiles a qualitative uncertainty assessment of the interpretation is attached to each interpretation point (Figure 5.4).

Table 3. Uncertainty classification for interpretation points (partly based on Høyer et al., 2024 and Sandersen, 2008)

Uncertainty class	Primary rationale	Secundary rationale
0 – Outside category	Points not related to data. Supporting points intended for helping interpolation only.	
1 – Low	Interpretation points linked to reliable borehole Data (with snap)	Interpretation points linked to less reliable borehole data or high quality geophysical data with well-resolved information about the layer boundary, consistent with the conceptual geological model.
2 – Intermediate	Interpretations in areas with less well-resolved information from geophysical data, but in areas where the conceptual model and/or neighbouring data support the interpretations (no snap).	Interpretations in areas far from neighbouring data, but with low geological complexity and a strong conceptual model.
3 – High	Interpretation points based solely on the conceptual model and data from greater distances (no snap).	Points placed in areas with less reliable data

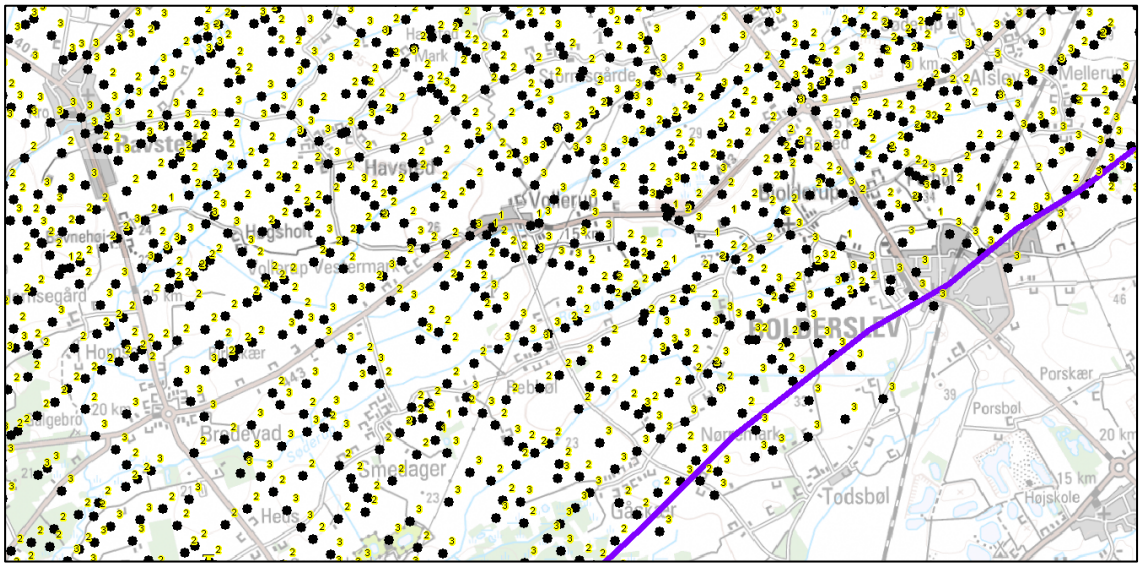

Figure 5.4. An example of uncertainty classes related to interpretation points.

5.3.4 Merging of interpretation points and interpolation of model layers

In order to produce one geological model for the area covered by the hydrological model area, the Bylderup-Bov and the Aabenraa models need to be merged with the FOHM model. As described in the sections above, it has been secured that all three models use the same layer terminology, meaning that the final model will include a merger of interpretation points for each boundary layer for all three models.

The procedure has been as follows:

- A copy of the interpretation points of all layers in the FOHM model inside the current scene extent is exported. (The GeoScene3D 'scene-extent' is the extent of the active model area)
- Within this copy, FOHM interpretation points for all layers inside the AA and BB model areas are deleted – except for the layers that have not been modelled in the AA and BB models
- Interpretation points from the AA and the BB models inside the individual model boundaries were copied and merged into the same point database

The individual layers in the merged interpretation points database are now interpolated using GeoScene3D's Interpolation Wizard. All points of all layer boundaries (surfaces) are gridded with Inverse Distance Weighting (IDW) in 25 m grids. The settings for the interpolation have been chosen to follow the Danish EPA ('Miljøstyrelsen') general settings used in the FOHM model; see Table 4 and Table 5. The terrain Digital Elevation Model (DEM; 25X25 m grid) is accessed via GeoScene's Geocloud.

Table 4. Interpolation settings

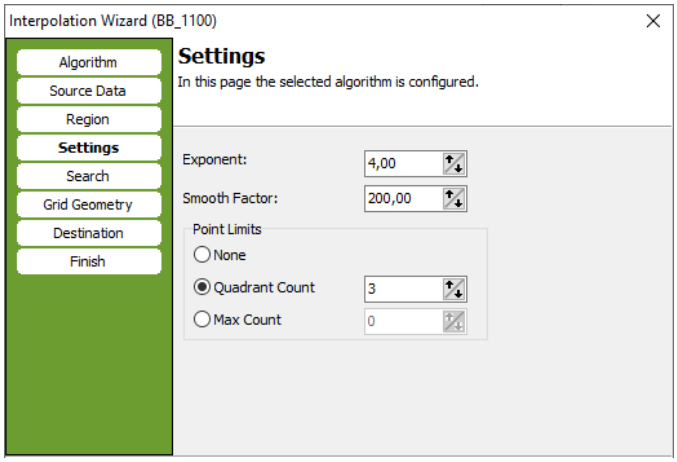

Table 5. Grid geometry and Scene extent

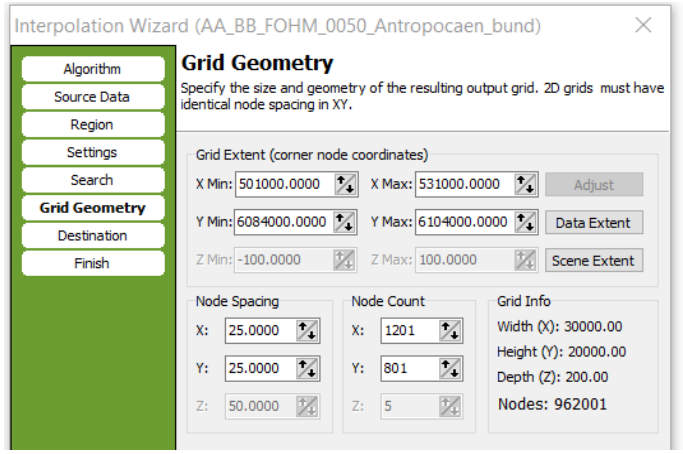

The interpolation led to minor adjustments in the interpretation points database and required re-interpolation:

- Artefacts were created in the interpolation of the uppermost layers of the AA model. This was solved by decreasing the search radius (see Table 1).
- The layer boundary ‘2400’ had a few unusual peaks in the area between the AA and the BB models. This was solved by deleting four FOHM model points, causing the peak within this small area (with sparse data)
- Interpretation points of the layer ‘400’ just northeast of the AA model was creating disturbances inside the AA model area. This problem was first attempted to be solved by deleting FOHM points of layer ‘400’ northeast of the AA model area. This was however not enough. Subsequently, points above terrain were added along ridges in the central part and along the north-eastern border of the model area. These specific points were given a point-type ‘7’ in the point database.

5.3.5 Grid adjustments

Once the grids have been made, an adjustment of the grid surfaces is performed using the Grid Adjustment tool in GeoScene3D. This adjustment is based on the defined layer succession and thereby the grid order (Table 1), minimum and maximum vertical distance between grids, and the maximum allowed grid adjustment. The grid adjustment produces a new set of grid files named with the postfix ‘Adjusted’ together with a set of grids containing the amount of adjustment for each grid, and a set of isopach grids for the resulting layer thicknesses.

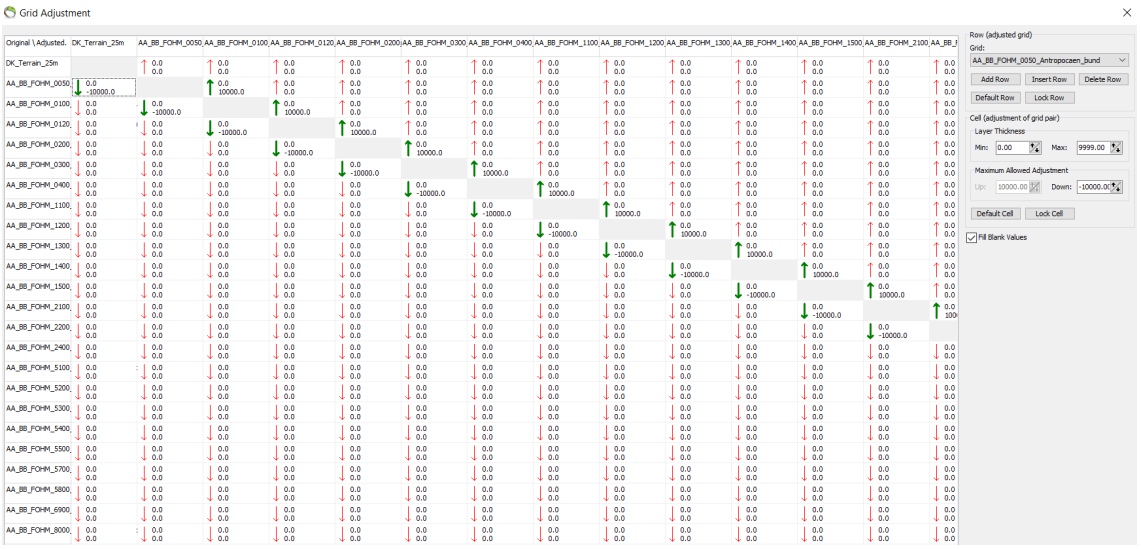

Figure 5.5. Grid adjustment dialogue box example.

The GeoScene3D Grid Adjustment dialogue box is shown in Figure 5.5. The example shows the initial setup, before defining details of the final grid adjustment of the model.

In the AA/BB-FOHM model, the minimum thickness of individual layers is set to 0.0 m. The surfaces Terrain (DK_Terrain_25m) and the Top pre-quaternary (layer 2400) are fixed and all other layers are adjusted up or down with respect to these layers. For further details, see the GeoScene-3D project.

6. Results

6.1 Geological interpretations of geological and geophysical data

6.1.1 TEM mean resistivity slices

A 3D gridding has been made based on the SkyTEM survey data in and around the BB model area, and in the following, selected mean resistivity slices at different elevations are shown and described. The slices give a birds-eye view of the area and visualizes large scale resistivity variations and trends. Mean resistivity slices from +20 to -200 m a.s.l. are shown in the following, starting from the top.

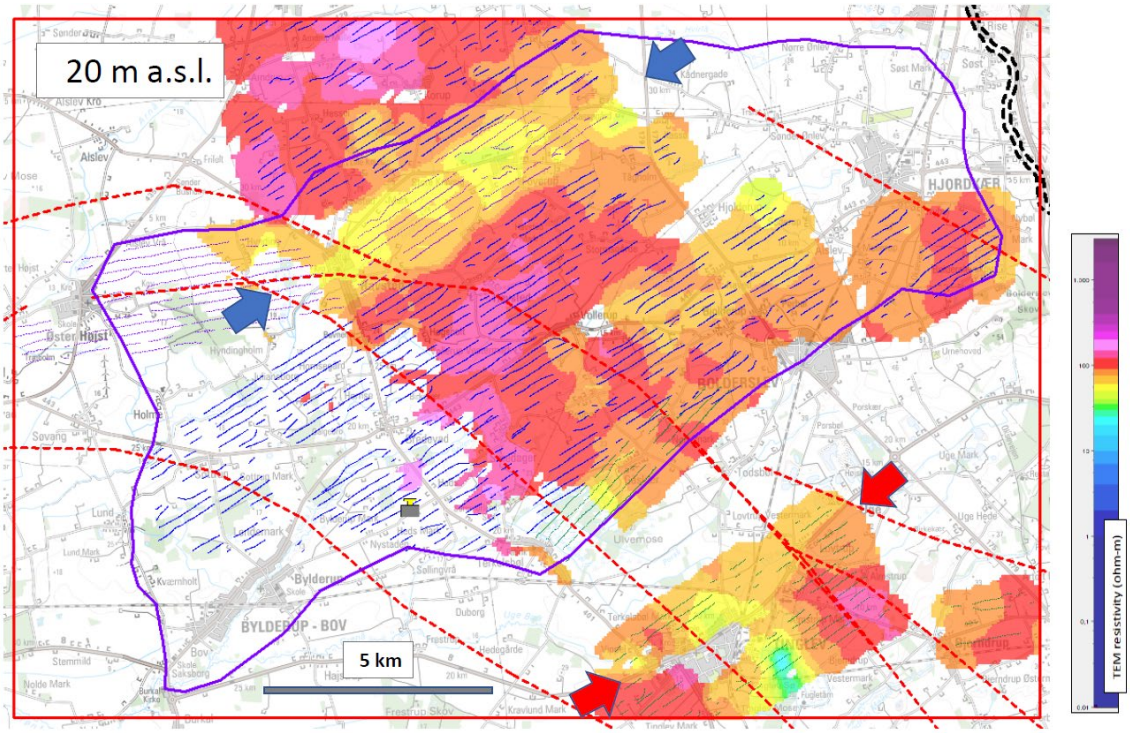

Figure 6.1. Mean resistivity slice 20 m above sea-level (a.s.l.). Red hatched lines show the approximate locations of deep faults. Purple line marks the BB model area. Arrows: see text for explanation.

Slice 20 m a.s.l (Figure 6.1) shows generally high resistivities (red/orange colours) with smaller areas of slightly lower resistivities (yellow/greenish colours). The lower resistivities tend to follow a WSW-ENE orientation, as highlighted by the arrows on the figure. Borehole data shows that the high resistivities are Quaternary sand and gravel of the Lateglacial outwash plain, whereas the lower resistivities represent clay till.

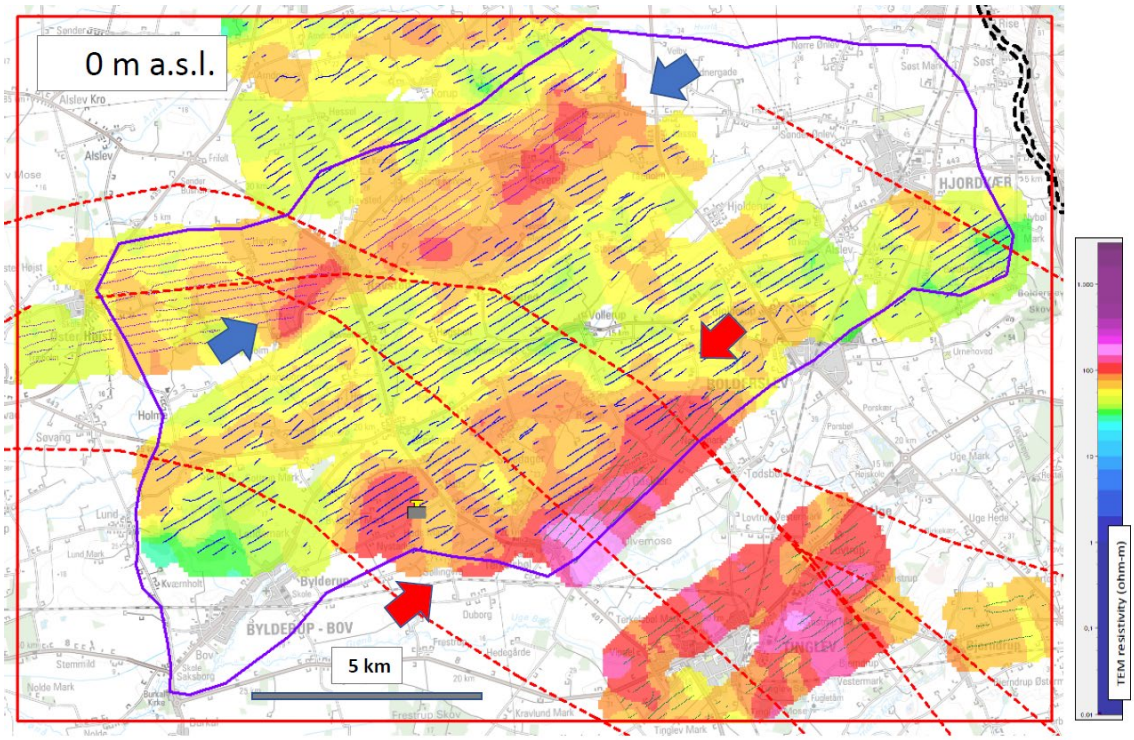

Figure 6.2. Mean resistivity slice 0 m above sea-level (a.s.l.). Red hatched lines show the approximate locations of deep faults. Purple line marks the BB model area. Arrows: see text for explanation.

Slice 0 m a.s.l (Figure 6.2) shows predominantly moderate resistivities (greenish colours) in the central and northern parts and high resistivities (red) in the southern part. Again, there is a tendency of a WSW-ENE trend in the resistivities. Highlighted by the blue arrows, for instance, is a band of high resistivities in an area, where the resistivities in the slice above shows lower resistivities (Figure 6.1). Compared with Figure 6.1, Figure 6.2 shows 'reversed' resistivities in the northern and central parts. According to borehole data, the moderate resistivities represent Quaternary clay till and the high resistivities represents meltwater sand and gravel.

On slice -30 m a.s.l. (Figure 6.3), the WSW-ENE trend, as seen above, is no longer present, and irregular patches of low resistivities emerge (bluish areas). At the blue arrow, the low resistivities represent the Miocene Maade Group Clays according to boreholes (e.g. DGU no. 159.1335). The low resistivity patches farther to the east, however, have slightly higher resistivities, pointing to clayey Quaternary sediments.

On slice -50 m a.s.l. (Figure 6.4), the low-resistivity areas to the west become more pronounced and the low-resistivity patches to the east now merge into larger areas. The green arrows highlight two NE-SW trending longitudinal stretches of low resistivities separated by a high-resistivity area. To the south, the purple arrows show a sharp boundary to high-resistive sediments to the northeast apparently matching with one of the major faults. The red arrows to the west highlight a longitudinal N-S stretch of high resistivities. This structure is a buried valley eroded into the low-resistive sediments. Just like it is seen on the -30 m slice (Figure 6.3), the southern end of the structure reaches the town of Bylderup-Bov.

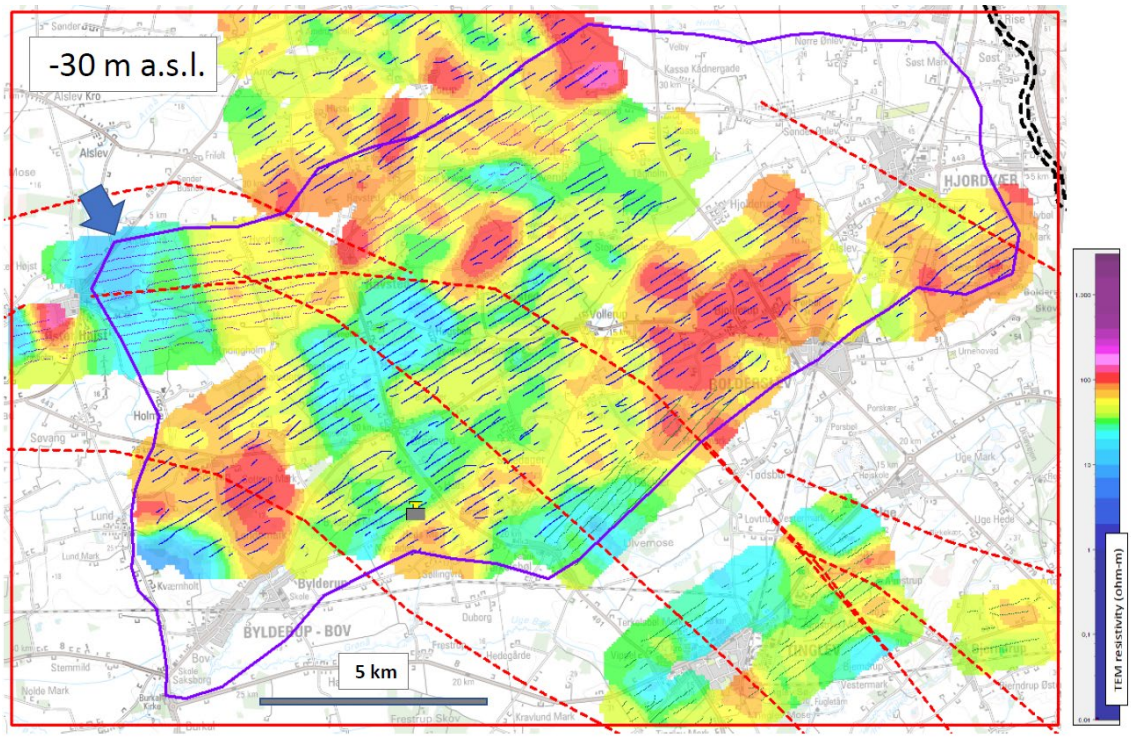

Figure 6.3. Mean resistivity slice -30 m above sea-level (a.s.l.). Red hatched lines show the approximate locations of deep faults. Purple line marks the BB model area. Arrows: see text for explanation.

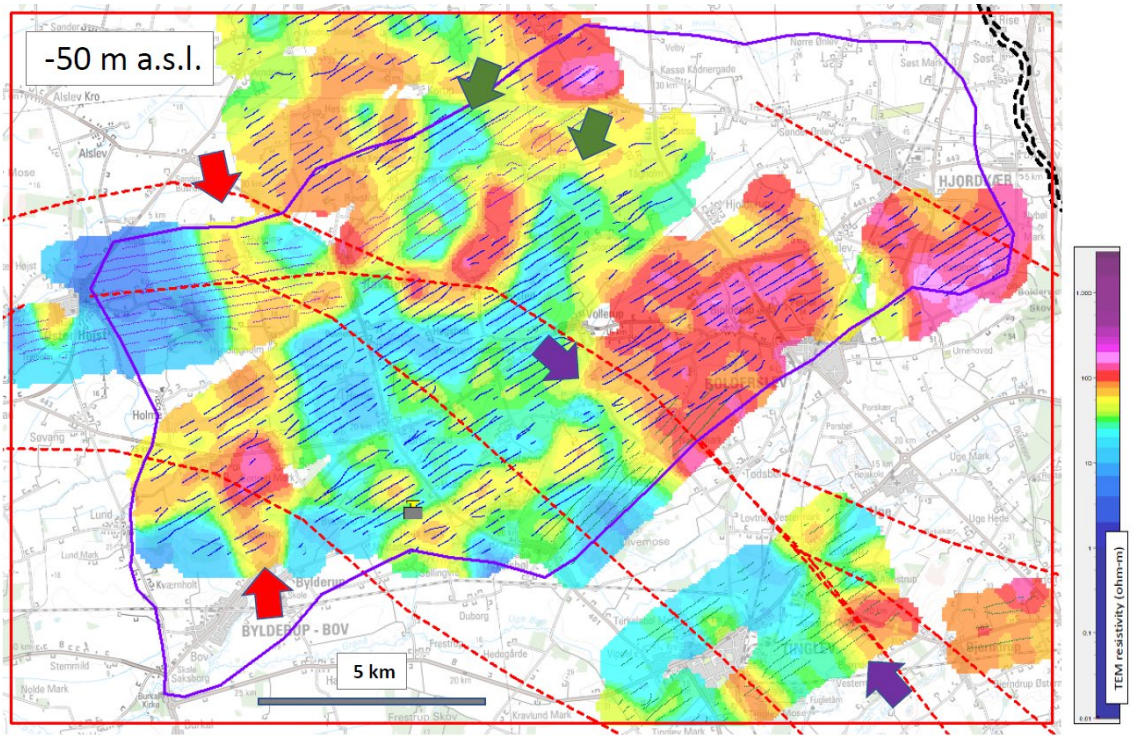

Figure 6.4. Mean resistivity slice -50 m above sea-level (a.s.l.). Red hatched lines show the approximate locations of deep faults. Purple line marks the BB model area. Arrows: see text for explanation.

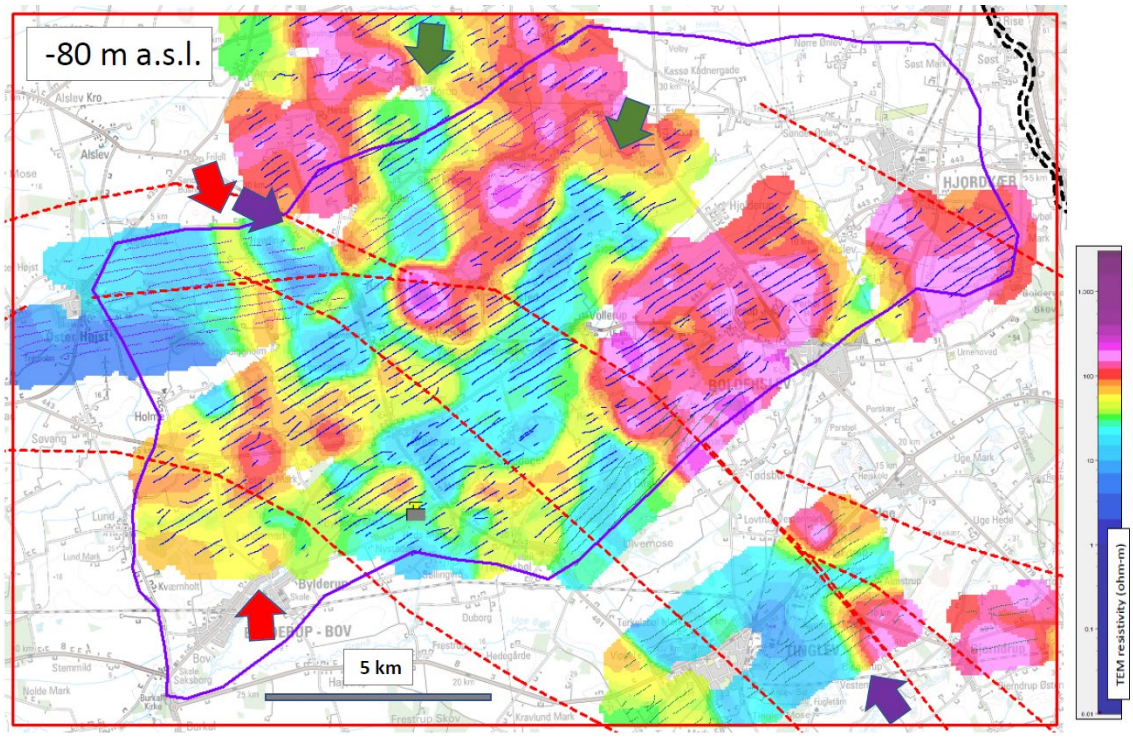

Figure 6.5. Mean resistivity slice -80 m above sea-level (a.s.l.). Red hatched lines show the approximate locations of deep faults. Purple line marks the BB model area. Arrows: see text for explanation.

The features of slice -50 m a.s.l. are also present in slice -80 m a.s.l. (Figure 6.5), but there appears to be a marked difference in the picture of the resistivities northeast and southwest of a NW-SE line, respectively (highlighted by the purple arrows). A relation to the fault as mentioned earlier seems to become more clear with depth. The low-resistive structures at the green arrows are still present, but the high resistivities in-between gets broader with depth.

At -80 m, the low-resistive structures are around 7-8 km long and up to 2½ km wide. The valley at the red arrows become narrower with depth. The high resistivities southwest of the N-S valley represent another buried valley which is broader and has an E-W orientation.

On the -120 m a.s.l. slice (Figure 6.6), the low-resistive structures at the green arrows retain their orientation, but the high-resistive sediments between widens even more. In 3D, this resembles a large NE-SW oriented fold in a succession of low-resistive sediments above high-resistive sediments. As it can be seen on the -120 m slice, the structure changes its appearance southwest of the line between the purple arrows.

On the -200 m slice (Figure 6.7), low resistivities dominate (blue colours), and high resistivities can only be found in an irregular NW-SE band inside the main faults of the Tønder Graben. The area with very high resistivities to the NW represents TEM models below the DOI (Depth Of Investigation), and therefore cannot be relied on. The low resistivities predominantly represent the deepest clay formations of the Miocene succession, and as the dark blue arrows indicate, there seems to be a WSW-ENE trend in the resistivity variations. This trend can be seen from -150 m to -250 m indicating faults in the deep parts of the sedimentary succession.

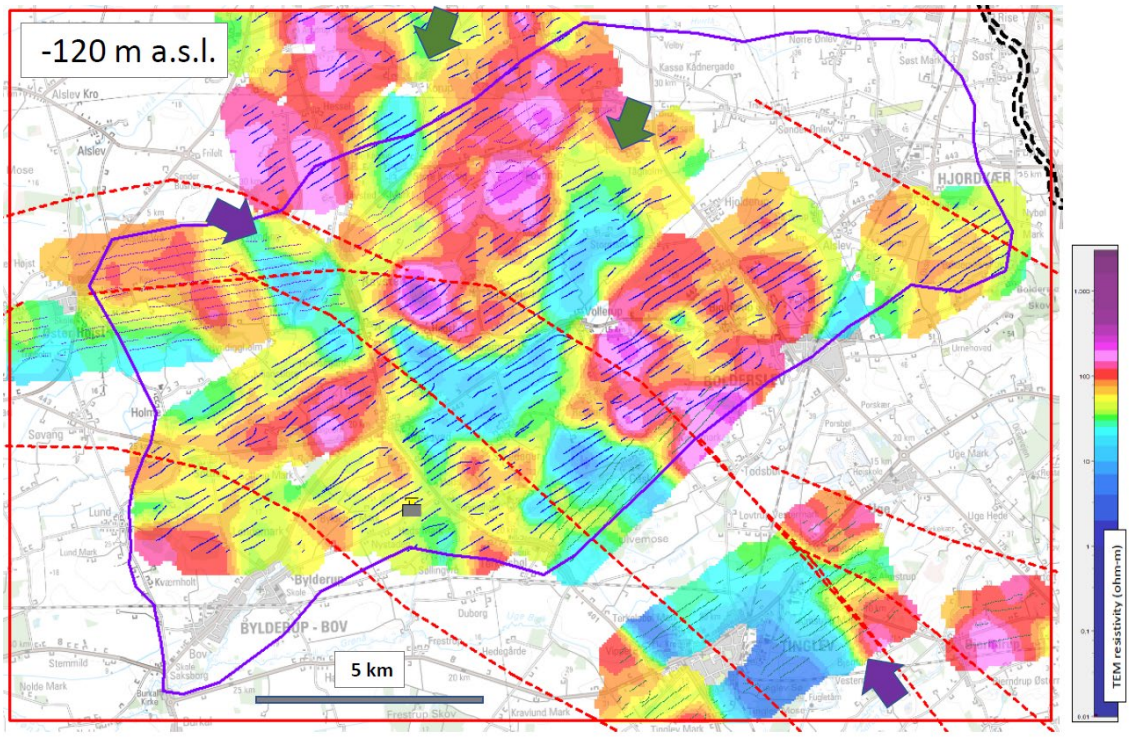

Figure 6.6. Mean resistivity slice -120 m above sea-level (a.s.l.). Red hatched lines show the approximate locations of deep faults. Purple line marks the BB model area. Arrows: see text for explanation.

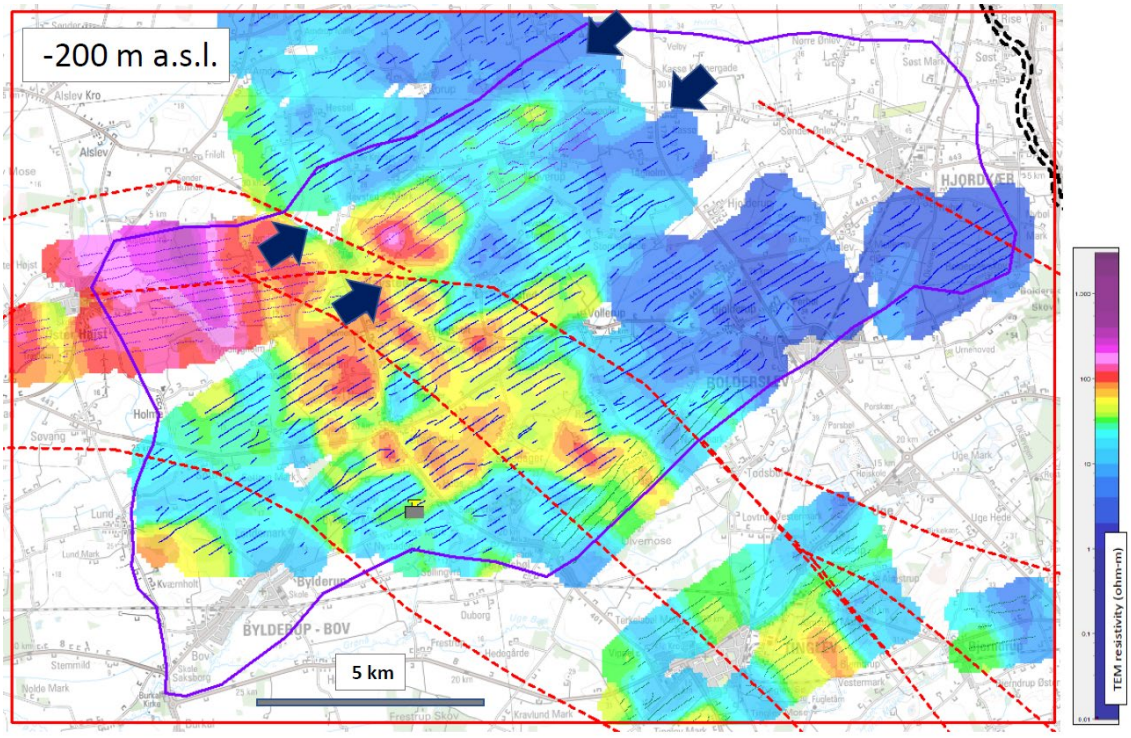

Figure 6.7. Mean resistivity slice -200 m above sea-level (a.s.l.). Red hatched lines show the approximate locations of deep faults. Purple line marks the BB model area. Arrows: see text for explanation.

6.1.2 Interpretations along selected vertical profiles

In the following, the geological model interpretations are sketched and described along six selected vertical profiles (Figure 6.8). It should be noted that the annotated interpretations are not the actual model interpretations along the defined layer boundaries but is a simpler visualisation of the performed interpretations based on TEM data and boreholes. To see the interpretation points and the interpolated layer boundaries we refer to the digital 3D model.

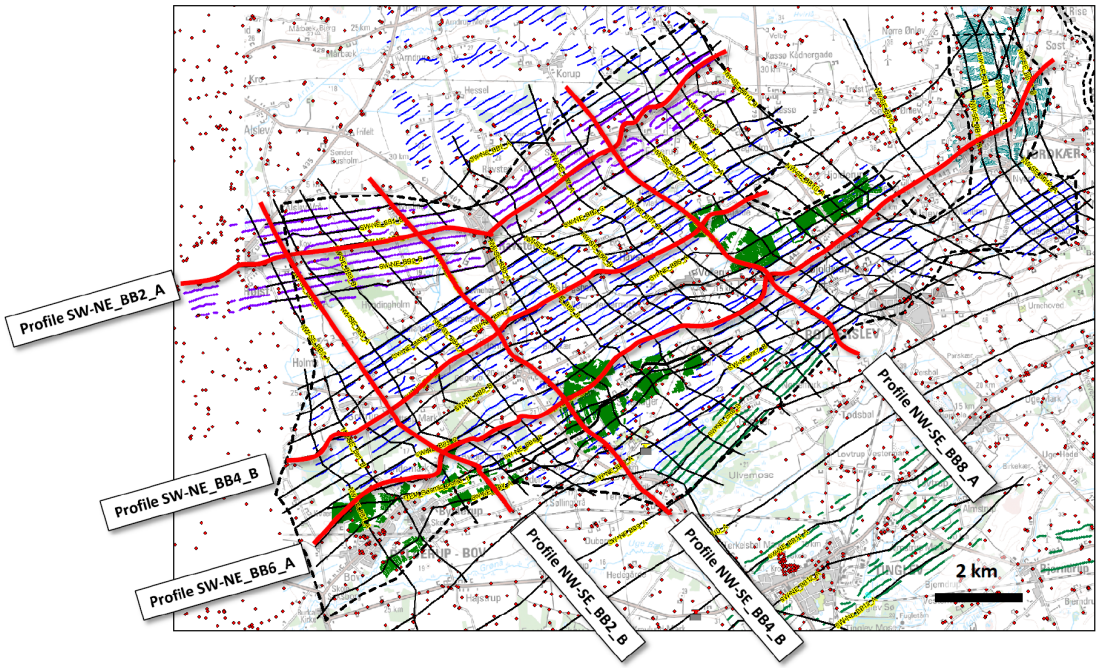

Figure 6.8. Selected geological profiles

Profile SW-NE_BB2_A (Figure 6.9):

From 0 to 4,500 m:

- The depth of investigation (DOI) is only around 150 m and therefore, the deepest mapped layer is the 'Miocene sand' consisting of sands and clays of the Arnum and Odderup Formations (Lower-Middle Miocene; Dybkjær, 2010). These sediments predominantly show high resistivities. Above, the low-resistive 'Maade Group' of marine clays attains a thickness of around 80 m.
- A buried Quaternary valley has been eroded into the Maade Group, but this valley is located just outside the BB model area. Above, the TEM and borehole data find tills and meltwater sand.

From 4,500 to 11,500 m:

- The deep Miocene sand and Quaternary meltwater sand cannot be distinguished from each other in the TEM data. Because of the depth, clay layers may be present but cannot be resolved in the SkyTEM data.
- The section appears to be deformed and offset by faults. Presumably due to a combination of glaciotectonics and deep tectonics related to the Tønder Graben

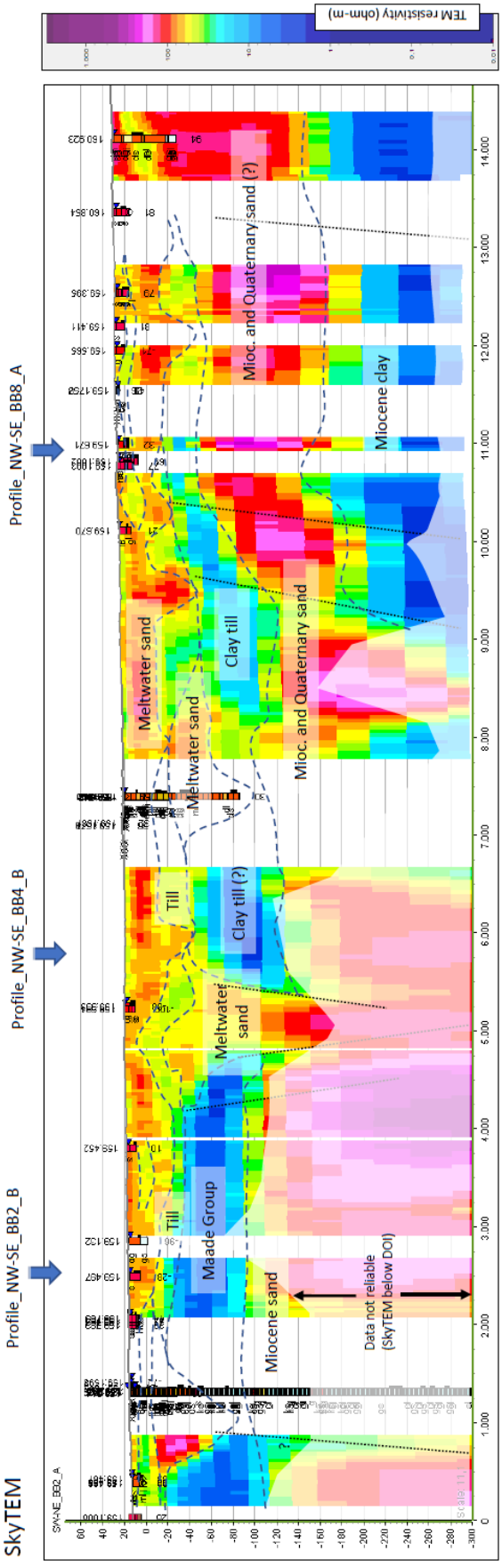

Figure 6.9. Sketch of geological interpretations along Profile SW-NE_BB2_A. For location, see Figure 6.8.

- Two valleys have been eroded through the thick low-resistive clay. The clays resemble the Maade Group clays, but they are interpreted as tills because of the deformation and mixing with Quaternary sediments (according to boreholes around the profile)

From 11,500 to 14,500 m:

- According to borehole data, the deep sand is expected to be dominated by Quaternary sand. The tills above thin out towards the northeast.
- The deep Miocene sediments most likely consist of clays of the Lower Miocene Klintinghoved Formation and older marine formations. This is suggested by biostratigraphy in deep boreholes to the south. There is, however, no well-control along the profile.

Profile SW-NE_BB4_B (Figure 6.10):

From 0 to 2,500 m:

- Above low-resistive Miocene clays, the SkyTEM finds high and moderate resistive sediments which are interpreted as Quaternary sand and clay layers representing buried valley infill (The Abild valley; Sandersen & Jørgensen, 2016).
- The valley is eroded through the Maade Group clays down to -140 to -150 m (see profile NW-SE_BB1_A to the left; Figure 6.11).

From 2,500 to 10,500 m:

- The elevation of the deep Miocene clay varies with a low around -280 m at 6,000 m and presumably even deeper at 7,000 m. This is interpreted to be caused by downfaulting within the Tønder Graben. The Miocene and Quaternary sands above are thickest here.
- The clay tills above are deformed and varies greatly in thickness

From 10,500 to 12,500 m:

- The deep Miocene clays are found at higher levels and the sand between the Miocene clay and the clay tills becomes thinner towards the east.

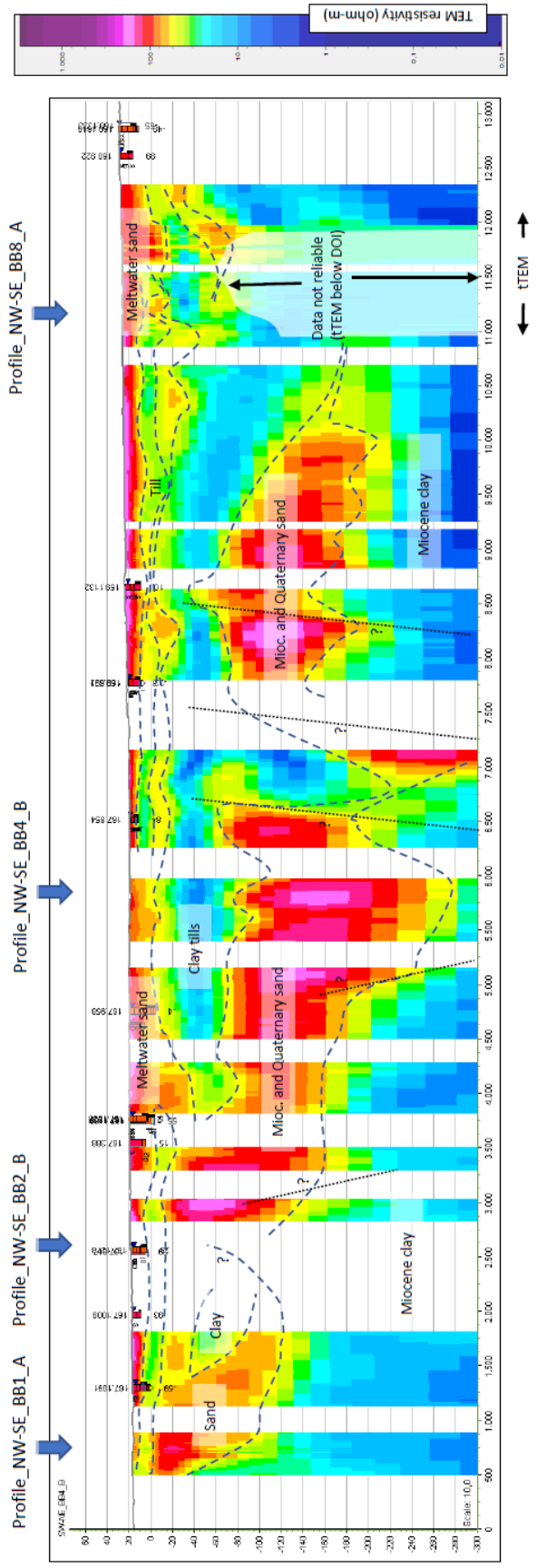

Figure 6.10. Sketch of geological interpretations along Profile SW-NE_BB4_B. For location, see Figure 6.8.

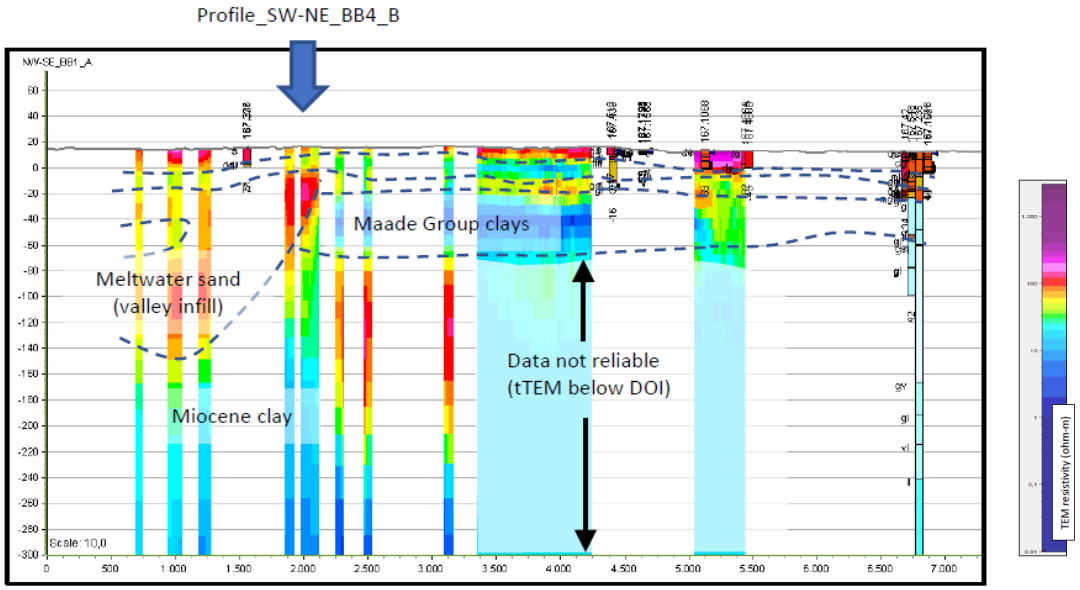

Figure 6.11. Sketch of geological interpretations along Profile NW-SE_BB1_A. The profile is the southwesternmost NW-SE profile, see Figure 6.8.

Profile SW-NE_BB6_A (Figure 6.12):

- The interpretations on this profile are to a large extent as on profile SW-NE_BB4_B
- The parts of the Tønder Graben with the largest subsidence are between 7,000 and 11,000 m
- The deep borehole DGU no. 160.1378 at 13,200 m shows a Quaternary succession down to the Miocene clays at around 200 meters depth.

From 3,500 to 8,500 m:

- The deep low-resistivity Miocene clay is found below -180 m
- The Miocene sediments above consists of alternating layers of sand, clayey sand, and clay
- A buried valley is eroded into the Miocene succession; the valley is filled with high-resistive meltwater sand
- The uppermost 40 to 60 m consists of Quaternary meltwater sand with an interlayered till. These layers are only slightly deformed.

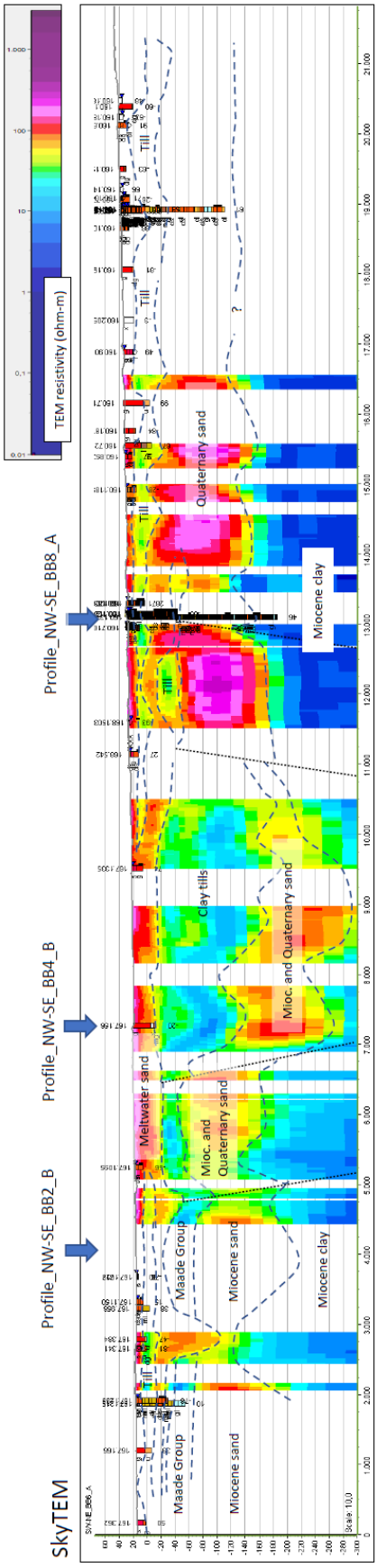

Figure 6.12. Sketch of geological interpretations along Profile SW-NE_BB6_A. For location, see Figure 6.8.

Profile NW-SE_BB2_B (Figure 6.13):

From 0 to 4,500 m:

- Because of the reduced DOI, the SkyTEM cannot resolve the deep parts of the succession
- The Maade Group clays are around 80 to 100 m thick and are offset by a fault at 2,000 m and probably also at 3,500 m. The offset is around 20 m.

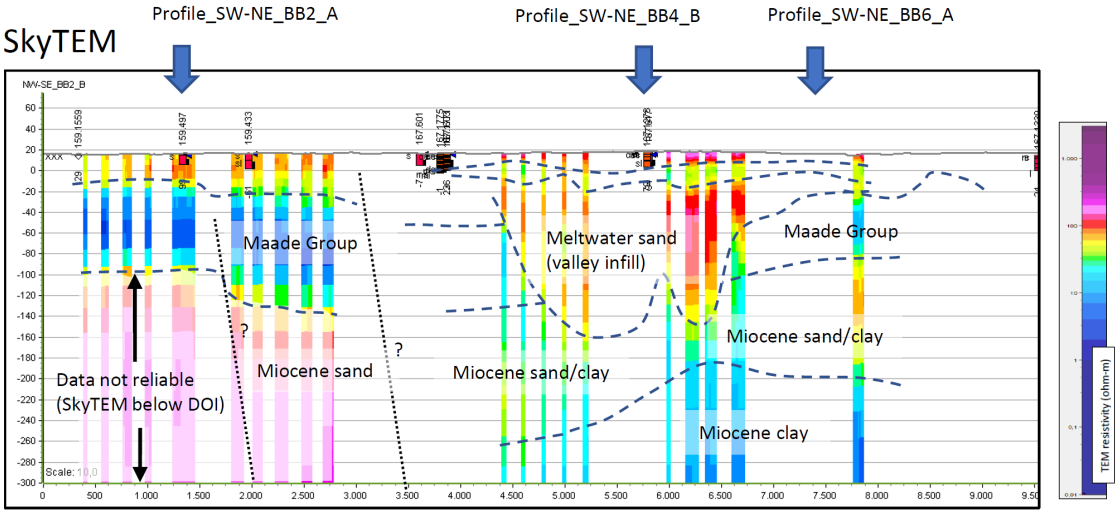

Figure 6.13. Sketch of geological interpretations along Profile NW-SE_BB2_B. For location, see Figure 6.8.

From 4,500 to 7,500 m:

- The SkyTEM shows mainly high-resistive sediments interpreted as predominantly Quaternary sand representing buried valley infill (The Abild valley; Sandersen & Jørgensen, 2016).
- The valley is eroded through the Maade Group clays down to -140 to -150 m (see also profile NW-SE_BB1_A to the right; Figure 6.11).
- A layer of moderate resistivities of up to 20 m thickness is seen around 0 m a.s.l. The layer is interpreted as till.

Profile NW-SE_BB4_B (Figure 6.14):

From 0 to 3,000 m:

- Because of the reduced DOI, the SkyTEM cannot resolve the deep parts of the succession
- The resistivity of the around 80 m thick clay till shows a strong resemblance with the Maade Group clays and the clay till most likely represent glaciotectonically deformed Maade clays
- The succession appears to be offset by a fault at 3,000 m – probably related to the Tønder Graben.

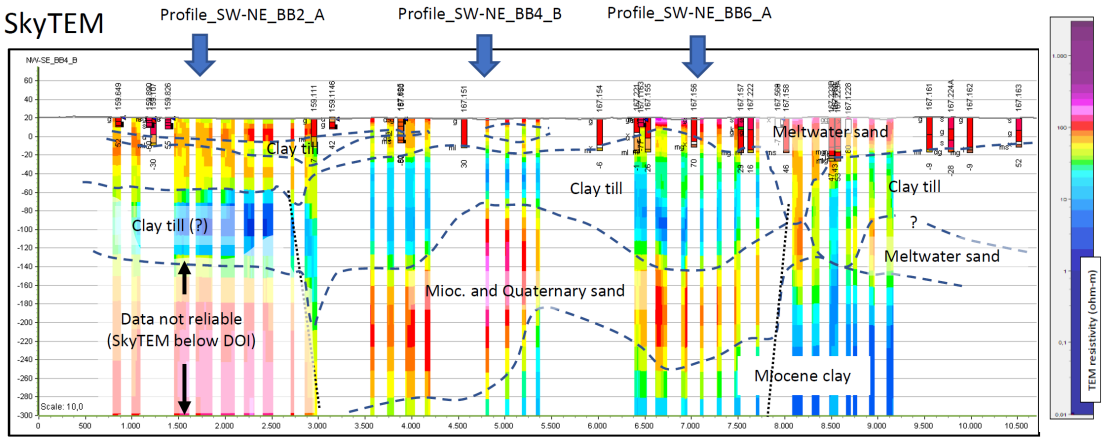

Figure 6.14. Sketch of geological interpretations along Profile NW-SE_BB4_B. For location, see Figure 6.8.

From 3,000 to 8,000 m:

- Deep low-resistive Miocene clays are found below -200 m
- The succession above (up to sea-level) is deformed and consists of clay tills and Quaternary sand, and presumably also Miocene sand. The clay till is glaciotectonically deformed
- The uppermost 40 m consists of meltwater sand and an interlayered till. These layers are only slightly deformed

From 8,000 to 10,000 m:

- The deep low-resistive Miocene clay is found at around -150 m, which is 50-150 m higher in elevation compared to the northern 3/4 of the profile
- The meltwater sand above the Miocene clay have a reduced thickness compared to the central part of the profile
- The clay till is glaciotectonically deformed and apparently thrusting in some parts increases its thickness
- The uppermost meltwater sand is between 25 and 40 m thick, except between 8,000 and 8,500 m, where a valley erosion makes the Quaternary succession around 120 m thick.

Profile NW-SE_BB8_A (Figure 6.15):

- The Miocene clay is found at elevations between -120 to -200 m.
- Above, it appears as if only Quaternary sediments are present: An around 200 m thick and heavily deformed succession of predominantly meltwater sand with a few layers of clay till.
- In the uppermost parts, a 40-50 m thick Quaternary succession of meltwater sand and till is present. These layers appear to be only slightly deformed

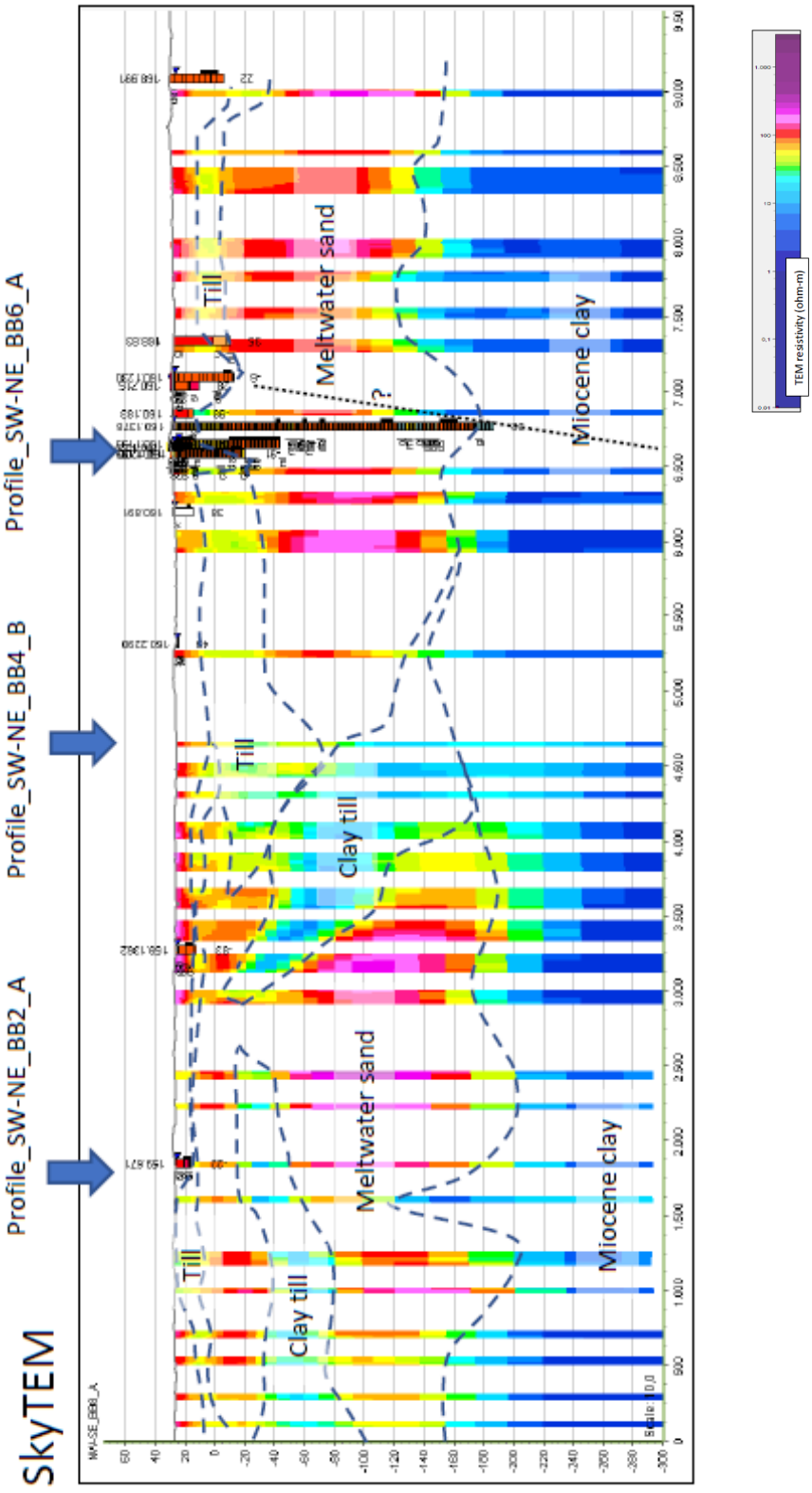

Figure 6.15. Sketch of geological interpretations along Profile NW-SE_BB8_A. For location, see Figure 6.8.

6.1.3 The sediments

As the descriptions of the selected profiles above show, both the pre-Quaternary and the Quaternary sedimentary successions appear to have been subject to not only deep tectonic events but also erosion and deformation by ice and meltwater during the Pleistocene glaciations. This has had a large impact on the geological architecture resulting in a high subsurface complexity. Especially the structural complexity can be difficult to interpret from the geophysical data, but it is also evident from borehole data that a distinction between pre-Quaternary and Quaternary sediments in many cases can be very challenging.

6.1.3.1 The pre-Quaternary succession

The expected Miocene succession in the model area is shown in Figure 3.7 and described in the text (Section 3.3.1). The borehole with the most complete Miocene succession and the most reliable descriptions is the DGU no. 159.1335 at Øster Højst just west of the model area (Figure 6.16; see also the profile in Figure 6.9).

The resistivity log of borehole DGU no. 159.1335 (Figure 6.16) shows that the deep Miocene Klintinghoved Formation and the deeper Palaeogene clays have resistivities predominantly below 5 ohmm (left logs). The Palaeogene clay of the Søvind Marl in the deepest part of the borehole, for instance, shows a resistivity below 3 ohmm and is described as 'very sticky' and very calcareous.

The sands of the Miocene Odderup Formation and the Bastrup Sand have resistivities below 40 ohmm, which is fairly low compared to the Quaternary meltwater sand in the upper parts of the borehole where the resistivities typically lie between 60 and 80 ohmm. Sample descriptions of the Miocene sand show that a clay content is very common, especially in the deep 50 m thick Bastrup sand where the resistivity is very low for a fine to medium-grained sandy deposit (15-25 ohmm). The Odderup and Bastrup sands are dark greyish-brown.

The Bastrup sand and the Odderup Formation are interlayered with blackish brown, slightly silty clays of the Arnum Formation with resistivities typically between 10 and 20 ohmm.

The uppermost Miocene, the Maade Group, consists of clay with a resistivity of around 5 ohmm. The rather high clay content in the Miocene sands is confirmed by the counts of the Gammalog (log to the right). The Maade Group clay is sticky, mica-rich, and black to blackish brown and non-calcareous.

Occasionally, metre-thick shell layers are found in the Miocene succession. These are in some cases categorized as 'Gravel' with reference to the grain size, but described as 'Shells, sandy, gravelly, grey brown'. Concretions in sand, gravel and stone fractions are also found in several horizons.

The Miocene succession as it is found in borehole DGU no. 159.1335 is expected to be representative for the Miocene sediments in and around the BB model area, and it consists mainly of clay with interlayering of usually thinner layers of clayey sand. The colours of the Miocene sediments are typically ranging from black to dark grey-brown.

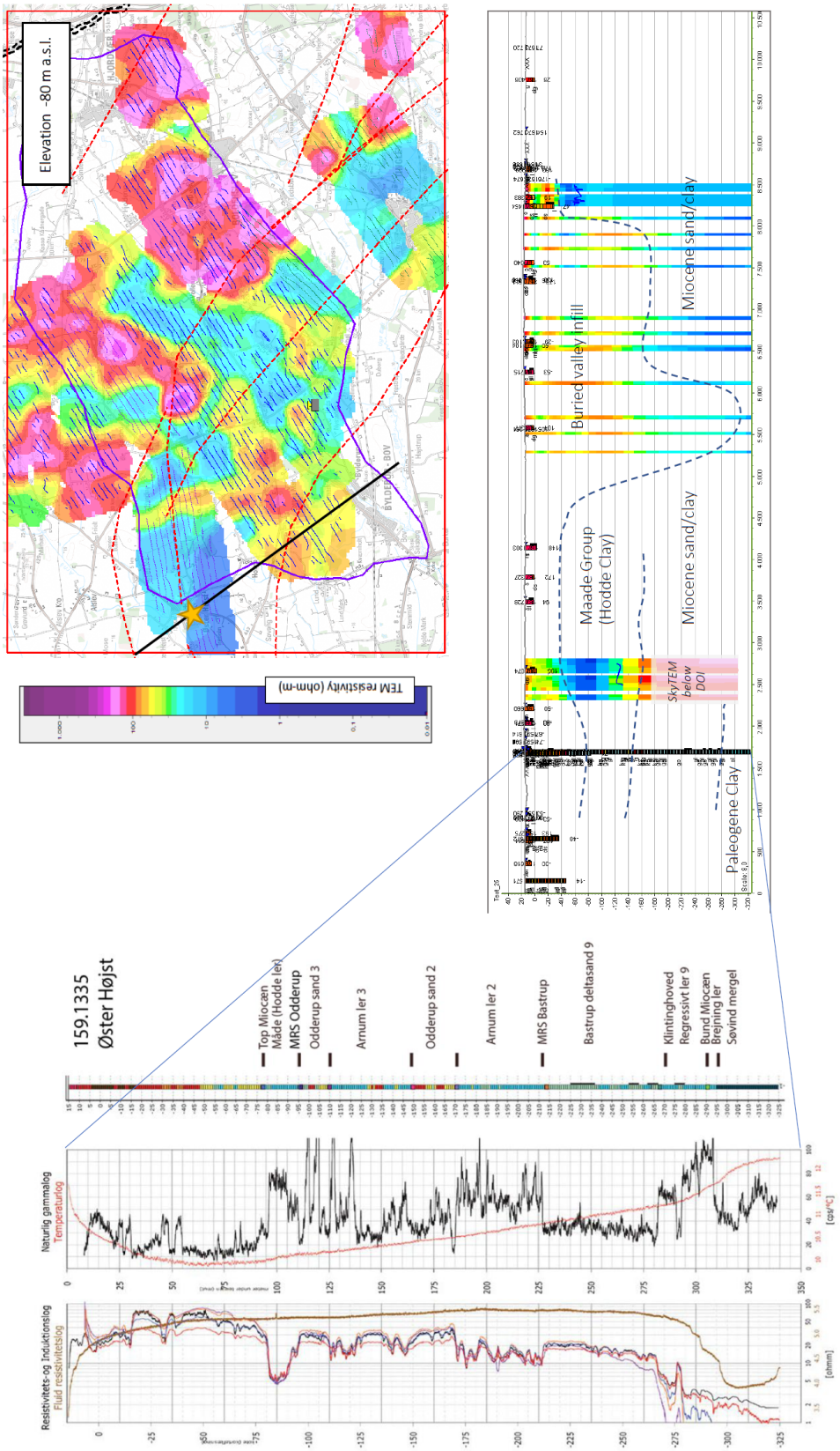

Figure 6.16. Borehole DGU no. 159.1335 at Øster Højst. To the left geophysical logs and biostratigraphic interpretations (From Kristensen et al., 2015). Lower right: a NW-SE profile with general interpretations and the borehole inserted. Top right: a mean TEM resistivity map at -70 m a.s.l. (black line shows the location of the profile and the yellow star shows the location of the borehole. Red hatched lines: faults. Purple polygon: the BB model area.

6.1.3.2 The Quaternary succession

The lithological characteristics of the Quaternary succession is described in the following primarily by using the descriptions from two deep boreholes, DGU no. 159.1444 and 160.1378 (The blue star is located just north of the borehole DGU no. 159.1444 and the yellow star just north of DGU 160.1378 in Figure 6.17).

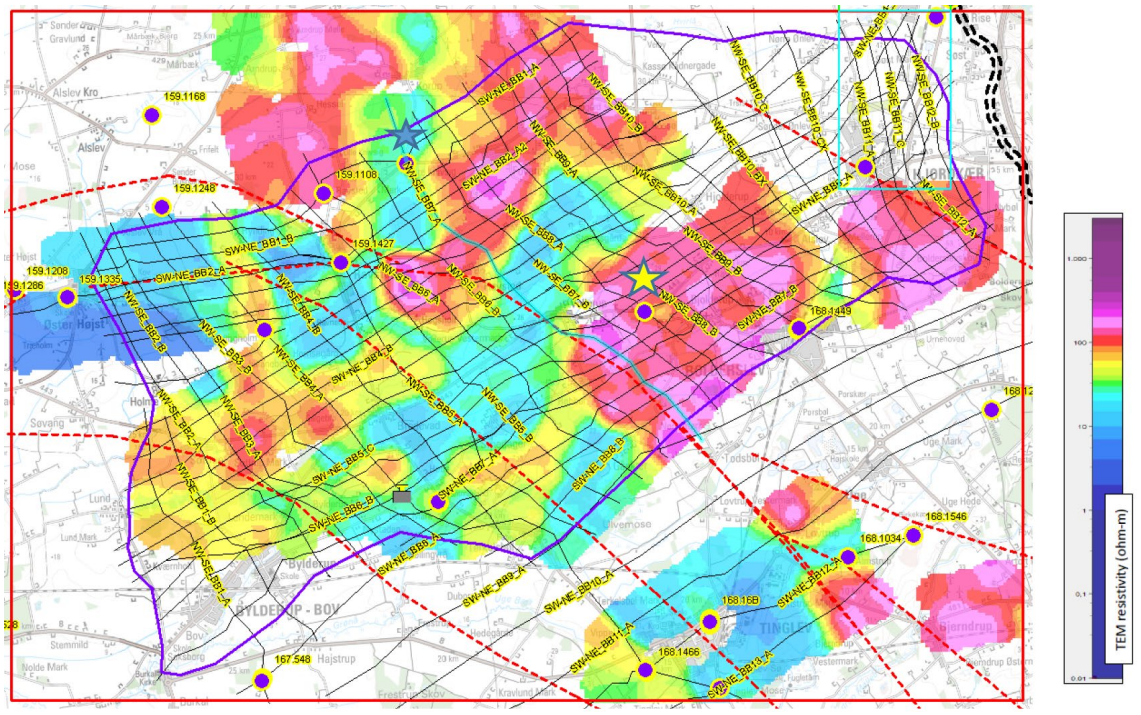

Figure 6.17. TEM mean resistivity map at -80 m a.s.l. BB model profiles are shown as thin black lines, and the model area is within the purple polygon. Purple dots show the locations of boreholes deeper than 75 m. The blue star is located just north of borehole DGU no. 159.1444 and the yellow star just north of DGU 160.1378 (see text). The profile highlighted with the light blue line is shown below in Figure 6.18.

DGU no. 159.1444

The sediments in the 215 m deep borehole DGU no. 159.1444 are made up of alternating layers of sand and clay with a close to 1/1 ratio (see location on Figure 6.17 and Figure 6.18 at the blue star). Apart from the uppermost meter the sediments are dark grey, greyish-brown to blackish-brown in colour.

The deepest samples from 209-215 metes depth consists of sticky, silty clay, and above a high-resistive and predominantly sandy succession of 50 to 60 meters thickness is found. Above these layers, an approximately 80 m thick clay layer interpreted as predominantly clay till described as grey-brown to blackish grey, sandy, silty, clay with fragments of chalk/lime-stone is found. A fine to medium sand layer of 20 m thickness is found interlayering the clay. In the TEM data, the clay is seen as a thick, irregular, low-resistive layer (Figure 6.18), but the TEM cannot resolve the interlayered sand. Above the clay is a 70 m thick succession of clay tills and meltwater sand/gravel with moderate and high resistivities, respectably.

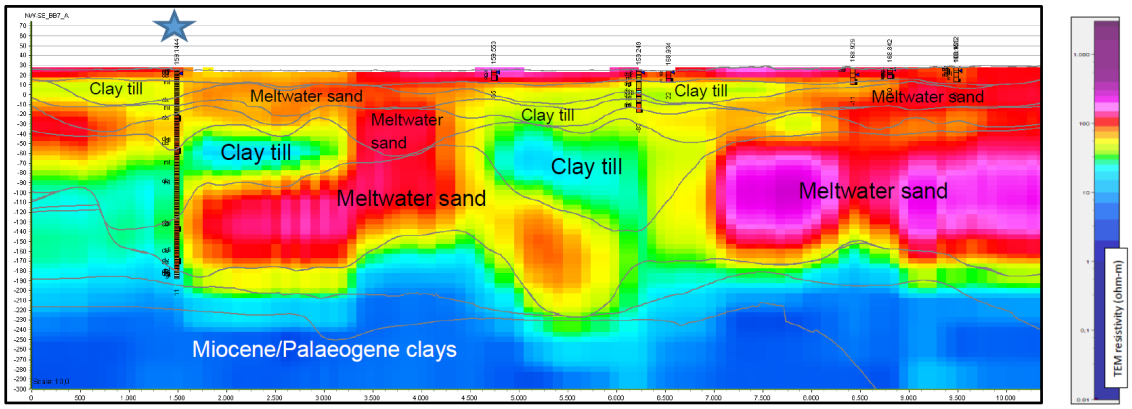

Figure 6.18. Profile NW-SE_BB7_A northeast of Ravsted. The profile shows a vertical profile through the 3D grid of the SkyTEM data. Boreholes are seen as coloured vertical rods with outline and annotations. The blue star marks the location of borehole DGU no. 159.1444 (see Figure 6.17). The grey lines are the layer boundaries modelled in the BB model.

Palynological investigations performed on four samples from the borehole referred the deepest sample (214–215 m depth) to the Miocene Klintinghoved Formation. Three samples above (201–202 m, 194–195 m and 57–58 m depths) all contained palynomorphic assemblages of different ages, and the sediment was therefore interpreted as Quaternary reworked sediments (Dybkjær 2015). In other words, the sedimentary succession down to -182,5 m a.s.l. can be considered to be of Quaternary age and presumably the sediments up to -40 m a.s.l. can be considered as reworked and deformed during the Quaternary, most likely by glaciotectonics. The palynological investigations point to reworking of the Miocene Maade Group clays (Dybkjær 2015). This conclusion fits well with the colours of the Miocene Formations described in the previous section from borehole DGU no. 159.1335.

DGU 160.1378

The Quaternary sediments in the 216 m deep borehole DGU no. 160.1378 are made up of alternating layers of sand and clay with a 3/1 ratio (see location on Figure 6.19 at the yellow star). Apart from the uppermost few meters, the sediments have a grey to greyish-brown colour. The Miocene clay in the bottom of the borehole is greyish-black.

The deepest layer is a 12 m thick greyish black clay layer that is interpreted to be mixed with Quaternary material. Above is 35 m of poorly sorted grey to dark grey calcareous sand followed by 17 m layers of dark grey to black sandy and silty clay. Above lies close to 150 m of predominantly grey brown to dark grey calcareous meltwater sand with minor interlayering of greyish brown to greyish black clays interpreted as clay tills.

Foraminiferal analyses find the deepest samples to be the Miocene Klintinghoved Formation, whereas the sediments above have foraminiferal assemblages that show signs of transport and reworking. However, as shown in Kristensen et al. (2015), palynological analyses find that the sediments from a depth of 80 m and down to the bottom of the borehole are Miocene. The description in the Jupiter database appears credible and is supported not only by the foraminiferal analyses, but also by the interpretations of the SkyTEM made in the BB model pointing to a glaciotectonically deformed succession. This example of contradictory descriptions can also be seen elsewhere, for instance in a 218 m deep borehole in Tinglev just southeast of the BB model (DGU no. 160.1228). Here, a succession that might visually be

seen as Miocene has been interpreted as Quaternary because of finds of both Miocene and Quaternary shell fragments, and fragments of crystalline rocks throughout the samples (Note by L.F. Jørgensen dated 17.7.1998 in the Jupiter database). It was also concluded that the clayey sediments were clay tills consisting of reworked Miocene sediments which have only been transported for relatively short distances. The high resistivities in the interval between ca. -20 and -140 m a.s.l. are in high contrast to the low to moderate resistivities of the Miocene sediments in borehole DGU no. 159.1335 (Figure 6.16).

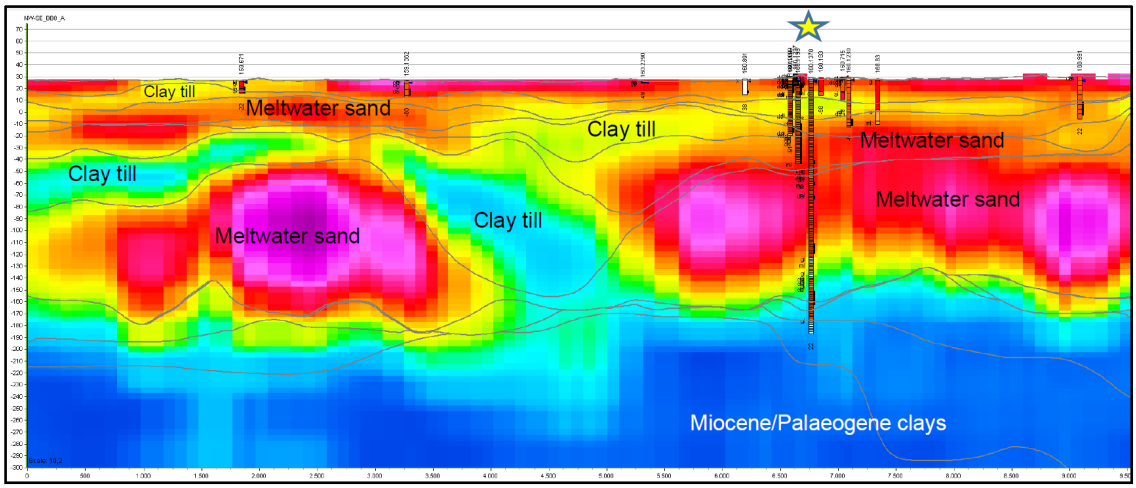

Figure 6.19. Profile NW-SE_BB8_A northeast of Ravsted. The profile shows a vertical profile through the 3D grid of the SkyTEM data. Boreholes are seen as coloured vertical rods with outline and annotations. The yellow star marks the location of borehole DGU no. 160.1378 (see Figure 6.17). The grey lines are the layer boundaries modelled in the BB model. NB: Please be aware that the 3D interpolation of the SkyTEM 1D models creates an evenly distributed grid that fills areas without data. The layer boundary interpretations shown in the profile is solely based on the 1D SkyTEM models (see Figure 6.15 for comparison).

Interglacial deposits

What is interpreted to be interglacial marine deposits have been found in boreholes in and around the BB model area. In borehole DGU no. 159.1108 north of Ravsted, a layer from -40 to -77 m a.s.l. described as fine olive-grey sand with intact shells, shell fragments, and mica is interpreted as interglacial marine sand in the Jupiter database. The sediment samples have not been biostratigraphically investigated and the interpretation is therefore based primarily on the content of shells of which no formal description and interpretation has been performed. Miocene sediments can contain a high amount of shell material, and reworking during the Quaternary may lead to numerous shell fragments in the Quaternary sediments. However, the presence of intact, thin-shelled molluscs in the samples points to very little reworking. Whether the sand represents an in-situ interglacial marine sediment deposited in a depression, or a Quaternary sediment containing reworked Miocene shells cannot be determined with certainty. The sand is found just north of the large scale glaciotectonic fold mentioned in the preceding text thereby suggesting deposition in the low-lying parts of a hill-hole-pair (Aber & Ber, 2007) – see Figure 6.20.

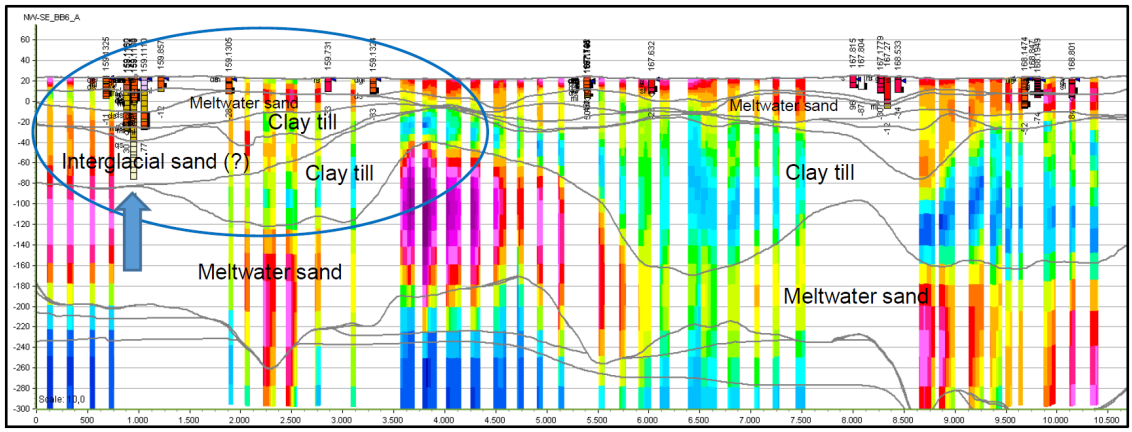

Figure 6.20. Profile NW-SE_BB6_A just east of Ravsted. The blue arrow shows the location of borehole DGU no. 159.1108, and the ellipse shows the interpreted hill-hole pair mentioned in the text (hill: the thick clay till; hole: the depression to the left – now filled with Quaternary sand.

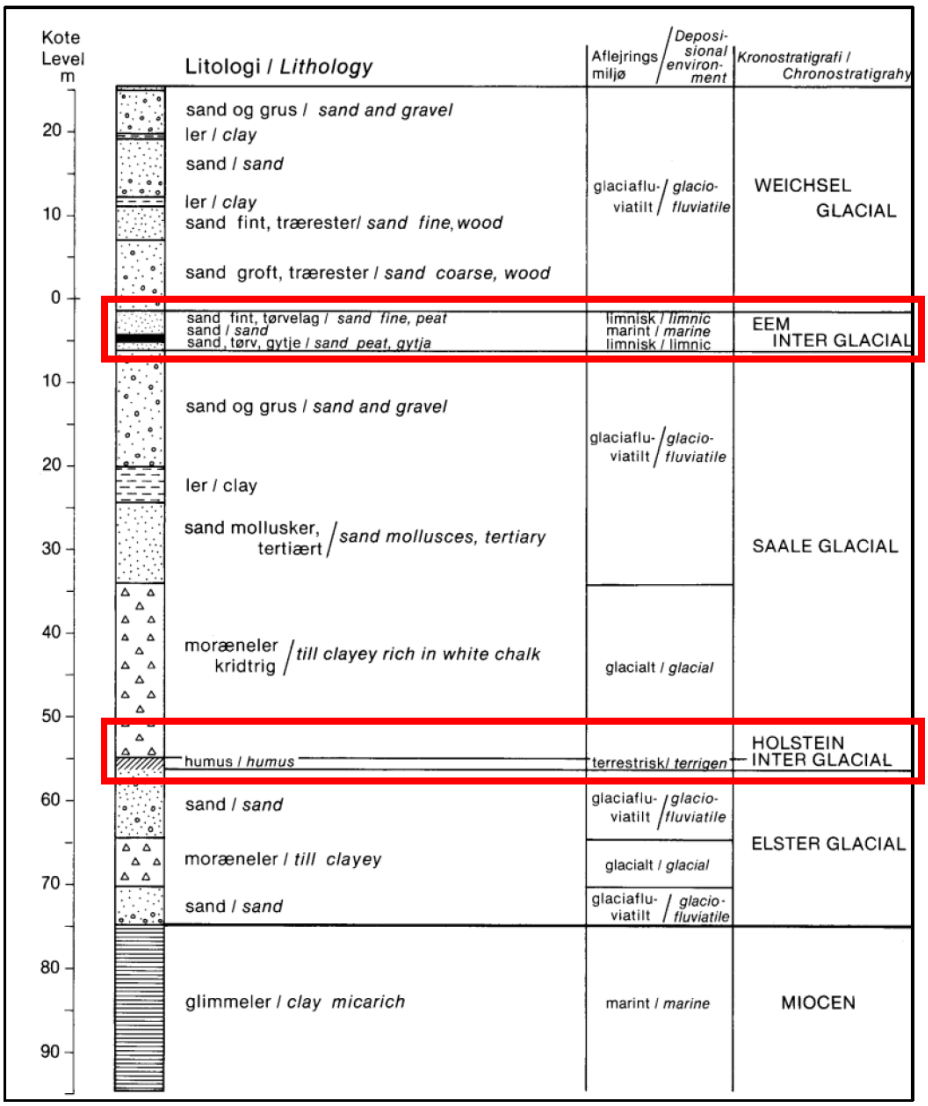

Figure 6.21. Sediment description of the borehole DGU. no. 168.16B at Tinglev Waterworks (drilled in 1938). Modified after Hansen (1989). Interval with interpreted interglacial sediments are highlighted with red rectangles.

In the town of Tinglev just south of the BB model, the borehole DGU no. 168.16 showed mainly sand and gravel down to a depth of 27 m (-2 m a.s.l), but below this interval peaty sand with molluscs with an indisputably Eemian age were found (Ødum 1933). A deeper borehole (DGU no. 168.16b) confirmed the find, but also a thin layer with organic material was found well below the Eemian interval (-55 m a.s.l.), and it was interpreted to represent terrestric interglacial Holsteinian sediments (Hansen 1989). The interglacial sediments were found below a chalk-rich clay till that was referred to the Saalian glaciation. In a borehole located farther to the south-west of (DGU no. 168.1466), 10 m of dark grey marine clay was found at a depth of 39 m (-14.5 to -24,5 m a.s.l.) – also below a chalk-rich clay till. The boreholes are located above the Tønder Graben and therefore the findings of both marine Eemian and marine Holsteinian sediments suggest the possibility of marine incursions into depressions related to the graben structure (Sandersen & Jørgensen, 2015).

However, with the new observations of pervasive glaciotectonics, the observations of interglacial sediments should be treated with caution – mostly in relation to the elevation of the finds and the place in the layer succession. But the findings of Eemian marine sediments cannot have been disturbed by the subsequent Weichselian glaciation because it did not reach past the Main Stationary Line. So, marine Eemian sediments found in the area can only be seen as evidence of marine transgressions into low-lying parts of the terrain during the Eemian.

As described in Sandersen & Jørgensen (2015), depressions in the present-day terrain were formed in the beginning of the Holocene, creating the large NW-SE oriented low-lying area now partly filled with peat and gyttja (see Figure 3.1). The subsidence was caused by early Holocene reactivations of the Tønder Graben due to the relief from the weight of the Weichselian ice sheet. If this mechanism was active just after the end of the Weichselian glaciation, it is likely that the analogous reactivations may have happened after previous glaciations as well. The findings of Eemian and Holsteinian marine sediments in boreholes support this. In addition to this, numerical simulations of the Coulomb Failure Stress (CFS) variations in the lithosphere during the last 200,000 years show that positive values for the CFS change point to unstable conditions and possible reactivation of deep faults as the result of the weight relief from the ice sheets (Figure 6.22; Brandes et al., 2024). From the figure it can be seen that positive values of the CFS changes are most pronounced at the end of the Saalian glaciation around 130,000 years, during the last 50,000 years of the Weichselian, and also into the Holocene. Even though the Weichselian ice sheet did not cover the Tønder Graben, it was able to destabilize the deep faults outside the ice sheet margin because of the large subsurface volume that was influenced by the stress changes. In the Blue Transition seismic survey most of the normal faults found apparently did not reach as far as the present-day terrain, but they clearly offset the relatively deep and thick clay till in the model area. Being located outside the Main Stationary Line, this clay is from the Saalian glaciation or older, thereby confirming the CFS modelling pointing to tectonic instability also following earlier glaciations.

In other words, the findings of postglacial and interglacial sediments in the area together with the knowledge from the numerical CFS simulations (Brandes et al., 2024), the mapped normal faults, and the deformations of the present-day topography (Sandersen & Jørgensen,

2015), the conclusions are that the Tønder Graben have experienced active faulting intermittently throughout the Quaternary. This appears to have opened up for sedimentation in narrow depressions and even temporary marine sedimentation in narrow fjords deep inland.

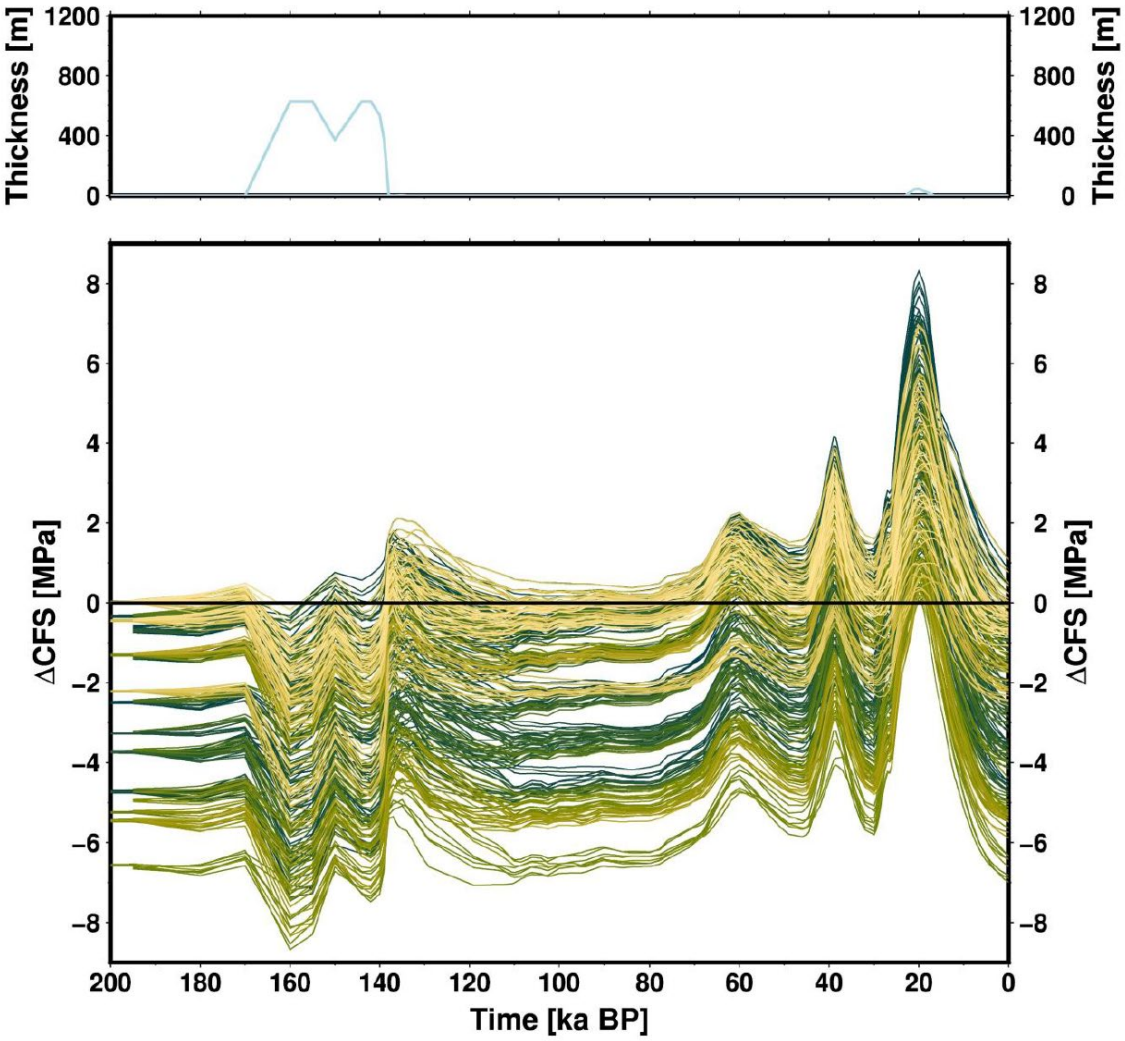

Figure 6.22. Numerical simulations of Coulomb failure stress (CFS) for the Tønder Graben area; lower panel. The upper panel shows the thickness of the ice sheets. From Brandes et al. (2024). Positive values for the CFS change point to unstable conditions and possible reactivation of faults.

Holocene organic deposits

As mentioned above, Holocene peat and gyttja has been deposited in low-lying areas during the Holocene (see for instance Figure 3.1). The performed tTEM survey was focused on mapping along the presumed ENE-WSW groundwater flow in the model area, the low-lying areas, and the areas around Bylderup-Bov. This has resulted in very good input for the geological modelling, but as the survey areas are patchy, the tTEM cannot produce a map of the Holocene organic sediments. The best overview of these sediments can instead be obtained from the surface geology map, Figure 6.23.

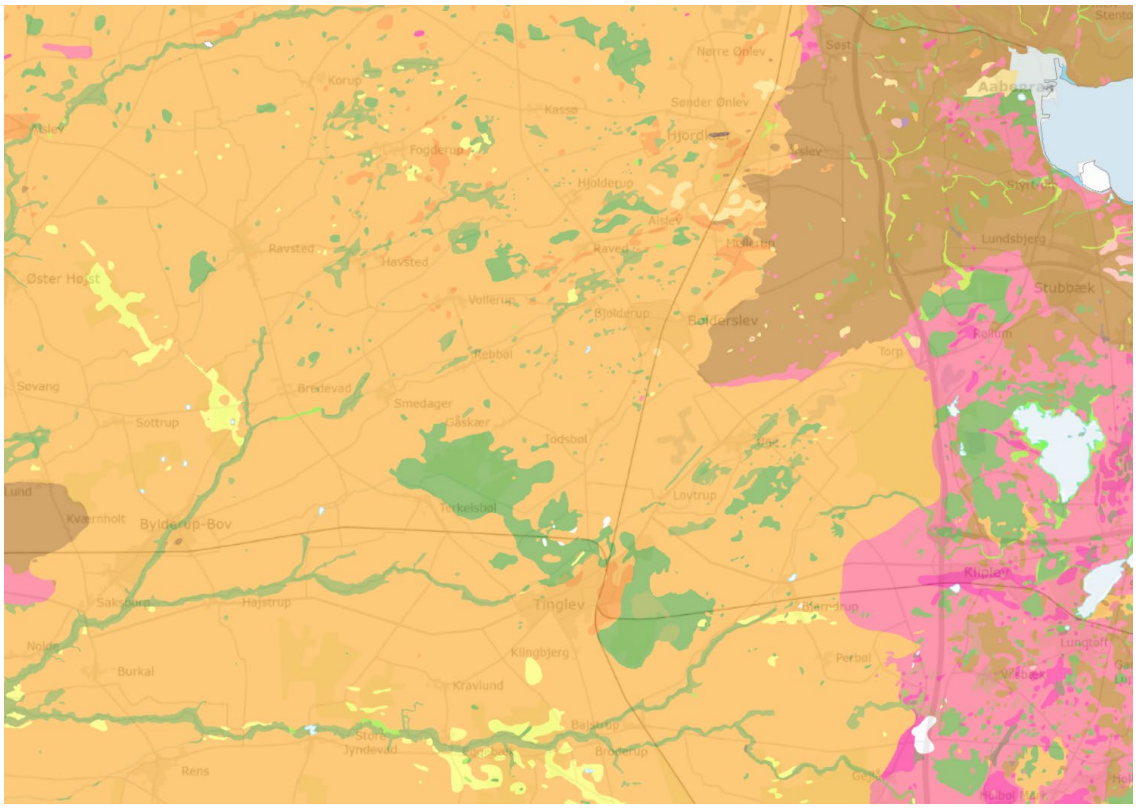

Figure 6.23. Surface geology map; 1:25,000 (Andersen et al., 2024). Green = Fresh water deposits (Holocene), Orange = Outwash plain sand and gravel (Lateglacial), Yellow = Aeolian deposits (Holocene), Brown/red = Glacial sediments (Weichselian).

Apart from the large areas over the Tønder Graben around Tinglev (lower centre of the map), all other occurrences are generally small and difficult to include in a geological layer model. The Holocene sediments have therefore not been designated a specific layer in the BB model.

6.2 Geological interpretation of the Blue Transition seismic survey

The geological interpretations of the seismic survey are described in the following. Primarily due to time constraints, the interpretations are focused on the southwestern part (Part 1), whereas the interpretations of the central and northeastern parts (Parts 2 and 3) are more tentative (Figure 6.24). The interpretations of the layer boundaries of Part 2 and 3 and the interpreted faults are therefore of a more sketchy nature than shown for Part 1.

6.2.1 Interpretation of the western seismic section (Part 1):

The seismic interpretation (Figure 6.25) started in the western part (Part 1) of the three seismic section segments due to the location of the nearby well Tinglev-1 (DGU no. 167.234A, Figure 6.24), which provided well-control for the seismic interpretation. The well was drilled in 1948 and now located 362 m south of the nearest profiling location at the NE end of the seismic section Part 1. The well has a terminal depth of 595 m and at a depth of about 160 m Neogene deposits were penetrated.

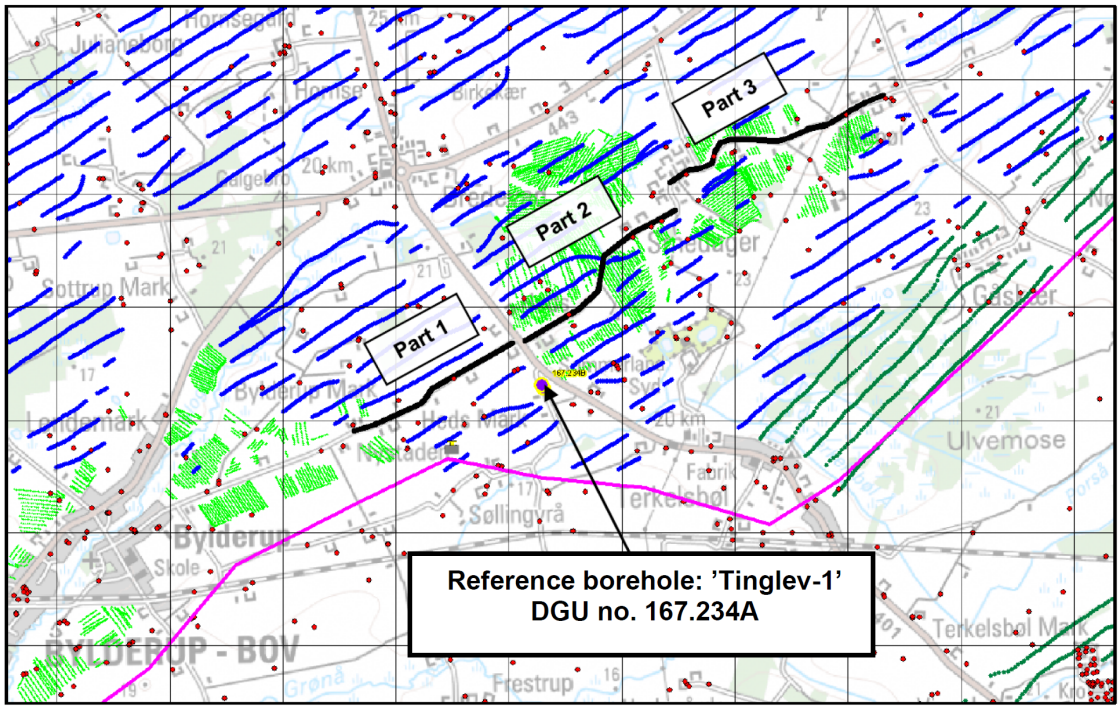

Figure 6.24. The three parts of the Blue Transition seismic survey marked with black lines. The reference borehole 'Tinglev-1' is used for the interpretations. Boreholes from the Jupiter database are shown as small red dots. This figure is a copy of Figure 4.3.

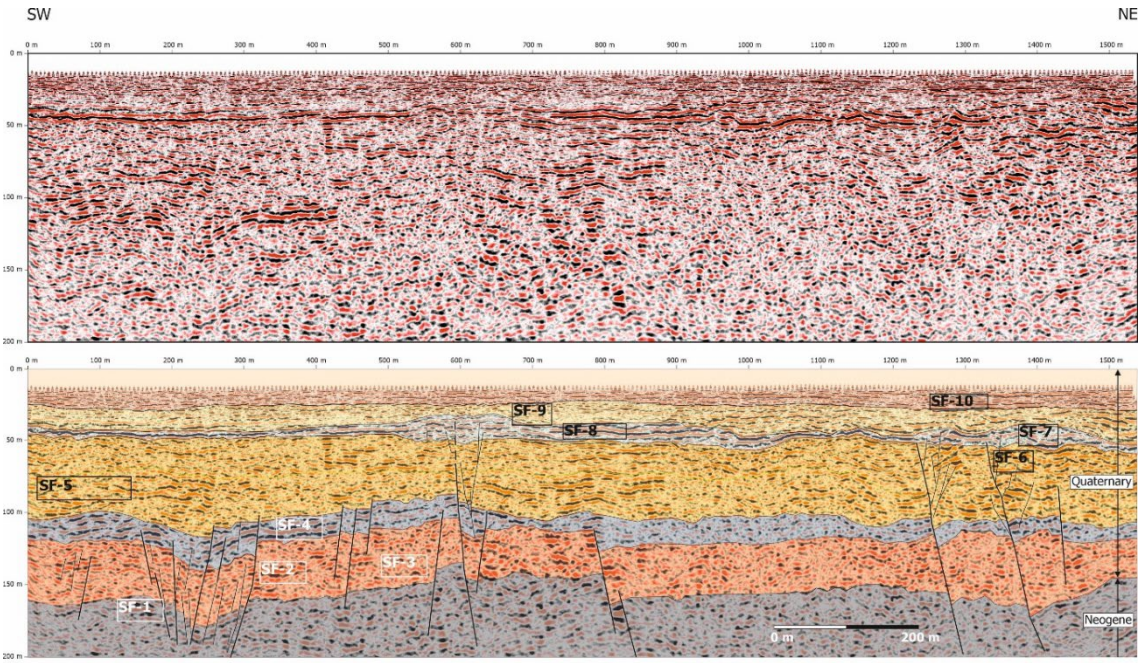

Figure 6.25. Seismic section, Part 1: Depth section image (top) and detailed interpretation (bottom). Elevation reference level (zero m line) is +30 m DNN. Approximately 2X vertical exaggeration.

The seismic interpretation carried out is largely based on the reflector attributes (e.g., strong, continuous, thick, narrow, diffuse) and the reflector pattern (e.g., parallel, inclined, convex, concave, lobe-shaped). Based on the geometries and the reflector pattern seven seismic

units and ten seismic facies types were defined based on Part 1 of the seismic survey (Figure 6.26). These units are subparallel and form a layer-cake structure (Figure 6.25).
Some seismic facies types are characterized by very continuous and subparallel, high amplitude reflectors that might represent the glacial tills that were drilled in the area. However, some lobe shaped reflector patterns resemble sedimentary bodies formed in a glaciolacustrine environment.

Based on well data, the material at the base of the seismic section is interpreted as top of the Neogene (indicated with the grey colour overlay). The material above is interpreted as the Quaternary, with different glacial tills included. The uppermost till is interpreted to have a Saalian age and the tills below are likely older. The material at the top of the seismic section is interpreted as the glacial outwash plain that is developed in this region. Based on the reflector pattern it is possible to subdivide the glacial outwash plain into two layers. This fits well with the idea of Friborg (1996) who noticed that there are two glacial outwash plains developed in parts of southern Denmark, a Saalian and a Weichselian one.

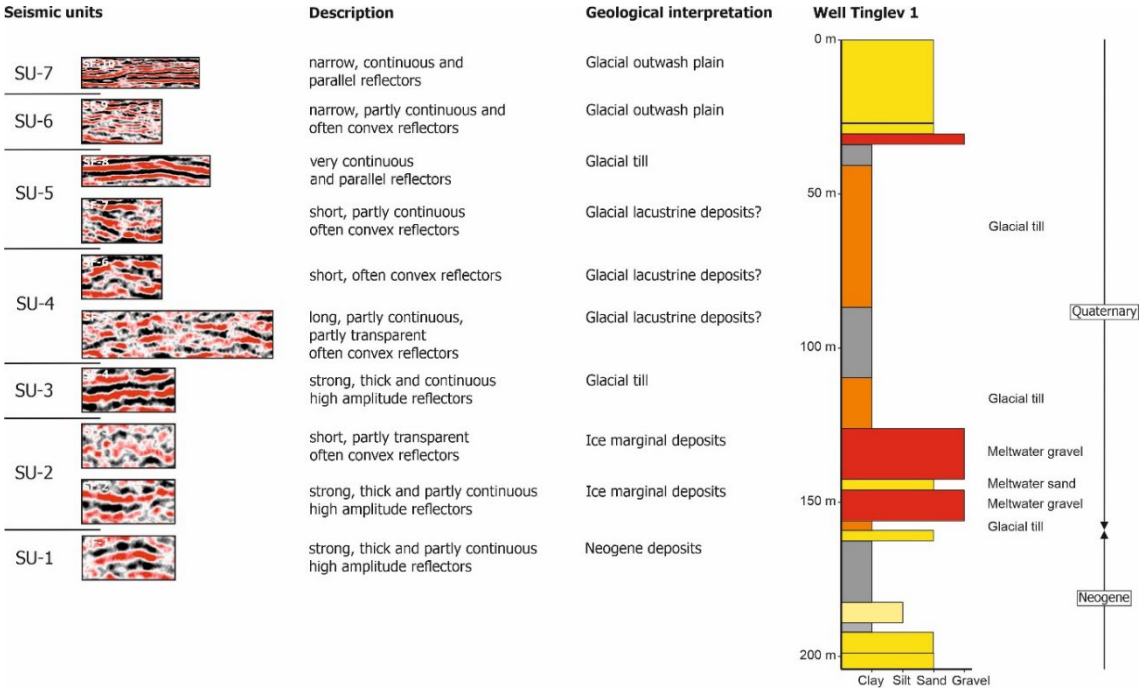

Figure 6.26. Seismic facies, their description and geological interpretation tied to Well Tinglev 1 (DGU no. 167.234A), which is located 362 m south of the NE end of the seismic section (regarding profiling position 1530 m at the horizontal axes).

The faults on the shear wave seismic sections are interpreted based on three different indicators that are summarized in Figure 6.27**.** At least two of the three fault indicators have to be present to interpret a fault. First of all, faults were interpreted by connecting a series of systematic reflector offsets and it is crucial that these reflector offsets can be traced vertically. Frequently, it can be observed that in a closely related group of faults, all faults show nearly the same dip angle. This supports the fault interpretation and reduces alternative interpretations, such as a coincidental alignment of reflector discontinuities that only mimic a fault. Furthermore, faults on the shear wave reflection seismic sections are often imaged as steeply dipping, thin transparent zones separating a stacked pattern of the reflector offsets. Faults

were also identified by abrupt lateral changes in the reflector pattern, regarding amplitude or phase characteristics. In rare cases, a fault shadow (a diffuse zone on a seismic section below a fault can be developed), also enables the identification of a fault trace. All faults interpreted in the seismic sections are normal faults. In most cases the displacement along the faults is in a range of several meters. The maximum fault displacement observed is approximately 16 m, near the centre of Part 1.

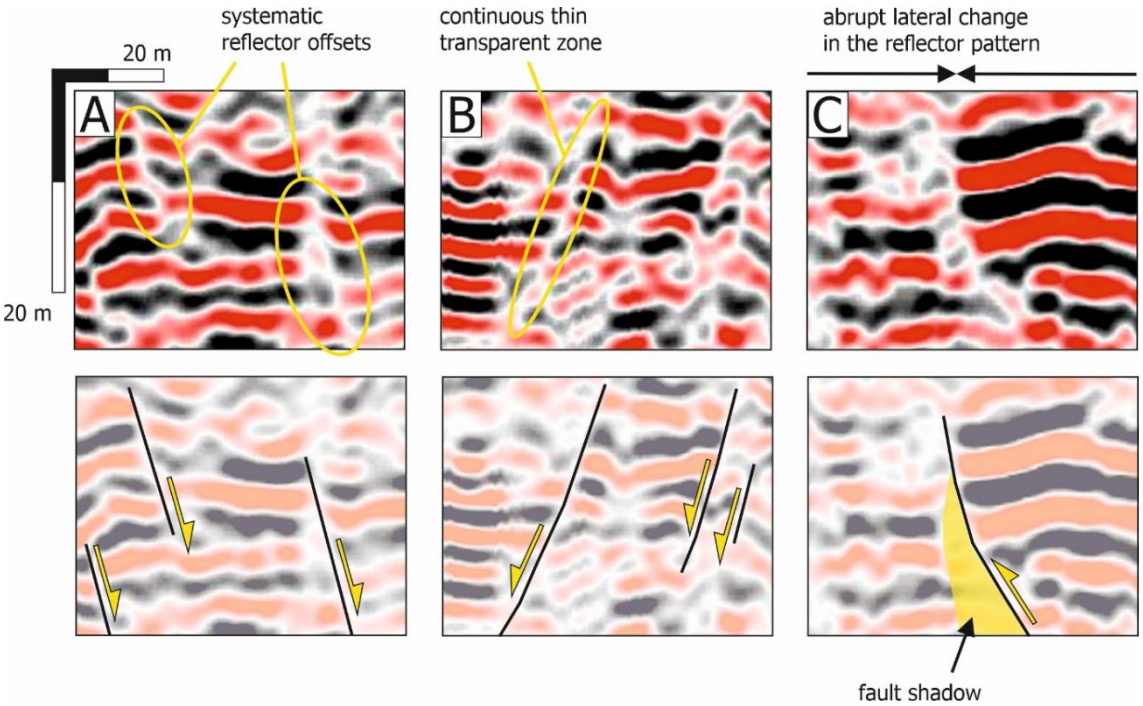

Figure 6.27. Indications for faults on the shear wave seismic sections (based on Brandes et al., 2022).

The faults were interpreted in detail on the western segment of the seismic survey (Part 1), which has a length of nearly 1530 m. The faults have mostly planar geometries, in rare cases faults show slight bends. There are clearly several normal faults developed, but a small graben structure at the southwestern end of the seismic section stands out (Figure 6.25). The seismic interpretation is supported by the seismic data derived shear wave interval velocity field, which is imaged below the interpreted section in Figure 6.28. There are no strong lateral changes in the interval velocities, which supports that the graben structure at the southwestern end of the section is a real feature and not caused by e.g. velocity driven pull-downs during depth conversion.

The tip lines of many of the faults stop at a depth of approximately 100 m. Based on the sediment thickness it becomes evident that the little graben (Figure 6.25, between 150 and 300 m) was active before the last till was deposited and there seems to be no later fault activity. In case of some of the faults, there was likely later fault activity and the faults may die out in the locally thick layer above interpreted as a till. No faults cut the Saalian till on this part of the seismic section, meaning that the fault activity seen on this part of the seismic section likely stopped during the Saalian glaciation or the following Eemian interglacial.

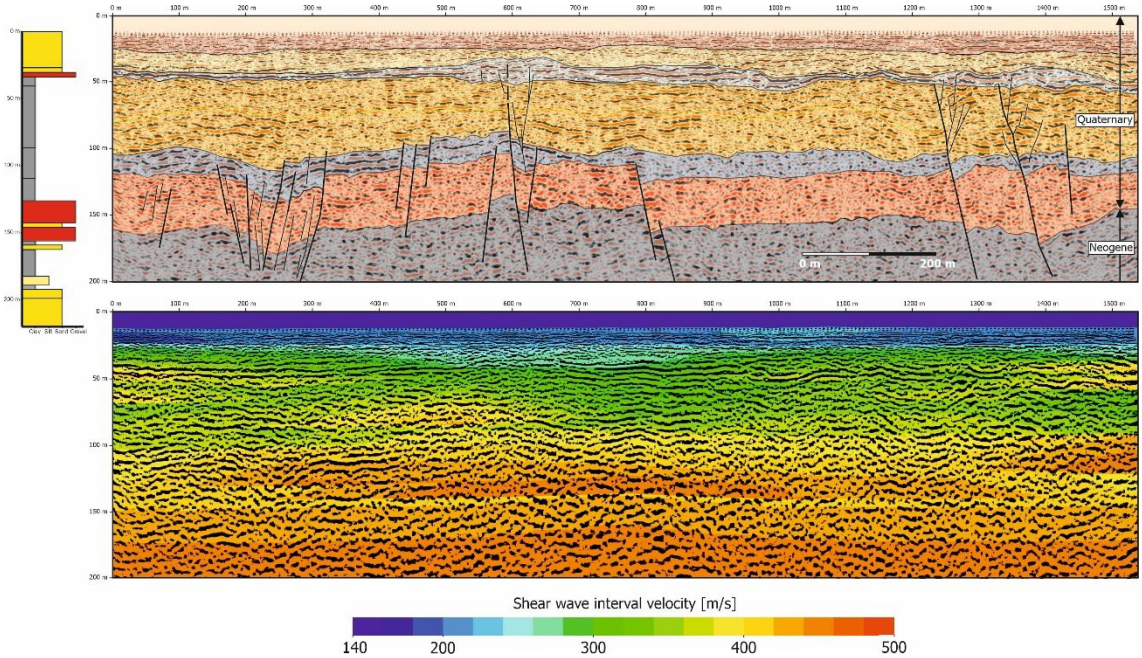

Figure 6.28. Interpreted seismic section (top panel) and the combined shear wave structure response and data derived interval velocity image (lower panel). Typically, shear wave interval velocity values below 250 m/s indicate less compacted young material, values of 250-400 m/s represent stiffer material, often indicating a higher clay content as a granular cementation. Values above 400 m/s indicate stiff sedimentary material, probably also compacted by glacial gravitation loads. Approximately 2X vertical exaggeration.

6.2.2 Interpretation of the central seismic section (Part 2):

Based on the detailed analysis and interpretations of Part 1 (Figure 6.25 to Figure 6.28), interpretations were continued towards the north-eastern parts of the profiling segments. The central section (Part 2) is shown in Figure 6.29.

With increasing distance towards northeast to the reference well Tinglev-1, the interpretation is hampered by the lack of well data, and therefore the interpretation of especially the deeper parts remains difficult. The Part 2 section images a synclinal structure in the western central part to at least 50 m depth (relative to the datum level 30 m DNN). The closely related faults at the south-western margin indicate a tectonic origin of this structure. However, an origin of this structure as an erosional feature cannot be ruled out, depending on the axis of the structure relative to the seismic profiling direction. Whereas the western part is dominated by fault traces following a NE dipping trend in the eastern part of the section Part 1 (Figure 6.25), the fault dip trend changes to mainly SW dipping faults towards the east in section Part 2. These features may reflect the uppermost part of the flanks of the Tønder Graben shown in the Figure 3.4 and Figure 3.5.

The upper parts of the section in Figure 6.29 shows a fair continuation of the layer-cake style that is common in the analysed sections. Horizons of strong amplitude response are seen at approximately 40 m depth, but in the part below 100 m depth the pattern tends to show predominant chaotic reflections without significant layer responses, indicating a disturbed or overprinted sedimentation. A trend of this change in seismic pattern image is also visible in the NE part of Part 1 (Figure 6.25**)**.

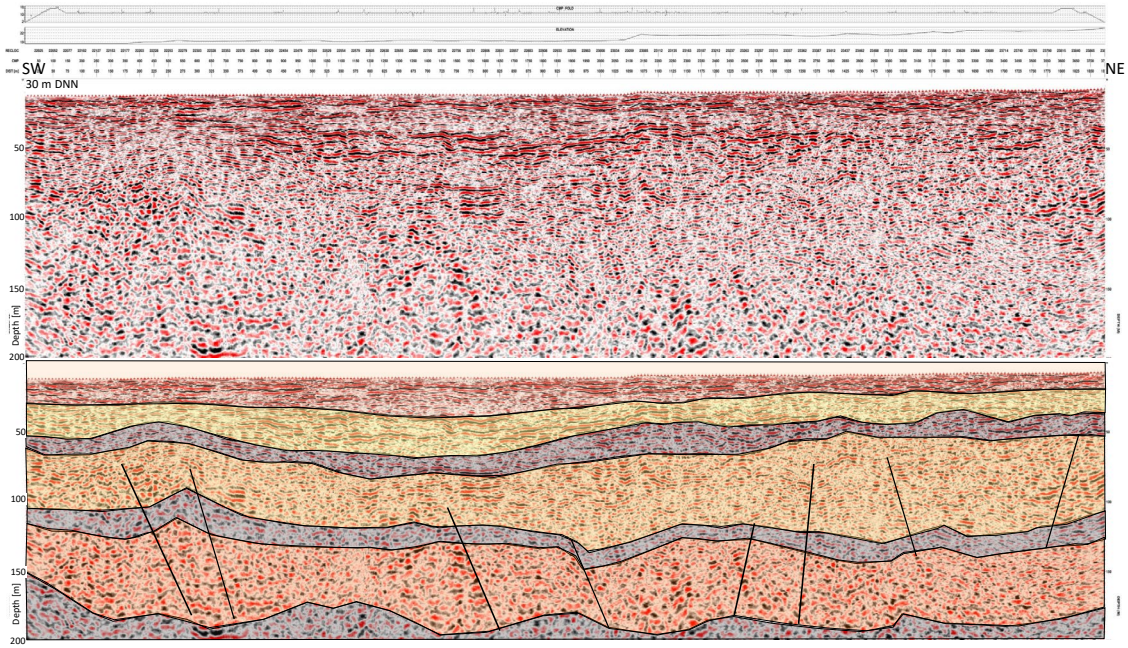

Figure 6.29. Seismic section, Part 2: Tentative interpretation of the seismic section in the centre part of the seismic profiling. Approximately 2X vertical exaggeration.

6.2.3 Interpretation of the easternmost seismic section (Part 3):

The eastern section (Part 3) is shown in Figure 6.30. Between sections Part 2 and Part 3 there is a gap of nearly 230 m perpendicular to the general profiling direction due to logistic reasons, so the direct profiling continuation was interrupted.

Compared to the section Part 2 (Figure 6.29) the reflection pattern in the upper layers (units SF8-10) within the 50 m depth range is more continuous, also reflector elements in the units SF6-7 are partly imaged. The fault traces show a mainly south-west dipping pattern and partly form a small local graben structure. The reflector pattern is less chaotic than in the section Part 2. The meltwater sand and gravel in the 30 m deep water abstraction well DGU no. 167.1497, shows that the uppermost units SF9 and SF10 represent the outwash plain sediments.

Figure 6.31 shows the SkyTEM profile SW-NE_BB6_A with geological interpretations made from SkyTEM and boreholes (see Figure 6.12). This SkyTEM profile is aligned nearly parallel to the seismic profile in about 1 km distance to the north (Figure 6.8). The red rectangle shown in Figure 6.31 represents the three parts of the seismic profiles shown in Figure 6.25, Figure 6.29, and Figure 6.30.

The combined figure of the SkyTEM and the geological interpretation in Figure 6.31, also shows the extent of the seismic sections as a red rectangle. In Figure 6.32, the seismic section interpretation results within the red rectangle are shown on top of the geological interpretations of boreholes and SkyTEM for comparison.

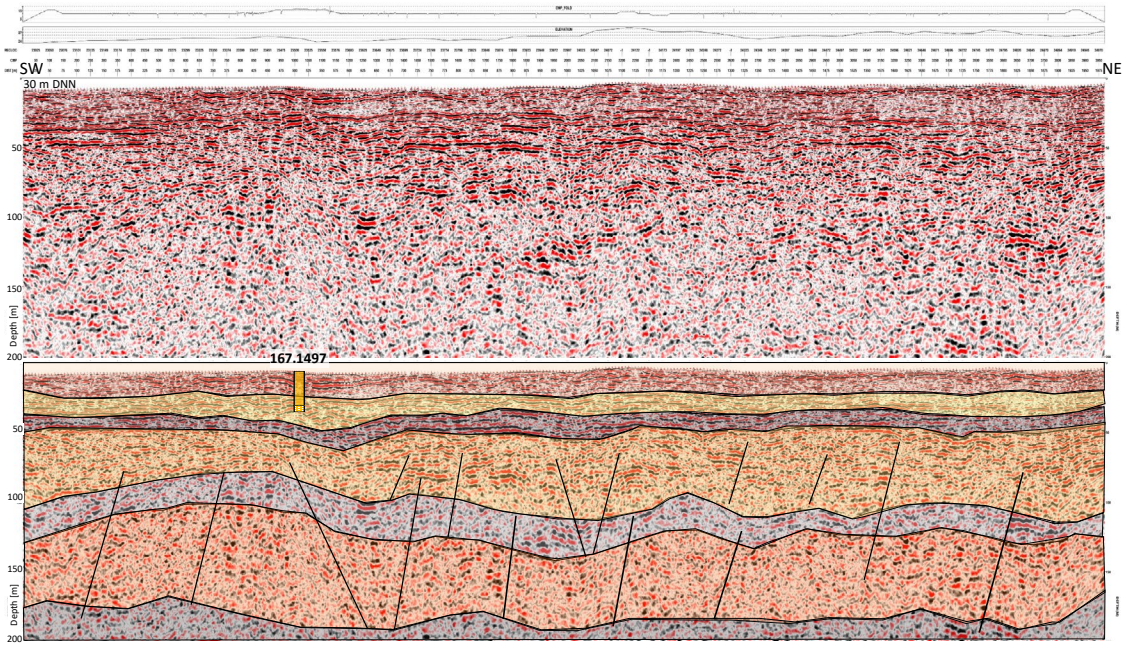

Figure 6.30. Seismic section, Part 3: Tentative interpretations of the northeastern seismic part of the seismic profiling. Approximately 2X vertical exaggeration.

Both interpretations show similar features regarding the upper depositional units, denoted by SF 9 and SF10 in the seismic sections and the “meltwater sand” layer with high resistivities in the SkyTEM. Also, the main normal faults that were interpreted in the south-east part is imaged at nearly the same position. The seismic units SF 4 to SF 8 are represented by relatively low resistivity in the SkyTEM, interpreted as clay tills. Below, the SF 2 and SF 3 units show high resistivity values in the SkyTEM, interpreted as sand units of Miocene and Quaternary age. Remaining differences in detail between SkyTEM and seismic results may result from the different location (~ 1 km distance) of the profiles.

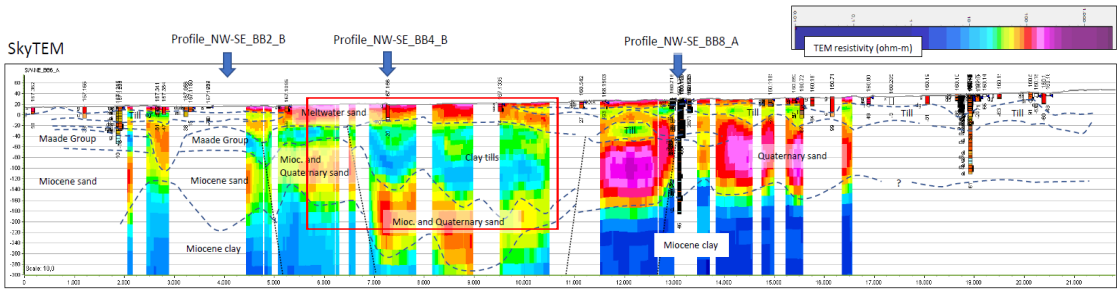

Figure 6.31. SkyTEM profile SW-NE_BB6_A (Figure 6.12) with geological interpretation included, running nearly parallel 1 km North of the seismic profiles. The red rectangle indicates the area of the seismic profiling results. Approximately 10X vertical exaggeration.

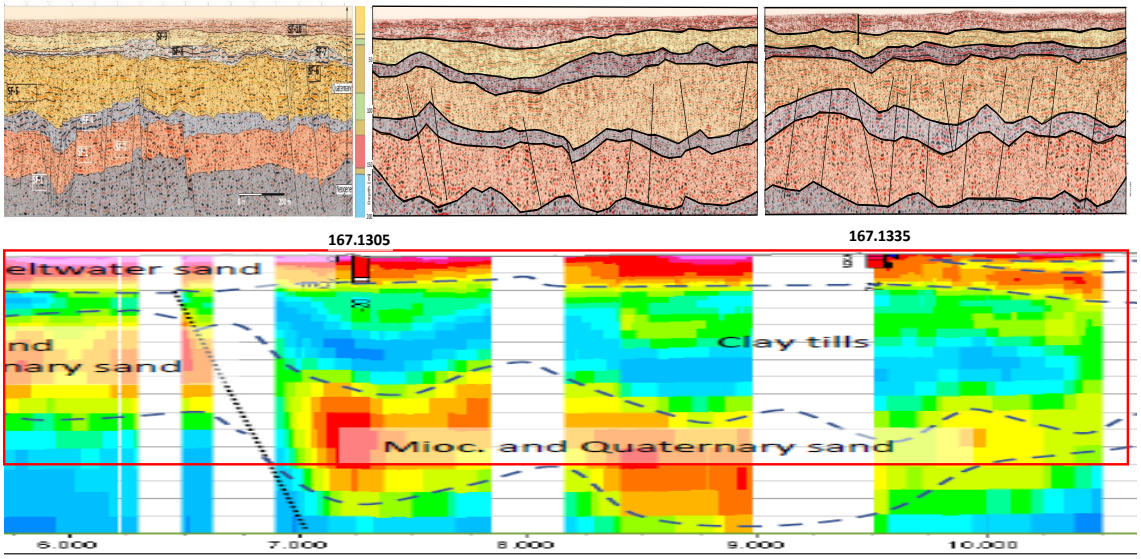

Figure 6.32. Joint image of a part of SkyTEM profile SW-NE_BB6_A with interpretation, and the seismic interpretation of the three profiling parts. Due to the nearly 1 km distance between the profiles of the SkyTEM and the seismic, different reference wells are annotated on section tops.

6.3 The geological architecture

6.3.1 Faults

As mentioned earlier, the Tønder Graben is expressed in the Top Chalk surface as elongate depressions oriented NW−SE and W−E (Figure 3.3; Ter-Borch 1991). These depressions are caused by faults offsetting the Chalk Group sediments in the order of up to a couple of hundreds of metres. Fault-related subsidence during the Neogene has been described, and some of the faults of the Tønder Graben are found to offset the sedimentary succession including the youngest Miocene deposits (Friborg et al. 2002; Jørgensen et al. 2012). Topographic analyses of the present-day terrain over the Tønder Graben have found that faults were reactivated in the early Holocene following the weight-relief from the Pleistocene ice sheets (Sandersen & Jørgensen, 2015). Even indications of strike-slip movements along the faults were found.

The subsurface architecture of the deep parts of the Tønder Graben is well illustrated by the seismic profile in Figure 3.4, and it is obvious that both the fault density and the amount of offset varies. The sketched geological profile in Figure 3.6 is based on a shallow seismic profile at Tinglev (Friborg et al., 2002), but basically it shows the same overall geological setting.

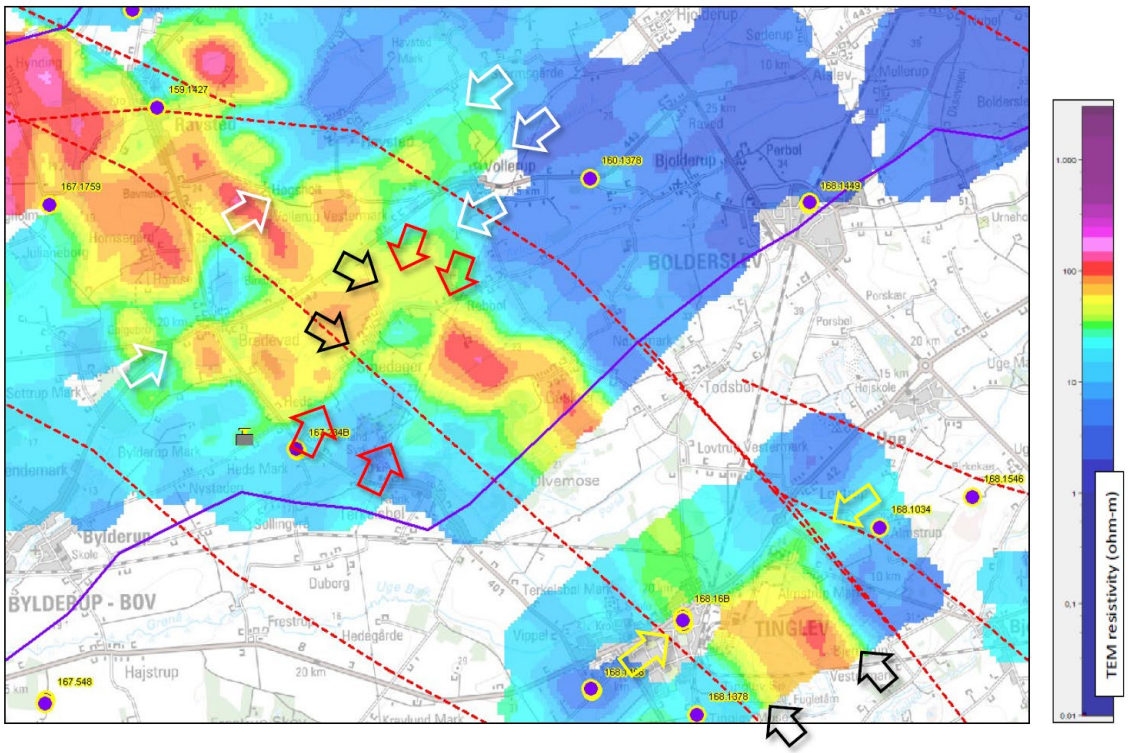

Figure 6.33. SkyTEM mean resistivity slice at -220 m a.s.l. (3D grid). Arrows highlights inferred faults Hatched red lines represent known deep faults, and purple dots mark boreholes deeper than 75 m.

Figure 6.33 shows the deep parts of the subsurface as a mean resistivity slice at -220 m a.s.l. The low resistivities (blue colours) represent Miocene and Palaeogene clays, whereas the high resistivities (yellow/red colours) represent deep sandy Quaternary sediments. The SkyTEM method is especially capable of mapping the depth to a good conductor, even at depths below 200 to 250 m, and the resistivity variations in Figure 6.33 are therefore considered credible.

As it can be seen, there appears to be orientational trends in the resistivity pattern:

- The black arrows outline the high-resistivity sediments in the deepest parts WNW-ESE to NW-SE trending parts of the graben structure
- The red arrows highlight resistivity shifts along NNE to SSW trends
- The yellow and white arrows highlights resistivity shifts along WSW-ENE trends

The WNW-ESE to NW-SE trend fits well with the main faults of the graben reaching the Top Chalk surface (red hatched lines), whereas the NNE-SSW to WSW-ENE trends are perpendicular or slightly oblique to the deepest high-resistivity parts of the graben.

Comparable observations of orientations were made by Sandersen & Jørgensen (2015) for the present-day topography (Figure 6.34). The overall orientation of areas with the highest variations in slope magnitude and slope orientation match the known orientation and location of the Tønder Graben, and – as highlighted by yellow arrows – there are sharp boundaries between areas with marked differences in the topography. The orientation of these lineaments falls into the same NNE-SSW to WSW-ENE interval as observed for the deep trends at -200 m a.s.l. (Figure 6.33). This strong correlation between the structures at depth and in the topography underlines that the structure of the Tønder Graben is reflected all the way

from the deep Mesozoic sediments to the present-day terrain. This also means that numerous faults offsetting parts or all of the sedimentary succession can be expected to be present, creating a complex geological architecture.

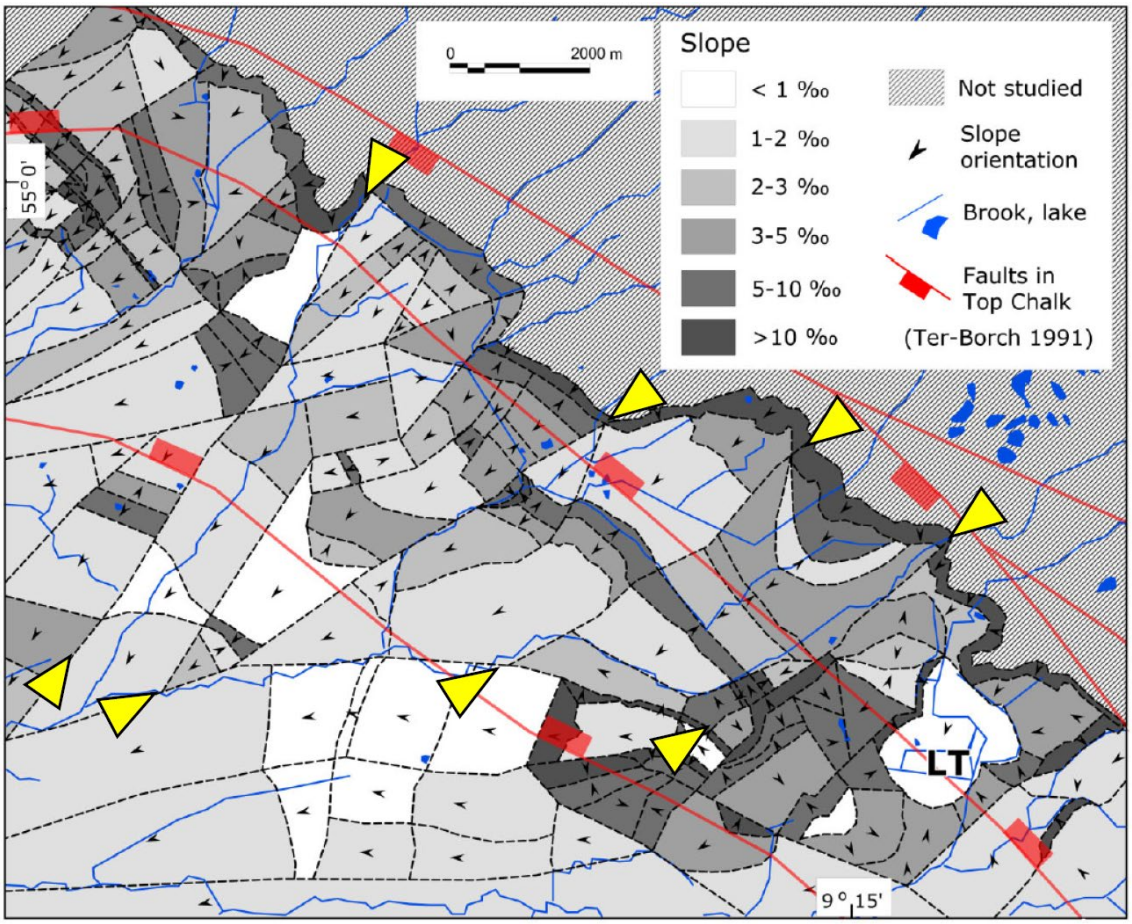

Figure 6.34. Slope magnitude (grey shades) and slope orientation (small black arrows) for the Bylderup-Bov -Tinglev area (modified from Sandersen & Jørgensen, 2015). The map view is more or less the same as seen in Figure 6.33.

6.3.2 Glaciotectonics and erosion

In the preceding sections it has been described that large parts of the sedimentary succession have been deformed and reworked by the Pleistocene glaciers. On Figure 6.17, it can be seen that the low-resistive clay – which on this figure is shown at -80 m a.s.l. – appears to have a NNE-SSW orientation extending to south of Ravsted. The similar low-resistivity structure to the southeast (between Ravsted and Vollerup) – as mentioned earlier – is the other flank of a large anticlinal fold shown to the left on the profile in Figure 6.19. The fold is also seen in Figure 6.18, but here the folded clay till seems to have been eroded away at the top of the anticline. The high-resistive sediments between the two low-resistive structures represent the Quaternary sand underneath the folded clay till.

This anticlinal clay structure seems to reach farther to the southwest than a line between the purple arrows in Figure 6.5, but here the clay layer changes from an anticline to stacked clay

layers in a more complicated setting of low-resistive layers. In the central part of Figure 6.35 a stacking of two till successions is clearly seen: here a slab of clay tills has obviously been pushed to the southeast (to the right) over deeper-lying clay tills. This shift to a more complicated picture coincides with where the Tønder Graben attains the largest depths. As the profile in Figure 6.35 is located just southwest of the profile in Figure 6.19, this most likely indicates a more intense south-eastward deformation of the anticline and eventually thrusting of the clay tills.

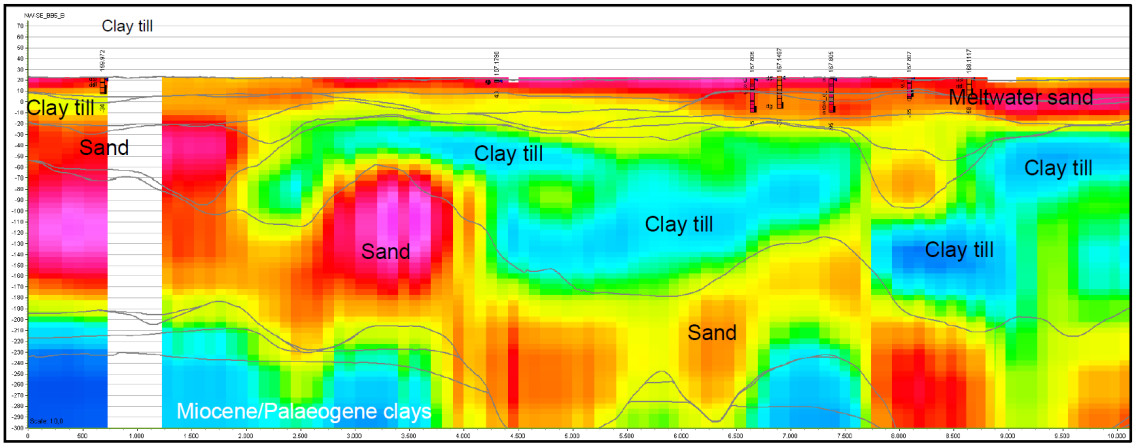

Figure 6.35. Profile NW-SE_BB5_B just northeast of Ravsted. The profile shows a vertical profile through the 3D grid of the SkyTEM data. Boreholes are seen as coloured vertical rods with outline and annotations. Thrusting of the clay tills is seen in the centre of the profile.

The deformations, as they can be seen on Figure 6.35, reaches from ca. -20 m and down to at least -180 m a.s.l. which is more or less the same as for the fold just to the northeast (Figure 6.19). The folded structure covers an area of around 5 x 7 km or more, and the deformations involve the sediments from -20 to -30 m and as deep as -200 to -250 m a.s.l. Even though the deformations have a pronounced impact on the sedimentary succession, the shape of the folded structure shows that this probably is the result of one major episode of glaciotectonics that affected all of the sediments down to the top of the deep Miocene clay sediments. The apparently higher intensity of deformation inside the main parts of the Tønder Graben, could indicate differences in the subglacial hydrostatic pressure inside the deep, sandy parts of the graben compared to outside the graben.

To the northeast, the folded clay layer gets thinner and is found at a higher elevation, where the thinning is the result of erosion. Glaciotectonic deformation is seen here as well, and the sediments are also reworked, and thus have a Quaternary age presumably all the way down to the oldest clayey Miocene sediments.

The deep boreholes within the Tønder Graben in the Tinglev area south of the BB model area also point to deep Quaternary deformations. In borehole DGU no. 168.1228, for instance, clay samples down to a depth of 218 m contain shell fragments of both Miocene and Quaternary species, feldspar, and fragments of igneous rocks. This points to a sedimentary succession of reworked Miocene sediments mixed with Quaternary material. Previous interpretations of a very thick succession of Miocene Maade Group clay within the graben caused

by subsidence during the Miocene (Friborg et al. 2002; Rasmussen et al. 2010) may therefore instead be the result of stacking of thrusted clayey slabs of reworked Miocene clayey sediments within the graben. Other deep boreholes point in the same direction.

6.3.3 How to distinguish between glaciotectonic faults and faults related to the movements of the Tønder Graben?

As shown above, there is a match in orientations between the deep parts of the mapped sedimentary succession and lineaments in the topography. This points to an impact from the faults of the Tønder Graben on all of the sediments above. However, between around -30 and -160 m a.s.l., the sedimentary succession has been disturbed by glaciotectonics, and the orientation of the large-scale folding has an orientation that is different from the orientations of the faults mentioned above. Judged by the orientation and by the stacking of the clay layers, the folding is likely the result of an ice advance from the NW, presumably during the Elsterian Glaciation or alternatively by the Drenthe ice advance in the Saalian (Drenthe; c.f. Sjørring & Frederiksen, 1980). The upper parts of the Quaternary succession have not been deformed by this ice advance, but instead by a later ice advance during the Saalian with comparatively less deformation.

The deformations caused by the older ice advance may have destroyed or overprinted most of the faults (between ca. -20 to -200 m a.s.l.) created by the reactivation of the Tønder Graben, so only the deep parts of these faults (below the glaciotectonic deformations) would have a chance of being recognized on the seismic sections. As described in the preceding, the data and the modelling point to reactivations of the faults of the Tønder Graben after at least the two latest glaciations and probably also after older ones, so a series of subsequent fault reactivation events can be expected in the area during the Quaternary.

The glaciotectonic deformations would theoretically be dominated by low-angle thrust faults (e.g. Aber & Ber, 2007), whereas faults related to offset along the Tønder Graben faults would be expected to be rather steep normal, reverse and strike-slip faults.

6.3.4 Buried valleys

Several buried valleys mapped with varying uncertainty are found within the BB model area:

Øster Højst/Bylderup-Bov: A buried valley is found from east of Øster Højst and towards south to Bylderup-Bov (see red arrows on Figure 6.36). The valley is around 1 to 1½ km wide and reaches down to around -140 m a.s.l. The valley is clearly eroded into the low-resistivity clay layers as seen on Figure 6.9 at 5,000 m on the profile. The valley is filled with meltwater sand and gravel.

Marked by a yellow arrow on Figure 6.36 is a W-E oriented buried valley that appears to be eroded by the N-S valley. The two valleys appear to have more or less the same depth. The E-W valley is the eastward continuation of a large, 20 km long primarily W-E oriented buried valley (Sandersen & Jørgensen, 2016), but according to the SkyTEM the valley appears to

stop a few kilometres into the BB model area. The valley reaches down to around -320 m a.s.l. farther to the west outside the BB model area.

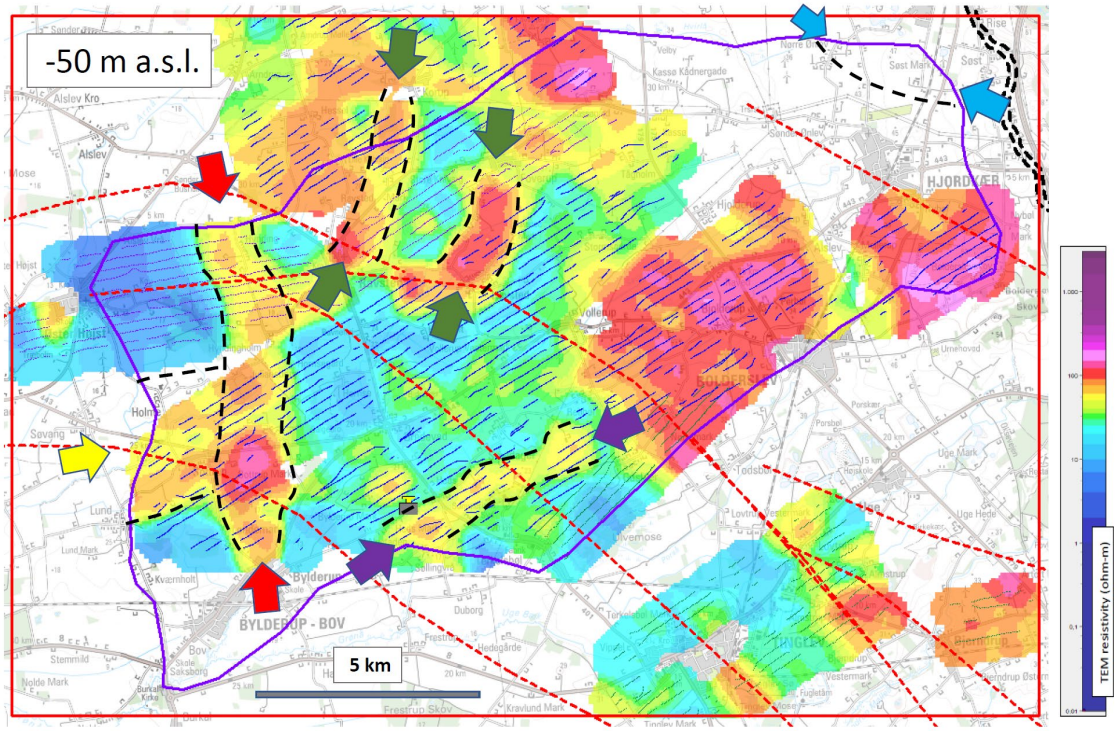

Figure 6.36. Buried valleys sketched on the SkyTEM mean resistivity map (-50 m a.s.l.). Arrows highlight interpreted buried valleys; see text for explanation.

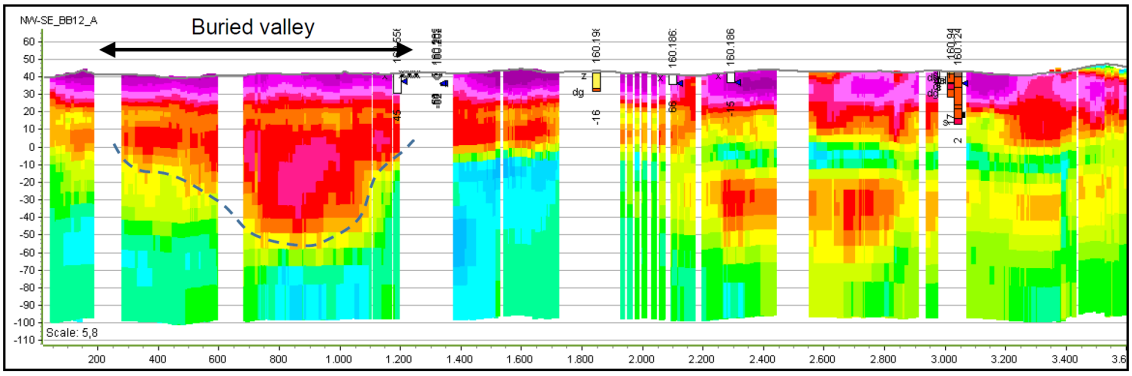

Figure 6.37. Profile NW-SE_BB12_A, oriented N-S. The extent of the buried valley is marked with a black arrow.

North of Terkelsbøl: A SW-NE oriented, 4½ km long and 1 km wide high-resistivity structure is tentatively interpreted as a mainly sand-filled buried valley (marked with purple arrows on Figure 6.36). The depth is varying, but maybe down to -100 m a.s.l. The structure appears to be erosive and may therefore be a buried tunnel valley (Profile NW-SE_BB4_B., Figure 6.14). But there is a possibility that the structure is sand in a syncline created by glaciotectonics or erosion along a fault zone perpendicular to the Tønder Graben.

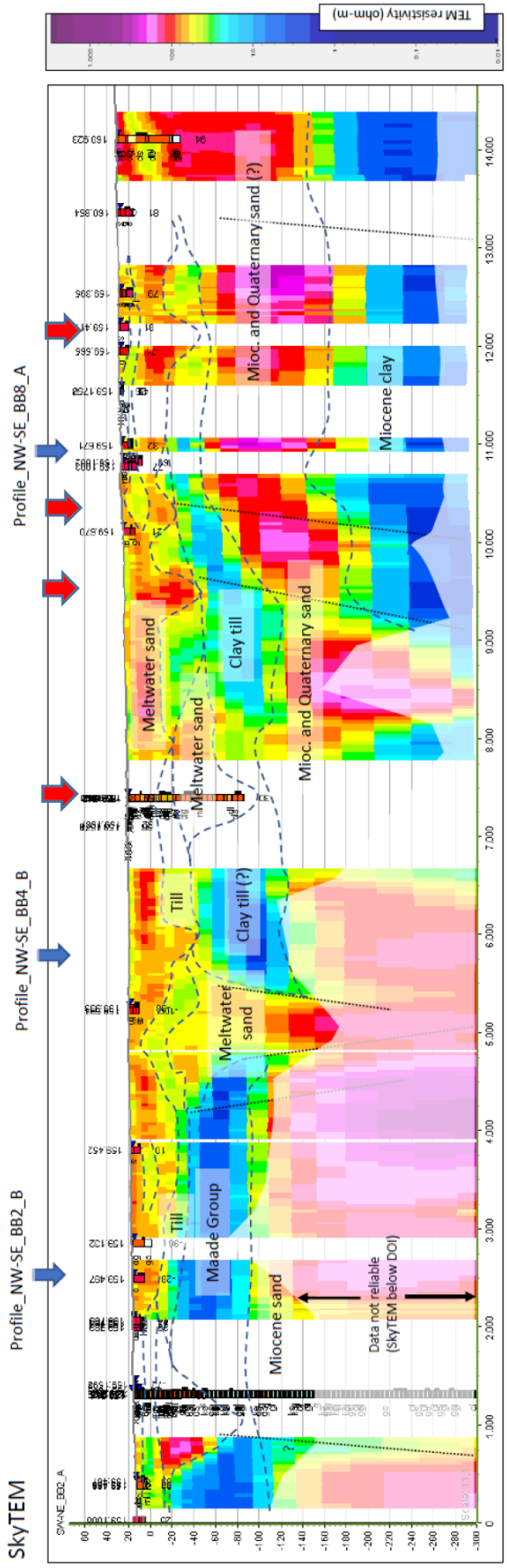

Figure 6.38. Shallow buried valleys marked with red arrows. Sketch of geological interpretations along Profile SW-NE_BB2_A. For location, see location on Figure 6.8.

Hjordkær/Aabenraa: A buried valley in the north-easternmost corner of the BB model just north of Hjordkær has been mapped with tTEM as seen on Figure 6.37. The valley is oriented WNW-ESE and is between 800 and 1200 m wide (see at blue arrows on Figure 6.36). The valley reaches down to around -50 m a.s.l. and is primarily sand-filled. The valley appears to be the westward continuation of a valley mapped earlier in the northern part of Aabenraa (Sandersen & Jørgensen, 2016). Another buried valley south of Hjordkær (also mapped earlier) by the use of gravimetry and seismic profiles, could not be verified by the SkyTEM or the tTEM data.

Ravsted: A number of possible shallow buried valleys around Ravsted are highlighted on Figure 6.36 with green arrows, and with red arrows on Figure 6.38.

The possible valleys shown on Figure 6.36 seem to be closely related to the large-scale fold described earlier. The easternmost structure is located parallel to and at the crest of the fold, where the fold appears to be eroded. Whether the high-resistivity structure is a result of glacial erosion of the top of the fold or actually is a buried tunnel valley eroded by meltwater at the crest of the fold cannot be determined. At deeper levels, the sandy core of the fold emerges, and the high resistivity area widens, as described earlier. The high-resistive structure just to the west is poorly documented but could represent a valley structure also related to the fold.

The shallow valleys, marked with red arrows on Figure 6.38 are only 20 to 40 meters deep and have widths of up to ½ km. The lengths and orientations of the structures are difficult to determine and it is questionable if they are valley erosions per se. Some of them have erosional characteristics pointing in that direction, but others do not. Some could be elongated structures created by glaciotectonics, such as for instance a syncline with sand layers.

6.4 Overview

The BB model area can be divided into 7 sub-areas with different geological architectures (Figure 6.39). The sub-areas are shortly summarized in the following:

Sub-areas A and B (see to the left on Profile SW-NE_BB2_A, Figure 6.9, and Profile SW-NE_BB6_A, Figure 6.12):

Here the Miocene succession is more or less undeformed with up to 80 m clay of the Maade Group at the top. Above, the Quaternary succession consists of clay tills and meltwater sand/gravel of a total thickness of up to 50 m. Faults are interpreted to be present along the boundary to sub-area E.

Sub-areas C and D (see at 5,000 m on Profile SW-NE_BB2_A, Figure 6.9, and at the centre of Profile NW-SE_BB2_B, Figure 6.13):

The two buried valleys E-W (sub-area C) and N-S (sub-area D) are both eroded into the Miocene clay and filled with mostly sandy meltwater sediments. The N-S valley is eroded into

the E-W valley and is therefore youngest. To the north, the 'D'-valley appears to be located over the fault zone along the boundary between sub-area A and E (Profile SW-NE_BB2_A).

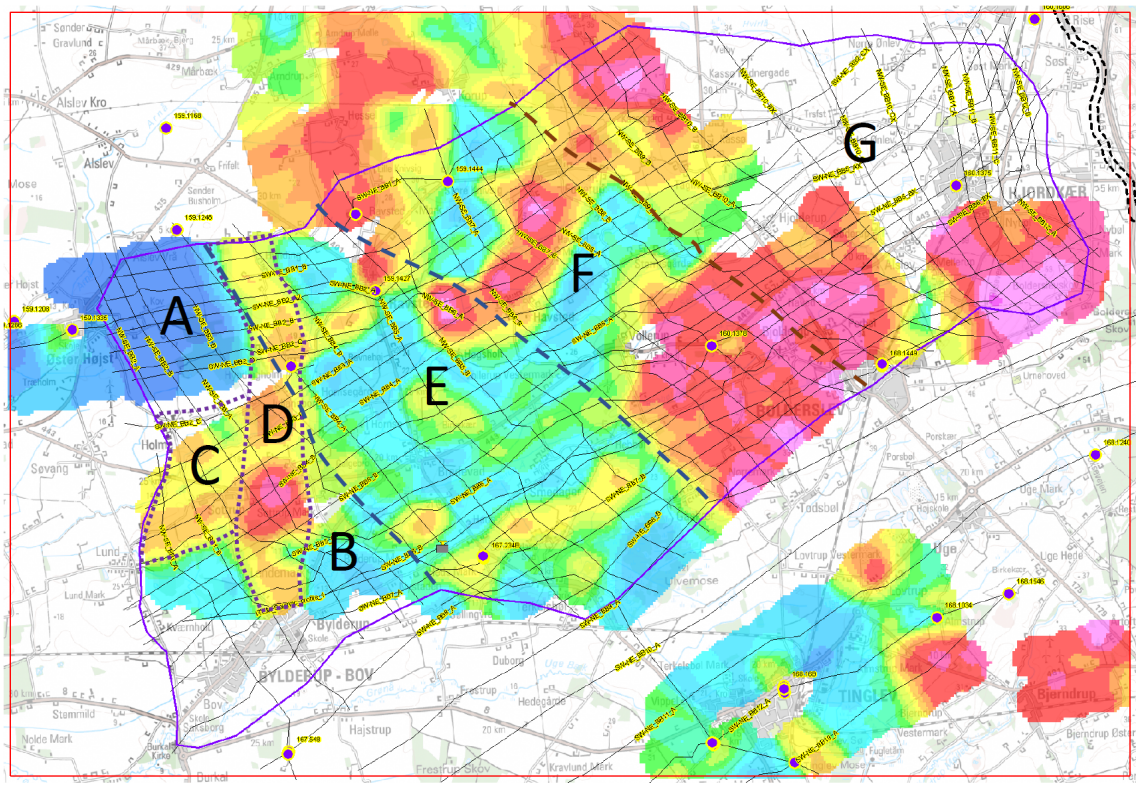

Figure 6.39. Selected sub-areas with different geological architecture within the BB model area. Background is SkyTEM mean resistivity slice at -50 m a.s.l. See text for explanation.

Sub-area E (see on Profile SW-NE_BB6_A between 5,000 and 11,000 m, Figure 6.12, and along Profile NW-SE_BB4_B, Figure 6.14):

This area lies over the deepest parts of the Tønder Graben, where the clayey and oldest parts of the Miocene in places are downfaulted to below -300 m a.s.l. or maybe even more, as it can be seen on Profile SW-NE_BB6_A. The Quaternary sediments above has a sand dominated lower part, and above a thick and clearly deformed layer of clay tills. Thrusting of the clay from a north-westerly direction is evident on some profiles (see earlier descriptions). The succession is presumably deformed by both glaciotectonics and deep tectonics. The clay thickness is up to around 150 m. Faults are interpreted to be present at the boundary to sub-area F.

Sub-area F (see Profile NW-SE_BB8_A, Figure 6.15):

In this area, the top of the oldest low-resistive Miocene sediments lies around 150 m higher than within the main part of the Tønder Graben to the southwest. The Quaternary succession above, from -160 up to around -20 m a.s.l., is heavily deformed – especially visible for the clayey parts as a large-scale fold that reaches across the entire sub-area. The clay, however, is only present in the northern two-thirds, whereas to the south, the clay abruptly diminishes and only attains negligible thicknesses farther south. The uppermost parts of the Quaternary

succession are only slightly deformed and clearly younger than the event that created the deeper deformations.

Sub-area G (see from 10,000 to 12,000 m on Profile SW-NE_BB2_A, Figure 6.9):

In sub-area G, the degree of glaciotectonic deformation is less pronounced as to the south-west, despite its location at the MSL and the clay till layers attain far lesser thicknesses. The deep parts of the Miocene succession are interpreted to lie at more or less the same elevation as in sub-area G. The Quaternary succession is dominated by sand, and as in sub-area G, the southern part is almost totally dominated by sand. In the north-easternmost corner of sub-area G, the southern flank of a buried valley is seen as a high-resistive structure. The elevation of the top of the Miocene sediments is uncertain.

6.5 Geological event chronology

The geological events which are interpreted to have formed the subsurface of the BB model area are sketched in Table 6. The Geological Event Chronology (GEC) is based on observations and interpretations within and outside the model area and it serves as a chronological framework supporting the understanding of which events likely created the subsurface as we see it today (e.g. Sandersen & Kallesøe, 2021). The GEC for the area is not complete, lacks dating of sediments, and has many unknowns, but it can serve as a basis for further work in the area because all new observations should be able to fit into the series of events. If they do not, the new interpretations should lead to a revision of the GEC adding details about new, previously unknown events.

6.6 Uncertainties related to the geological model

As described previously, an uncertainty assessment has been appointed to every interpretation point of the BB model. This is an estimation of the interpretation uncertainty at specific locations along the profiles that can be used to illustrate the uncertainty related to the individual layer boundaries of the model, that can be used in subsequent groundwater modelling (Høyer et al., 2024).

Apart from this way of conveying the modellers evaluation of the interpretation uncertainties, more general issues can be put forward (see Høyer et al. 2024 and Sandersen et al. 2018):

<u>Uncertainties related to borehole data:</u>
Boreholes may have very detailed sample descriptions and be very accurately located, but if the drilling depth is limited, information is only gained of the near-surface geology. Only very few boreholes are penetrating all of the sedimentary succession that is of interest in the modelling. This is a common problem, but the consequence is that the deeper we get, the more uncertain are the interpretations of lithology and thereby origin of the sediments. If deep borehole data is present, the quality of the borehole descriptions is very important. Standard drilling procedures vary, and the quality of the sediments samples is highly dependent on the

drilling method and the handling of the samples. As seen in the preceding, due to glaciotectonic deformation and glacial reworking some deep boreholes have ambiguous sample descriptions and age determinations – are they Quaternary or are they Miocene? In the geological modelling, these issues have been discussed, a number of observations have been made, and interpretations performed.

Table 6. Proposed geological event chronology of the Bylderup-Bov model area

Suggested age	Event	Description
Middle to Late Miocene	Deep tectonics	Reactivation of the Tønder Graben faults. Downfaulting of the Miocene sediments within the graben structure.
Elsterian or older	Buried valley erosion	The E-W buried valley in the western part of the model area is formed as a tunnel valley.
Elsterian or older	Glaciotectonics	Deformation, reworking, and erosion of downfaulted Miocene sediments (ice advance presumably from NW). The resulting Quaternary succession has a large content of reworked Miocene material. Large scale folds and thrusts are formed. The deformations appear to have been most intense in the deepest downfaulted parts of the graben. Glacial erosion appears to have been most intense outside the Tønder Graben to the northeast.
Holsteinian or older interglacial	Marine sedimentation, deep tectonics	Reactivation of deep faults induced by the weight relief from the ice sheet. Possible marine sedimentation in low-lying areas created by glaciotectonic deformation, tunnel-valley erosion, or subsidence within the Tønder Graben.
Saalian (Drenthe?)	Buried valley erosion	Erosion of a N-S tunnel valley (to the NW in the model area) by an ice advance from a northerly direction.
Saalian (Warthe?)	Glacial sedimentation and erosion, glaciotectonics	Repeated ice-advances and retreats created a series of tills and meltwater sediments above the deeper and highly glaciotectonically deformed sediments. The sediments are slightly to moderately deformed presumably from northerly directions. Erosion and subsequent infilling of shallow valleys.
Eemian	Deep tectonics, marine sedimentation	Reactivation of deep faults induced by the weight relief from the ice sheet. Eemian marine sediments were occasionally deposited in depressions created by glaciotectonics, tunnel-valley erosion, or in subsided parts of the Tønder Graben.
Weichselian (around the Last Glacial Maximum)	Glaciotectonics	Glaciotectonics at the Main Stationary Line (MSL) in the easternmost part of the model area.
Weichselian/Late Weichselian	Outwash plain sedimentation	Sandy and gravelly sedimentation on the outwash plain west of the MSL
Early Holocene	Deep tectonics	Reactivation of the faults of the Tønder Graben and subsidence induced by the weight relief from the ice sheet. Creation of both highs and lows in the topography.
Early Holocene	Sedimentation in lakes and bogs	Sedimentation in the created depressions.

Uncertainties related to the geophysical data

The use of geophysics, especially the TEM, has enabled valuable mapping of the subsurface in 3D down to around 300 meters or more. However, because it is an indirect method it gives a picture of electrical resistivity variations of the subsurface which cannot directly be converted to lithology. As the foot-print is large at depth, the degree of detail diminishes as we

go deeper because the method creates resistivity averages over large volumes. This, in combination with 3-D effects due to a high degree of complexity inevitably creates interpretation uncertainty. Added to this are the common issues with data density and the interpretation of the lithology based on resistivities.

The three parts of the seismic survey are performed along one SW-NE oriented line with horizontal offsets between. Because the SkyTEM and the seismic are not located at the same geographical positions, differences between the interpretations of the two datasets when compared will inevitably be present. The SkyTEM survey has an aerial coverage enabling 3D interpretations, whereas the seismic is along a line which for obvious reasons limits the interpretations to 2D.

The area has a very complex geological setting with deep faults and glaciotectonics that shows large horizontal variability which challenges the interpretation of the geophysical data. The deep faults which are related to the Tønder Graben are expected to be steep, and related to the outline of the graben, while the glaciotectonic faults are expected to be predominantly low-angle thrusts dipping in N-NW directions more or less coinciding with the axis of the graben. The seismic sections are therefore presumably more or less perpendicular the bounding graben faults, but parallel to the strike of the glaciotectonic thrusts. This should be taken into consideration when interpreting the geophysical data.

Uncertainties related to the handling of layer boundaries

In a layer model, once the point interpretations have been made, interpolation creates the layer boundary surfaces. In this process, interpolation artefacts are commonly introduced. Some issues can be addressed when choosing interpolation method and procedure, but generally, intense variations in elevation of a given surface is problematic. For example, deep and narrow buried valley structures often cannot be correctly modelled at the bottom of the valleys because the interpolation is not reaching deep enough. A consequence of this is that some erosions are not modelled correctly unless fictitious interpretation points are introduced to force the interpolation deeper. Similar problems may occur for glaciotectonic structures.

The used FOHM layers in the area are generally based on relatively few interpretation points. This creates complex layer variations locally that not necessarily can be justified by data. The BB model focus on the uppermost parts of the succession but includes modelling of the bottom of the Quaternary sediments. In the BB model, the bottom of the Quaternary sediments (layer boundary ‘2400’) has been modelled to deeper levels than in the FOHM model. In the layer adjustment, this has resulted in pushing down of the Miocene FOHM layers below. This may have resulted in artefacts – especially where the ‘2400’ boundary experience the largest variations.

Uncertainties related to the Pre-Quaternary surface

As mentioned above, there are uncertainties related to the determination of the top of the Pre-Quaternary sediments, because borehole data in some cases are ambiguous and because the SkyTEM cannot resolve individual layers at depth. In addition to this, biostratigraphical analyses are scarce.

Uncertainties related to layer-cake modeling of complex geology

The Bylderup-Bov geological model is made as a layer-cake model where boundary surfaces define the layer succession. This has been chosen because the intention was to fit the new geological model into the national hydrostratigraphic 'FOHM model' by using the same layer definitions. Using a layer-cake modelling approach in a very complex geological setting, however, has limitations because all lithological and structural variations must be modelled with 2-D layer boundary surfaces. In complex geology, the use of voxel modelling (cube stacking in the 3-D space), or a combination of layer-cake modelling, and voxel modelling would be preferable (Jørgensen et al., 2015). Using only layer modelling therefore adds uncertainties because complex lithology will be simplified to fit the layer sequence, deep erosions will create steep layer boundaries, and faults will be treated as flexures. This should be taken into consideration when evaluating the results of the final model.

7. Focus points for the hydrological modelling

Compared to earlier geological model interpretations, the impact of large-scale glaciotectonics, deep tectonics, and intense erosion has changed the 3D architectural conception of the model area. New data acquisition has given a better understanding of the subsurface, but this new conceptual understanding has added geological complexity that may have consequences for the groundwater flow and vulnerability.

Based on the geological modelling, a few suggested focus points for the hydrological modelling can be sketched:

Presence of faults

- Faults related to the Tønder Graben can offset the sedimentary succession and can create obstructions for horizontal groundwater flow
- Faults can create possibilities for a larger vertical groundwater transport, owing to presence of offsets of clay layers otherwise shielding the aquifers from surface contamination

Glaciotectonic deformations, glacial reworking, and glacial erosion

- The glaciotectonic deformations and the glacial reworking of especially the sediments within the Tønder Graben means that deformed Quaternary sediments are surrounded by clayey Miocene sediments outside the deepest parts of the graben
- The deformed and reworked Quaternary sediments can be expected to have different physical properties compared to the Miocene sediments
- Large amounts of the Miocene and the Quaternary successions have been eroded away to the east and southeast. The thickness of the Quaternary clay layers has thereby been significantly reduced in large areas

Deep valley erosions

- Several deep, sand-filled valley erosions are present in the area, creating potential local corridors for both horizontal and vertical groundwater flow

Properties of the Miocene versus the Quaternary sediments

- The Miocene sediments in the area consists predominantly of clay layers and clayey sand
- The highly deformed Quaternary sediments at depth have higher resistivities compared to the resistivities of the Miocene sediments, pointing to a generally higher sand/silt content and thus higher hydraulic conductivity.

8. References

Aarhus University, 2025. tTEM Mapping Bylderup-Bov. Report number 13032025, March 2025. Hydrogeophysics Group, Aarhus University. Performed as a part of the Interreg Blue Transition project, 45 p.

Aber, J.S. & Ber, A., 2007. Developments in Quaternary Sciences, Glaciotectonism. Elsevier, Volume 6, 2007, ISSN 1571-0866, ISBN 9780444529435

Andersen, L. T., & Pedersen, S.A.S., 2025. Piggyback imbrications, duplex stacking and sequential superimposed deformation in the Fanø Bugt Glaciotectonic Complex, Danish North Sea. GEUS Bulletin, 59. https://doi.org/10.34194/t407hg84.

Andersen, L. T., Anthonsen, K. L., & Jakobsen, P. R., 2024. Danmarks Digitale Jordartskort 1:25.000. Version 7.0. GEUS. Danmarks og Grønlands Geologiske Undersøgelse Rapport Vol. 2023 No. 29, https://doi.org/10.22008/gpub/34696.

Andersen, L. T., Hansen, D. L., & Huuse, M., 2005. Numerical modelling of thrust structures in unconsolidated sediments: implications for glaciotectonic deformation. Journal of Structural Geology, 27(4), 587-596. https://doi.org/10.1016/j.jsg.2005.01.005.

Arnaud, E., Harvey, T., Weaver, L., Meyer, J.R. & Parker, B.L., 2025. Ice-marginal terrestrial landsystems: Sediment heterogeneity, architecture and hydrogeological implications. Earth-Science Reviews, Volume 262, 2025, 105059, ISSN 0012-8252, https://doi.org/10.1016/j.earscirev.2025.105059.

Bense, V.F., Van den Berg, E.H. & Van Balen, R.T., 2003. Deformation mechanisms and hydraulic properties of fault zones in unconsolidated sediments; the Roer Valley Rift System, The Netherlands. Hydrology Journal (2003), 11:319-332. Springer Verlag.

Brandes, C., Polom, U., Bentzen, A., Steffen, R., Steffen, H. & Sandersen, P., 2024. Neotectonic activity of the Tønder Graben, derived from a 2D shear wave seismic survey. Presentation at the Postglacial Fault Symposium, August 12th, 2024, Gävle Sweden.

Brandes, C., Polom, U., Winsemann, J., Sandersen, P.B.E., 2022. The near-surface structure in the area of the Børglum fault, Sorgenfrei-Tornquist Zone, northern Denmark: Implications for fault kinematics, timing of fault activity and fault control on tunnel valley formation, Quaternary Science Reviews, 289, 107619, DOI: https://doi.org/10.1016/j.quascirev.2022.107619.

Clausen, O. R., Nielsen, S. B., Egholm, D. L. & Gołedowski, B., 2012. Cenozoic structures in the eastern North Sea Basin − A case for salt tectonics. Tectonophysics 514–517, 156–167.

Clausen, O. R. & Huuse, M., 1999. Topography of the Top Chalk surface on- and offshore Denmark. Marine and Petroleum Geology 16, 677–691.

Clausen, O. R. & Pedersen, P. K., 1999. Late Triassic structural evolution of the southern margin of the Ringkøbing-Fyn High, Denmark. Marine and Petroleum Geology 16, 653–665.

Dybkjær, K., 2015. Palynologisk undersøgelse af 1 prøve fra DGU nr. 168.1546 (Uge) og 4 prøver fra boringen DGU nr. 159.1444. Udarbejdet for Naturstyrelsen, GEUS-notat nr.: 08-EN-15-02, dateret 30. januar 2015.

Friborg, R., 1996. The landscape below the Tinglev outwash plain: a reconstruction. Bulletin of the Geological Society of Denmark 43, 34–40.

Friborg, R., Kirsch, R., Scheer, W., Stoepker, K. & Thomsen, S., 2002. Grundvand til Sønderjylland og Schleswig – Grundwasser für Sønderjylland und Schleswig. 92 pp. Landesamt für Natur und Umwelt des Landes Schleswig-Holstein & Sønderjyllands Amt, Teknisk Forvaltning.

Hansen, S., 1978. Sidste istids maksimums-udbredelse i Syd- og Midtjylland. Danmarks Geolologiske Undersøgelser, Årbog 1976, 139–152.

Hansen, S., 1989. Geological map of Denmark. Map sheet Tinglev. Soil map & glacial morphological map. Geological Survey of Denmark, Map Series 9 & 10, Copenhagen.

Hansen, M., & Pjetursson, B., 2011. Free, online Danish shallow geological data. Geological Survey of Denmark and Greenland Bulletin, 23, 53-56. https://doi.org/10.34194/geusb.v23.4842.

Henriksen, H.J., Kragh, S.J., Gotfredsen, J., Ondracek, M. van til, M., Jakobsen, A., Schneider, R.J.M., Koch, J., Troldborg, L. Rasmussen, P., Pasten-Zapata, E. & Stisen, S., 2020. Udvikling af landsdækkende modelberegninger af terrænnære hydrologiske forhold i 100m grid ved anvendelse af DK-modellen: Dokumentationsrapport vedr. modelleverancer til Hydrologisk Informations- og Prognosesystem. Udarbejdet som en del af den fællesoffentlige digitaliseringsstrategi 2016-2020, Initiativet Fælles data om terræn, klima og vand. GEUS, Klima, Energi og Forsyningsministeriet.

Houmark-Nielsen, M., 2011. Pleistocene glaciations in Denmark: a closer look at chronology, ice dynamics and landforms. In: Ehlers, J., Gibbard, P.L., Hughes, P.D. (Eds.), Quaternary Glaciations: Extent and Chronology. A Closer Look. Developments in Quaternary Sciences, 15. Elsevier, Amsterdam, ISBN 978-0-444-53447-7, pp. 47–58. https://doi.org/10.1016/B978-0-444-53447-7.00005-2.

Houmark-Nielsen, M., 2007. Extent and age of Middle and Late Pleistocene glaciations and periglacial episodes in southern Jutland, Denmark. Bulletin of the Geological Society of Denmark 55, 9–35.

Høyer, A. S., Sandersen, P. B. E., Andersen, L. T., Madsen, R. B., Mortensen, M. H., & Møller, I., 2024. Evaluating the chain of uncertainties in the 3D geological modelling workflow. Engineering Geology, 343, 107792. https://doi.org/10.1016/j.enggeo.2024.107792

Jakobsen, P.R., 2022. Geomorphological map of Denmark, 1:200.000, Geological Survey of Denmark and Greenland. https://doi.org/10.22008/FK2/0U6ERA

Jørgensen, F. & Sandersen, P., 2006. Buried and open tunnel valleys in Denmark – Erosion beneath multiple ice sheets. Quaternary Science Reviews 25, 1339–1363. https://doi.org/10.1016/j.quascirev.2005.11.006.

Jørgensen, F., Høyer, A.-S., Sandersen, P.B.E., He, X. & Foged, N., 2015. Combining 3D geological modelling techniques to address variations in geology, data type and density – An example from Southern Denmark. Computers & Geosciences 81 (2015) p. 53–63 http://dx.doi.org/10.1016/j.cageo.2015.04.010.

Jørgensen, F., Sandersen, P., Høyer, A.-S., Møller, R. R., Pallesen, T. M., He, X., Kristensen, M., Sonnenborg, T., & von Platen-Hallermund, F., 2014. 3D geologisk model ved Tønder. GEUS. Danmarks og Grønlands Geologiske Undersøgelse Rapport Bind 2014 Nr. 39 https://doi.org/10.22008/gpub/30606.

Jørgensen, F., Scheer, W., Thomsen, S., Sonnenborg, T. O., Hinsby, K., Wiederhold, H., Schamper, C., Burschil, T., Roth, B., Kirsch, R. & Auken, E., 2012. Transboundary geophysical mapping of geological elements and salinity distribution critical for the assessment of future sea water intrusion in response to sea level rise. Hydrology and Earth System Sciences Discussions 9, 2629–2674.

Kidmose, J., Jessen, S., Sandersen, P. B. E., Nilsson, B., Koch, J., Thorling, L., Pedersen, J. B., Christiansen, A. V., & Møller, I., 2025. Remote sensing of preferential groundwater discharge with high-resolution geophysical measurements of FloaTEM and tTEM compared with lake surface temperature anomalies. Journal of Hydrology, 652, Artikel 132523. https://doi.org/10.1016/j.jhydrol.2024.132523.

Kolstrup, E. & Havemann, K., 1984. Weichselian Juniperus in the Frøslev alluvial fan (Denmark). Bulletin of the Geological Society of Denmark 32, 121–131.
Kristensen et al 2015 Miocæn 3D

Kristensen, M., Vangkilde-Pedersen, T., Rasmussen, E. S., Dybkjær, K., & Andersen, L. T. (2015). Miocæn 3D opdateret 2014. Den rumlige geologiske model. GEUS. Danmarks og Grønlands Geologiske Undersøgelse Rapport Bind 2014 Nr. 75 https://doi.org/10.22008/gpub/30643.

Lyngsie, S., 2007. Continental sutures and their influence on rifting in the North Sea. Ph.D. thesis, University of Copenhagen, 64 pp.

Miljøstyrelsen, 2020. Samling af Geologiske Modeller i Jylland, p. 54. FOHM – Fællesoffentlig hydrologisk model. June 26, 2020. In Danish. 54 p.

Niras, 2025. Opstilling af 3D hydrostratigrafisk model; Blue Transition – Aabenraa. Preliminary version (Ver.1). Performed for Region Syddanmark, 19. marts 2025.

Niras, 2024. tTEM-kortlægning Aabenraa og Tønder Tolkningsrapport. Performed for Miljøstyrelsen, March 2024.

Piasecki, S., & Rasmussen, E. S., 2010. Stratigrafisk analyse af boring DGU nr. 168.1467 ved Tinglev i Sønderjylland. GEUS. Danmarks og Grønlands Geologiske Undersøgelse Rapport Bind 2010 Nr. 4 https://doi.org/10.22008/gpub/27929.

Polom, U., Bagge, M., Wadas, S., Winsemann, J., Brandes, C., Binot, F., Krawczyk, C.M. 2013. Surveying near-surface depocentres by means of shear wave seismic. First Break, Vol. 31, p. 67-79, 2013.

Rambøll, 2012a. SkyTEM – Tinglev. Processering, tolkning og rapportering. Performed for Nature Agency Ribe, 32 p., april 2012.

Rambøll, 2012b. SkyTEM – Ravsted-Bedsted. Processering, tolkning og rapportering. Performed for Nature Agency Ribe, 28 p., March 2012.

Rasmussen, E. S., 2009. Neogene inversion of the Central Graben and Ringkøbing–Fyn High, Denmark. Tectonophysics 465, 84– 97.

Rasmussen, E.S., Dybkjær, K., Piasecki, S., 2010. Lithostratigraphy of the upper Oligocene-Miocene session in Denmark. Geological Survey of Denmark and Greenland Bulletin, 2010; 22:93.

Rasmussen, P., Kidmose, J., Kallesøe, A. J., Sandersen, P. B. E., Schneider, R., & Sonnenborg, T. O., 2023. Evaluation of adaptation measures to counteract rising groundwater levels in urban areas in response to climate change. Hydrogeology Journal, 31, 35–52. https://doi.org/10. https://doi.org/10.1007/s10040-022-02573-7.

Sandersen, P.B.E., 2008. Uncertainty assessment of geological models - a qualitative approach. IAHS-AISH Public. 345–349.

Sandersen, P.B.E. & Jørgensen, F., 2022. Tectonic impact on Pleistocene and Holocene erosional patterns in a formerly glaciated intra-plate area. Quaternary Science Reviews; https://doi.org/10.1016/j.quascirev.2022.107681.

Sandersen, P.B.E. & Jørgensen, F., 2016. Kortlægning af begravede dale i Danmark. Opdatering 2010-2015. Volumes 1 and 2. GEUS Special Publication. ISBN 978-87-7871-451-0/452-7.

Sandersen, P. B. E., & Jørgensen, F., 2015. Neotectonic deformation of a Late Weichselian outwash plain by deglaciation-induced fault reactivation of a deep-seated graben structure. Boreas, 44(2), 413-431. https://doi.org/10.1111/bor.12103.

Sandersen, P. B. E., & Jørgensen, F., 2003. Buried Quaternary valleys in western Denmark-occurrence and inferred implications for groundwater resources and vulnerability. Journal of Applied Geophysics, 53(4), 229-248. https://doi.org/10.1016/j.jappgeo.2003.08.006.

Sandersen, P.B.E. & Kallesøe, A.J., 2021. MapField study area LOOP 2: Establishing a geological event chronology. GEUS Report 2021/30.

Sandersen, P.B.E, Kallesøe, A.J., Møller, I, Høyer, A.-S., Jørgensen, F., Pedersen, J.B. & Christiansen, A.V., 2021. Utilizing the towed Transient ElectroMagnetic method (tTEM) for achieving unprecedented near-surface detail in geological mapping. Engineering Geology 288, 106125. https://doi.org/10.1016/j.enggeo.2021.106125.

Sandersen, P. B. E., Jørgensen, F., Kallesøe, A. J., & Møller, I., 2018. *Opstilling af geologiske modeller til grundvandsmodellering*. GEUS. Geo-vejledning Bind 2018 Nr. 1. Special publication. https://doi.org/10.22008/gpub/38283.

Seidenfaden, I. K., Sonnenborg, T. O., Stisen, S., & Kidmose, J., 2022. Quantification of climate change sensitivity of shallow and deep groundwater in Denmark. Journal of Hydrology: Regional Studies, 41, 101100. https://doi.org/10.1016/j.ejrh.2022.101100.

Sjørring, S. og Frederiksen, J., 1980. Glacialstratigrafiske observationer i de vestjyske bakkeøer. Dansk geol. Foren., Årsskrift for 1979, side 63-77, København, 18. January 1980.

SkyTEM Aps., 2023. SkyTEM kortlægning af Tinglev. Afrapportering af rådata. Survey performed for the Danish Environmental Agency (Miljøstyrelsen), March 2023.

Ter-Borch, N., 1991. Geological map of Denmark, 1:500.000. Structural map of the Top Chalk Group. Geological Survey of Denmark, Map Series 7, Copenhagen.

Vejbæk, O. V., 1997. Dybe strukturer i danske sedimentære bassiner. Geologisk Tidsskrift 4, 1–31.

Vejbæk, O. V. & Britze, P. (eds.), 1994: Geological map of Denmark, 1:750.000. Top pre-Zechstein (two-way traveltime and depth). Geological Survey of Denmark, Map Series 45, 8 pp.

Ødum, H., 1933. Mindre Meddelelser fra Danmarks geologiske Undersøgelses Borearkiv. Nr. 10. Tinglev. Meddelelser fra Dansk Geologisk Forening 8, 261–262.